Chiral Resorcinarenes as Enantioselective Receptors

Dissertation
University of Bielefeld
Department of Chemistry
submitted by
Marlene Elisabeth Paletta

in partial fulfillment of the requirements
for the degree *Doctor rerum naturalium*

May 2010

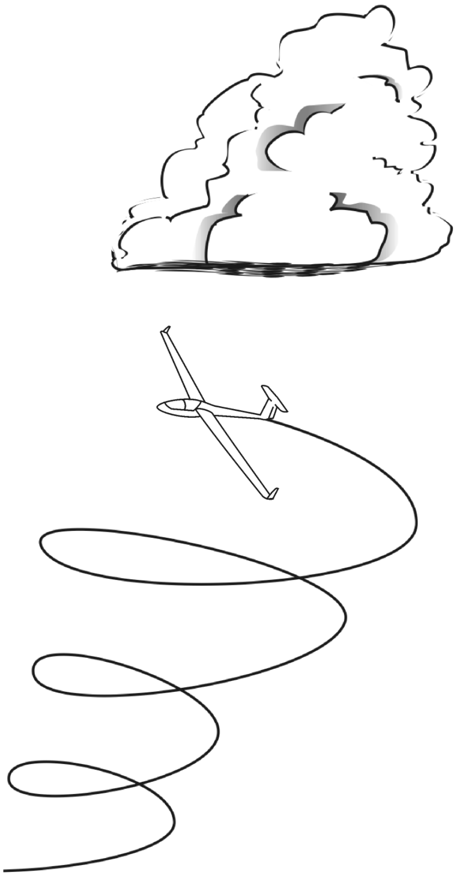

Referent:	Prof. Dr. J. Mattay
Koreferent:	PD Dr. N. Schaschke

Danksagung

Diese Arbeit enstand in der Arbeitsgruppe Organische Chemie I an der Universität Bielefeld und wurde unter der Anleitung von Prof. Dr. Jochen Mattay in der Zeit von November 2006 bis Mai 2010 angefertigt. Ihm danke ich für das spannende Thema, die hervorragende Atmosphäre in der Arbeitsgruppe und vor allem für das in mich gesetzte Vertrauen und die Gestaltungsfreiheit in dieser Arbeit.

PD Dr. Norbert Schaschke danke ich für die Übernahme des Koreferates.

Begleitet und unterstützt haben mich während der Dissertation viele Menschen, denen ich danke:
Thomas Geisler danke ich für Synthesen von Vorstufen sowie die Unterstützung bei GC-Fragen. Für die Lösung von technischen Problemen danke ich Dieter Barth. Heike Kosellek und Stefanie Boese danke ich für die Versorgung mit Material und Laborbedarf sowie Informationen aller Art. Den Auszubildenden Irina Langlitz, Daniela Niebuhr, Olga Fuchs und Olga Paustian danke ich für Synthesearbeiten während ihrer Zeit in der OCI.

Ich danke Peter Mester für die Durchführung von NMR-Messungen aller Art. Bei Dr. Andreas Mix bedanke ich mich für sein Engagement in vielen NMR-Experimenten und Diskussionen.

Der Massenspektrometrie-Abteilung danke ich für zahlreiche Messungen, insbesondere Dr. Matthias Letzel für aufwendige Experimente. Dr. Caterina Fraschetti gilt mein besonderer Dank für die Durchführung der Gasphasenexperimente und die vielen Diskussionen rund um Massenspektrometrie sowie rege Korrespondenz.

Dr. Alexander Rozhenko danke ich für wertvolle Hinweise und die quantenchemischen Rechnungen.

Beate Neumann und Dr. Hans-Georg Stammler danke ich für die Messung und Bearbeitung der Kristallstrukturanalysen.

Der Arbeitsgruppe OCI danke ich für die Zusammenarbeit, das Diskutieren von Ideen aller Art und die gemeinsamen Ausflüge. Ion Stoll, Björn Schnatwinkel, Michael Klaes, Olaf Barton, Christian Schäfer, Kai Altenhöhner, Michael Peter, Florian May, Jens Eberhard, Sebastian Wiegmann, Frank Strübe, Ramona Hartmann, Falk Wehmeier, Jens Linke und Tobias Schröder danke ich für viele Arbeitsgruppenaktivitäten. Ein ganz besonderer Dank gilt meinen Mitbewohnern in "207", Oliver Tosic und Sebastian Bringmann, für die einzigartige, harmonische Laborzeit.

Meiner Familie danke ich sehr für die mir entgegengebrachte Geduld und ihre humorvolle Art. Besonders herzlich ist der Dank an Rudi.

Marlene Paletta
Mai2010

Contents

1 Preface 1

2 Chiral Structures in Supramolecular Chemistry 3
2.1 Chiral Structures Based on Resorcinarenes and Cavitands 3
2.2 Cyclochiral and Inherently Chiral Resorcinarenes 7
2.3 Chiral Artificial Receptors 12

3 Objective 17

4 Amidoresorcinarenes 19
4.1 Synthesis of Resorcinarenes Functionalised with Amino Acids 19
4.2 Chiroptical Properties of the Amidoresorcinarenes and -Cavitands 23
4.3 Synthesis of Inherently Chiral Resorcinarenes Functionalised with Amino Acids 25

5 Cavity-Extended Chiral Resorcinarenes 29
5.1 Synthesis of a Biaryl Motif 29
5.2 Crystal Structures and Conformational Analysis 38
5.3 Chiroptical Properties of the Tetrabiaryl Ether 41

6 Chiral Resorcinarenes as Receptors for Chiral Molecular Recognition 45
6.1 Synthesis of Chiral Resorcinarenes 45
6.1.1 Synthesis of a Labelled Aldehyde 46
6.1.2 Synthesis of Racemic, Inherently Chiral Resorcinarenes 50
6.1.3 Enantiomer Resolution of Inherently Chiral Resorcinarenes 51
6.1.4 Achiral, Labelled Resorcinarenes 56
6.2 Chiroptical Properties of the Enantiomers 57
6.3 Enantioselectivity of Inherently Chiral Resorcinarenes 60
6.4 Diastereomeric Complexes in Solution 71

6.5 DFT-Calculations of the Diastereomeric Complexes 74

7 Summary **79**

8 Experimental Section **85**

8.1 General Remarks 85

8.2 ESI-FT-ICR Experiments 85

8.3 Synthesis of Amidoresorcinarenes and -Cavitands from Achiral Resorcinarenes . 86

8.3.1 Tetracarboxylic acid resorcinarene **39** 86

8.3.2 Tetracarboxylic acid cavitand **42** 87

8.3.3 General protocol of the amide formation 87

8.3.4 (*S*)-Tetrakisphenylalanine resorcinarene **44** 87

8.3.5 (*R*)-Tetrakisphenylalanine resorcinarene **45** 88

8.3.6 (*S*)-Tetrakisphenylalanine cavitand **46** 88

8.3.7 (*R*)-Tetrakisphenylalanine cavitand **47** 89

8.4 Synthesis of Tetrabiaryl ether **55** 90

8.4.1 Tetrakis-(2´-bromobenzyl)ether tetramethoxyresorcinarene *rac*-**54** . . . 90

8.4.2 Tetrakis-(2´-bromobenzyl)ether tetramethoxyresorcinarene (*M*,*R*)-(–)-**54** 91

8.4.3 Tetrakis-(2´-bromobenzyl)ether tetramethoxyresorcinarene (*P*,*S*)-(+)-**54** 91

8.4.4 Synthesis of Tetrakis-(2´-bromo-4´-(methoxycarbonyl))tetramethoxyresorcinarene **58** 93

8.5 Synthesis of the Labelled Aldehyde **76** 95

8.5.1 1-Dodecene-12,12,12-d_3 **73** 95

8.5.2 1-Undecanal-11,11,11-d_3 **76** 95

8.6 Synthesis of racemic Tetramethoxyresorcinarenes **79** and **80** 96

8.6.1 Tetramethoxyresorcinarene *rac*-**79** 96

8.6.2 Tetramethoxyresorcinarene-d_{12} *rac*-**80** 96

8.7 Resolution of the Tetramethoxyresorcinarene enantiomers 97

8.7.1 General Procedure of the Diastereomer Formation 97

8.7.2 Diastereomers **81a** and **81b** of Tetramethoxyresorcinarene **79** 97

8.7.3 Diastereomers **82a** and **82b** of Tetramethoxyresorcinarene **80** 99

8.7.4 General procedure cleavage of the auxiliaries 100

8.7.5 Tetramethoxyresorcinarene (*P*,*S*)-(+)-**79** 100

8.7.6 Tetramethoxyresorcinarene (*M*,*R*)-(–)-**79** 101

8.7.7 Tetramethoxyresorcinarene-d_{12} (*P*,*S*)-(+)-**80** 101

8.7.8 Tetramethoxyresorcinarene-d_{12} (M,R)-(–)-**80** 102
8.8 Synthesis of Octahydroxyresorcinarenes 102
8.8.1 General procedure Octahydroxyresorcinarenes 102
8.8.2 Octahydroxyresorcinarene **83** 102
8.8.3 Octahydroxyresorcinarene-d_{12} **84** 103
8.9 Synthesis of Octamethoxyresorcinarenes 103
8.9.1 General procedure of the methylation reaction 103
8.9.2 Octamethoxyresorcinarene **85** 103
8.9.3 Octamethoxyresorcinarene-d_{12} **86** 104

Abbreviations **105**

Glossary **107**

Bibliography **109**

Appendix **117**

1 Preface

Supramolecular chemistry is the field of specific interactions between structures due to their shape, their electrostatic surface, the steric fit and the spatial arrangement.[1,2] Non-covalent interactions govern the selective recognition of geometrically complementary binding sites of small substrates and receptors. Macrocyles provide a defined architecture with an inner cavity like a bowl and a specific arrangement of the substitutents. A non-planar surface is ideally suited to encapsulate small guest molecules to form a complex that is held together by non-covalent interactions. The investigation of these short-range forces is crucial to understand the mechanisms in molecular recognition.

The design and synthesis of receptors is the challenge in supramolecular chemistry. The class of resorcinarenes and cavitands offers a hollow space with adjustable flexibility and a wide range of functionalities that can be introduced into the macrocycle.[3–5] The enclosure properties of achiral structures are evident as shown in many examples, e.g. host-guest complexes,[6,7] anion receptors[8] or supramolecular assemblies.[9,10] From the vantage point of chirality there are e.g. cyclodextrines[11] known as natural receptors of a macrocyclic type and chiral crown ethers as artificial systems.[12] Calixarene-based receptors were able to enantiodiscriminate substrates with a change in colour upon complexation.[13]

Chiral resorcinarenes and cavitands are valuable building blocks in supramolecular chemistry as they offer a well-defined shape with various functionalities. The preparation of artificial receptors and their enantio discriminating potential is of considerable interest. With these macrocycles one can gain further insight into molecular recognition processes. This may open up the way to design host systems for enantioselective reactions.

2 Chiral Structures in Supramolecular Chemistry

2.1 Chiral Structures Based on Resorcinarenes and Cavitands

Resorcinarenes are three-dimensional macrocycles that are used in various aspects of supramolecular chemistry, for example, as building blocks and in molecular recognition[6,14,15] as well as in chiral assemblies.[5] In an acid catalysed condensation reaction these building blocks are generated from resorcinol and an aliphatic or aromatic aldehyde.[3,16] The possible conformations of the tetrameric macrocycles are shown in Figure 2.1, whereas the residues are arranged *axially* (R_a) or *equatorially* (R_e). The resorcin[4]arenes are denoted in the following as resorcinarenes.

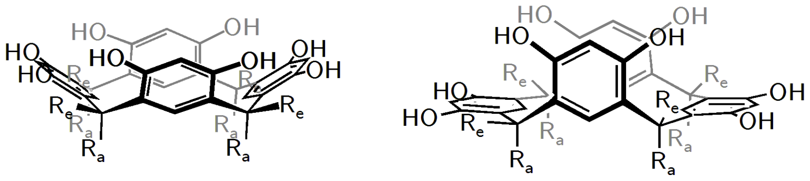
HO
OH
HO
HO
HO
OH
OH
OH
R_e
R_e
R_a
R_a
R_e
R_e
R_a
R_a
HO
OH
HO
OH
R_e
R_e
HO
OH
HO
R_e
R_a
R_e
OH
R_a
R_a
R_a

crown (C_{4v})
R_e = H, R_a = alkyl; *rccc*

boat (C_{2v})
R_e = H, R_a = alkyl; *rccc*

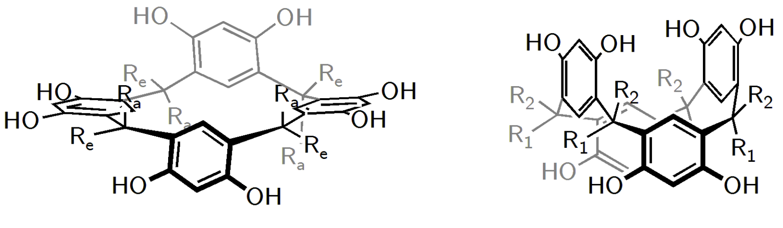
HO
OH
R_e
R_e
HO
R_a
R_a
OH
HO
R_a
OH
R_e
R_a
R_e
HO
OH
HO
OH
HO
OH
R_2
R_2
R_2
R_2
R_1
R_1
R_1
HO
HO
OH

1,2-alternate (C_s)

1,3-alternate (D_{2d})

Figure 2.1: Conformations of resorcinarenes.

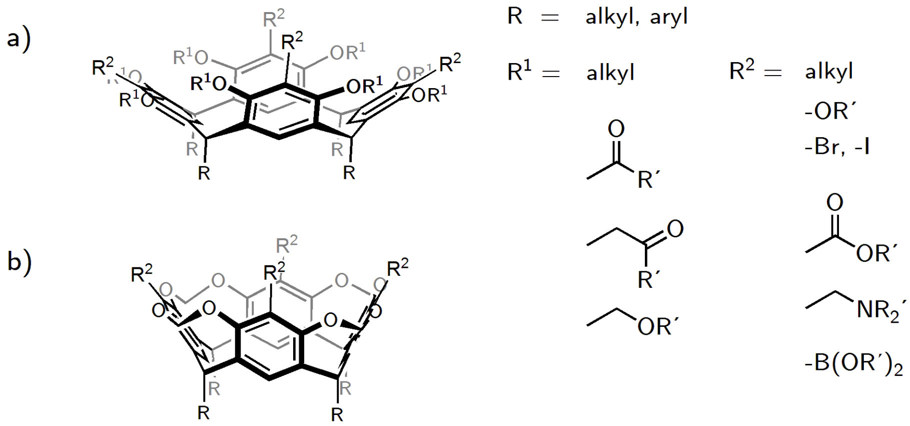

Figure 2.2: (a) Scaffolds of the resorcinarene and (b) the methylene-bridged cavitand. Examples for the substitution pattern at the *upper rim* are given for the residues R^1 and R^2.

The thermodynamically controlled reaction leads to products wherein the residues are all *cis*-oriented (*c*) to one reference moiety (*r*), giving a (*rccc*)-configuration for the *boat* and the *crown* conformation (e.g. R_e = H, R_a = alkyl). In solution, these two conformations interconvert. There are few examples given for functionalisations introduced in the *upper rim* shown in Figure 2.2 a. In methylene bridged cavitands the conformation is fixed (Figure 2.2 b) and the scaffold becomes very rigid. Both the resorcinarenes and the cavitands generate a bowl-shaped cavity that can easily be functionalised as shown for some examples given in the next sections.

The resorcinarene scaffold provides a platform for the attachment of various groups. In the following macromolecular systems are presented from the vantage point of chirality. To turn achiral resorcinarenes and cavitands into a chiral entity simply a chiral moiety can be attached either to the hydroxyl groups or to the *ortho* position at the *upper rim*. SCHURIG *et al.* prepared an octafunctionalised resorcinarene **1** in 1999, that was immobilised on dimethylpolysiloxane.[17] The material is suitable as stationary phase in gas chromatography (Figure 2.3 a). A series of *N*(*O*,*S*)-TFA-(*S*,*R*)-amino acid methyl esters was successfully separated with enantioselectivities indicating the degree of peak separation up to $\alpha_{S/R}$=1.10 for leucine derivatives.[18]

SHERMAN *et al.* presented 1995 a pyrogallol based cavitand **2** bearing four (*S*)-phenylalanine ethyl ester residues with a short linking (Figure 2.3 b).[19,20] This system was the precursor for a series of *de novo* synthetic proteins with *C*- and *N*-terminally linked peptides with native-like properties, offering the design of artificial proteins.[21,22] A benzyl amine cavitand was used

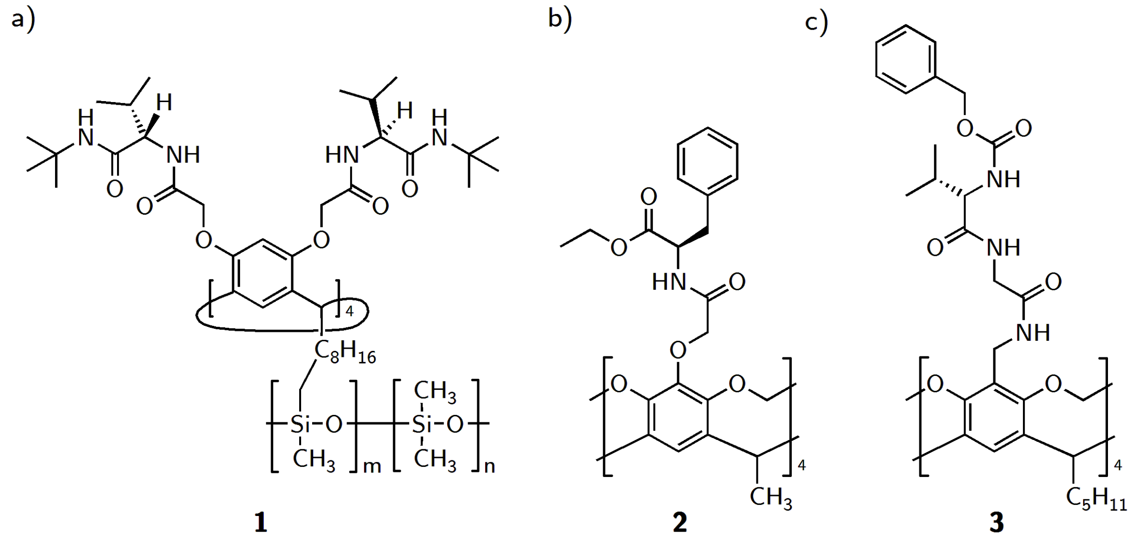

1 **2** **3**

Figure 2.3: (a) Resorcinarenes with amino acid residues by SCHURIG. Peptidocavitands by (b) SHERMAN and (c) FEIGEL.

by FEIGEL *et al.* as the rigid basis for the *C*-terminal attachment of dipeptides (Figure 2.3 c).[23,24] The cavity of compound **3** encloses acetonitrile and forms a very stable complex in chloroform solution.

Cavitands with phenyl ether bridges were prepared *via* nucleophilic aromatic substitution.[25,26] The extended *upper rim* was further functionalised with eight amide residues to give cavitand **4** (Figure 2.4 a). In crystal structure analysis the intramolecular hydrogen bonding was shown to be of cycloenantiomeric character that switches between the two cycloenantiomers in solution. Beside chiral substituentents, chirality in cavitands **5** and **6** originates from an unsymmetrical substitution pattern at the *upper rim* (Figure 2.4 b).[27] The vaselike cavity encloses aromatic compounds as well as solvent molecules.

The known examples of peptidocalixarenes based on resorcinarenes all have a very flexible linkage as there are benzylamine fuctionalities,[23,24] or 2-phenoxyacetyl groups.[17,19–22] The cavitands are more rigid than the resorcinarenes with chiral moieties at the *upper rim* that interconvert between the *crown* and the *boat* conformation. The most flexible systems are the methylated resorcinarenes with chiral lateral chains.[28–33] In complexation experiments in the gas phase and theoretical studies, the *upper rim* cavity of amido[4]resorcinarenes **7a**-**d** was shown to be less important to the complexation behaviour; in these systems the chiral lateral chains take part in enantioselective interactions. The chiral distinction depends strongly on the orientations the flexible chains adopt in the gas phase.[34]

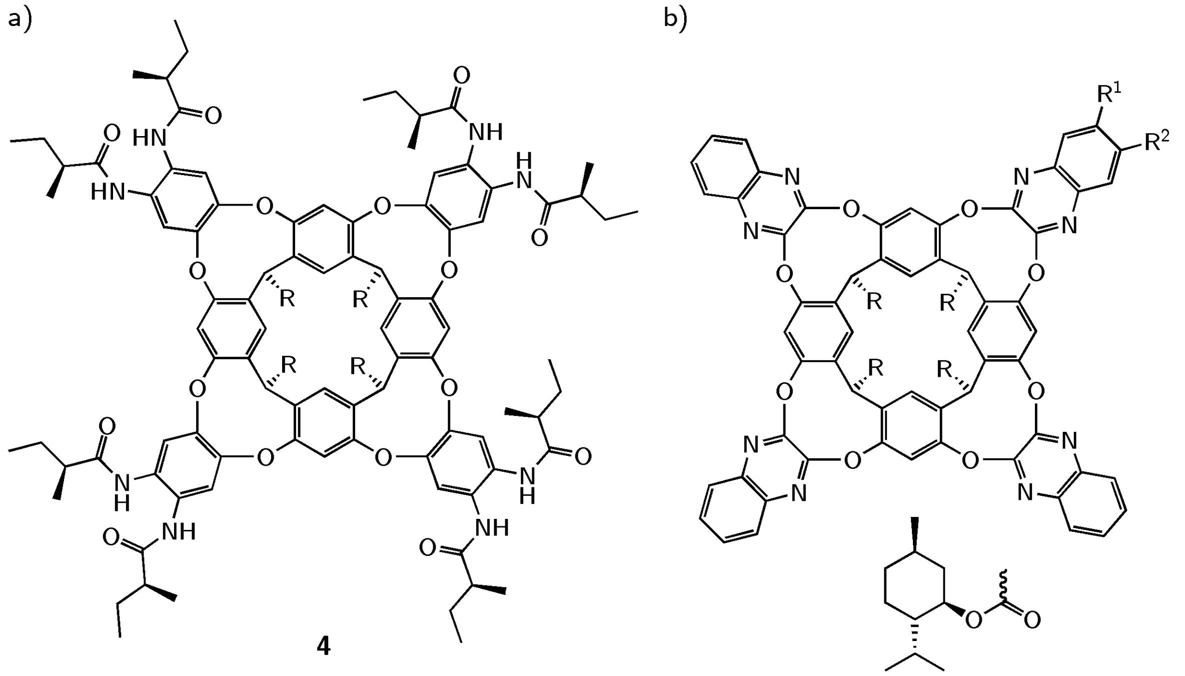
a)
b)
O
HN
NH
HN
H
N
O
N
H
NH
R
R¹
R²
N
O

4

$R = C_{11}H_{23}$

C(O)-Menthyl

5a $R = CH_3$, $R^1 = H$, $R^2 =$ C(O)-Menthyl

5b $R = CH_3$, $R^1 =$ C(O)-Menthyl, $R^2 = H$

(−)-6 $R = CH_3$, $R^1 = H$, $R^2 = CH_2OH$

(+)-6 $R = CH_3$, $R^1 = CH_2OH$, $R^2 = H$

Figure 2.4: (a) Cavitand with eight (*S*)-2-methylbutanamide residues and (b) unsymmetrically substituted cavitands.

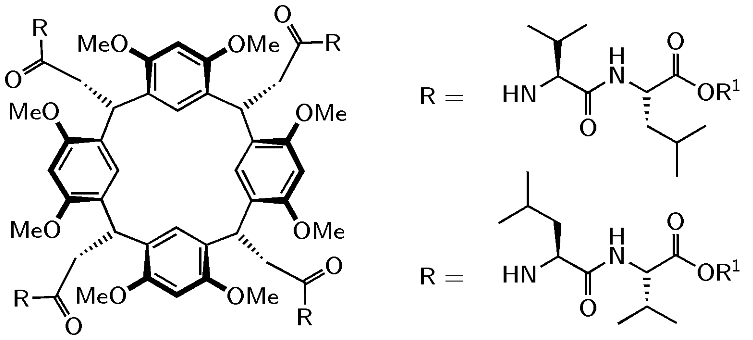
R
O
MeO
OMe
R =
HN
H
N
OR¹

$R^1 = H$ **7a**
$R^1 = CH_3$ **7b**

$R^1 = H$ **7c**
$R^1 = CH_3$ **7d**

Figure 2.5: Chiral amido[4]resorcinarenes with different side chains that contain valine and leucine residues.

The rigid structure of a resorcinarene with phosphorus bridging units was build up by Pietraszkiewicz *et al.* (Figure 2.6).[35] The bridges are substituted with (*S*)-1-phenylethanamine forming a chiral environment inside the cavity. In water, the cavitands of **8** form Langmuir monolayers that discriminate the (*S*)- and the (*R*)-enantiomers of thryptophane (**9**) and valine (**10**), respectively, at low pH values.

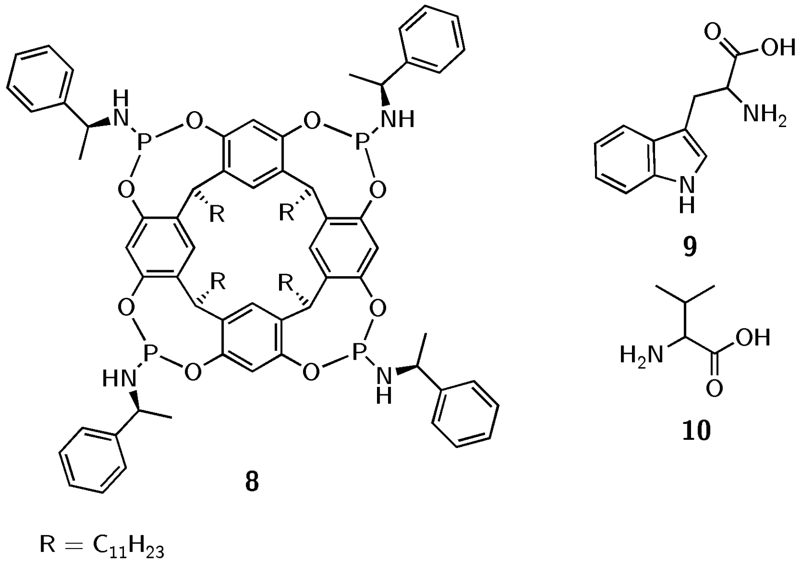

Figure 2.6: Phosphorus-bridged cavitand with (*S*)-1-phenylethanamine residues. Tryptophane (**9**) and valine (**10**) were investigated in aqueous solution.

2.2 Cyclochiral and Inherently Chiral Resorcinarenes

Chiral 1,3-oxazine derivatives were prepared from achiral resorcinarenes *via* Mannich reaction with (*R*)-and (*S*)-(1-phenylethyl)amine (Figure 2.7 a).[36] The cyclochiral, cavity extended diastereomers of macrocycle **11** form complexes with the enantiomerically pure phenylethylamine guests **12** in chloroform, benzene and THF.[37] Titration experiments were performed and monitored by differential UV/Vis spectroscopy. The association constants are different for each diastereomeric complex and the difference gives the chiral discrimination as a ratio of the formation constants (ratio of 0.79 for phenylethylamine; $K_{(+)-\mathrm{amine}}/K_{(-)-\mathrm{amine})}$). The absolute configuration of the benzylamine moieties in **11** was known, but at that time the configuration of the methylene bridges was not known so that the diastereomers of **11** were characterised by their optical rotation properties. Rissanen *et al.* investigated the chiral discrimination properties of the similar compound **13** towards chiral ammonium salts by MS (Figure 2.7 b).[38] The chiral ammonium salts **14** and **15** were investigated as *quasi*-racemate with one enantiomer isotopically labeled; in Figure 2.7 b one of the investigated *quasi*-racemates is displayed. The low mass difference of the *quasi*-enantiomers (3 amu) results in an insufficiently resolved isotope pattern. From analysis of the isotope pattern no significant difference in the relative peak intensities of the charged, diastereomeric complexes were obtained due to discrimination effects.

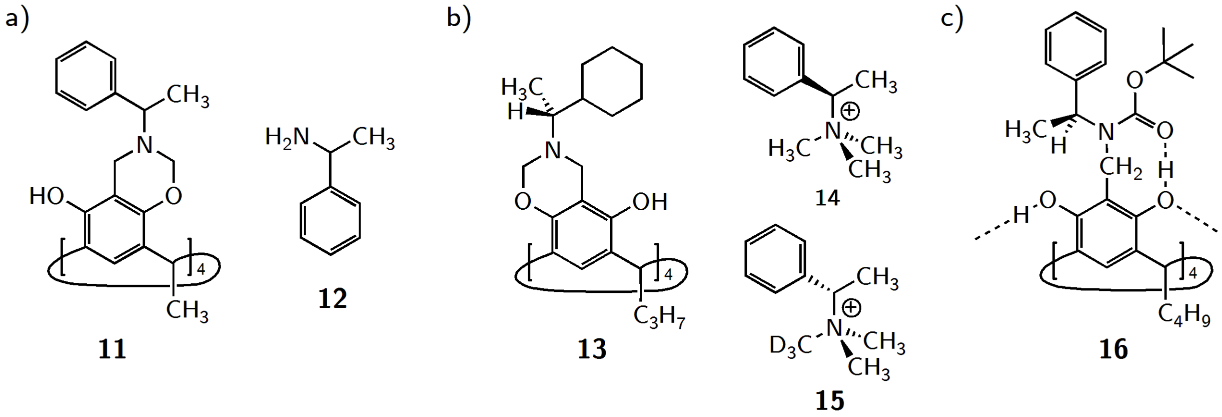

Figure 2.7: (a) 1,3-Oxazine derivative and a chiral guest investigated by Iwanek, (b) oxazines and *quasi*-enantiomers of ammonium guests, (c) (*S*)-1-phenylethylamine of a benzylamine resorcinarene.

A stable cyclochirality was observed for the benzylamine derivative **16** prepared by Szumna in the solid state as well as in solution (Figure 2.7 d).[39,40] The chiral residues are arranged in an inherently chiral manner of C_4 symmetry at the *upper rim*. The direction of the hydrogen bonds results from the diastereomeric preference depending on the chiral moiety. For **17a** and **17b** (Figure 2.8 a) the diastereomeric excess was determined by NMR spectroscopy as $> 95\%$ and for **17c** and **17d** as 72%. The split-Cotton effect displayed between 275 and 325 nm and arises from the inherently chiral hydrogen bonding (Figure 2.8 b). The chiral residues exhibit a monosignate signal < 260 nm. Semiempirical calculations (AM1) support the conformational stability based on hydrogen bonding.

Under acidic conditions, the tetrabenzoxazine diastereomers **11**, **13** and **16** are labile. The oxazine moiety can be transferred into the other C_4 symmetric regioisomer. Hence, for complexation experiments with e.g. chiral acids these systems are not suitable because epimerisation occurs.

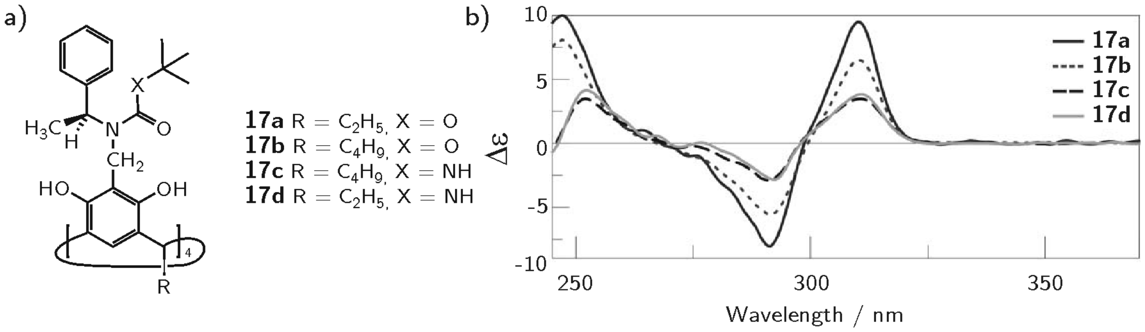

Figure 2.8: CD spectra of C_4 symmetric oxazine resorcinarenes **17a-d** in $CHCl_3$. This figure is taken from A. Szumna, *Org. Biomol. Chem.* **2007**, *5*, 1358-1368.

The chirality of inherently chiral resorcinarenes originates from the topology of the nonplanar structure (Figure 2.9). The C_4 symmetric resorcinarenes are prepared from achiral building blocks. The methylene bridges become stereogenic centers due to the substitution pattern at the *upper rim*. In contrast to benzoxazines derivatives, these scaffolds are stable towards moderate acidic and basic conditions.

The tetrameric macrocycles **18a-e** were synthesized in one step from 3-alkoxyphenols and an aldehyde or a corresponding acetal under Lewis acid catalysis. This procedure was first applied in 2000 by the group of MOCERINO[41] and improved substantially by HEANEY *et al.*[42] three years later. By starting from the dimethyl acetals of the aldehyde even 3-benzyloxy phenol was successfully reacted to the macrocycle **18e** despite the high lability of the benzyl ether functionality towards Lewis acids.

Recently, the absolute configuration of a C_4-symmetric tetramethylresorcinarene **19** with pendant isobutyl groups was determined by X-ray crystallographic analysis of the separated diastereomers **20a** and **20b** containing four (*S*)-(+)-10-camphorsulfonyl esters as auxiliaries.[43] The internal chirality reference revealed the configuration of the methylene bridges. After hydrolysis, the (−)-enantiomer of *rccc*-2,8,14,20-tetraisobutyl-6,12,18,24-tetra-*O*-methylresorcin[4]arene **19**, shortly denoted as tetramethoxyresorcin[4]arene, was shown to be of (*M*,*R*)-chirality and the (+)-enantiomer of **19** (*rccc*-2,8,14,20-tetraisobutyl-4,10,16,22-tetra-*O*-methylresorcin[4]arene) of (*P*,*S*)-chirality (Figure 2.10). The assignments were confirmed by analysis and alkaline hydrolysis of the tetra-(*R*)-(−)-10-camphorsulfonyl ester diastereomers. These results correct the assignment published in earlier studies[44,45] wherein the enantiomers were accidentally interchanged.

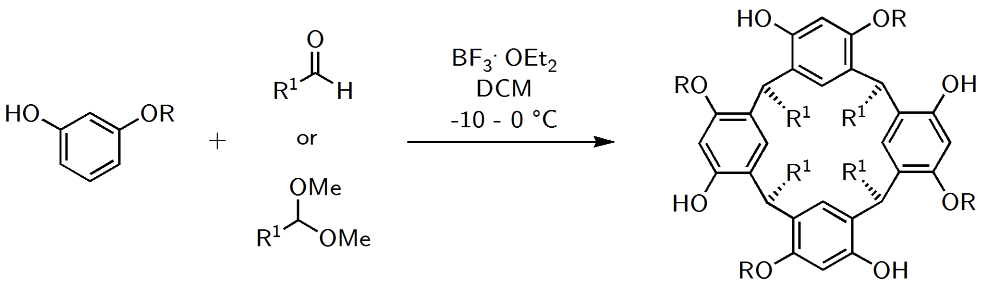
HO
OR
+
R1
H
O
or
OMe
R1
OMe
BF3· OEt2
DCM
-10 - 0 °C
HO
OR
RO
OH
R1
R1
R1
R1
HO
OR
RO
OH

18a R = CH_3, $R^1 = C_7H_{15}$
18b R = C_3H_7, $R^1 = C_{11}H_{23}$
18c R = cyclopentyl, $R^1 = C_5H_{11}$
18d R = (2S)-2-methylbutyl, $R^1 = C_{11}H_{23}$
18e R = benzyl, $R^1 = C_5H_{11}$

Figure 2.9: Synthesis of the inherently chiral resorcinarenes from 3-alkoxyphenols and an aldehyde or a corresponding acetal under Lewis acid catalysis.

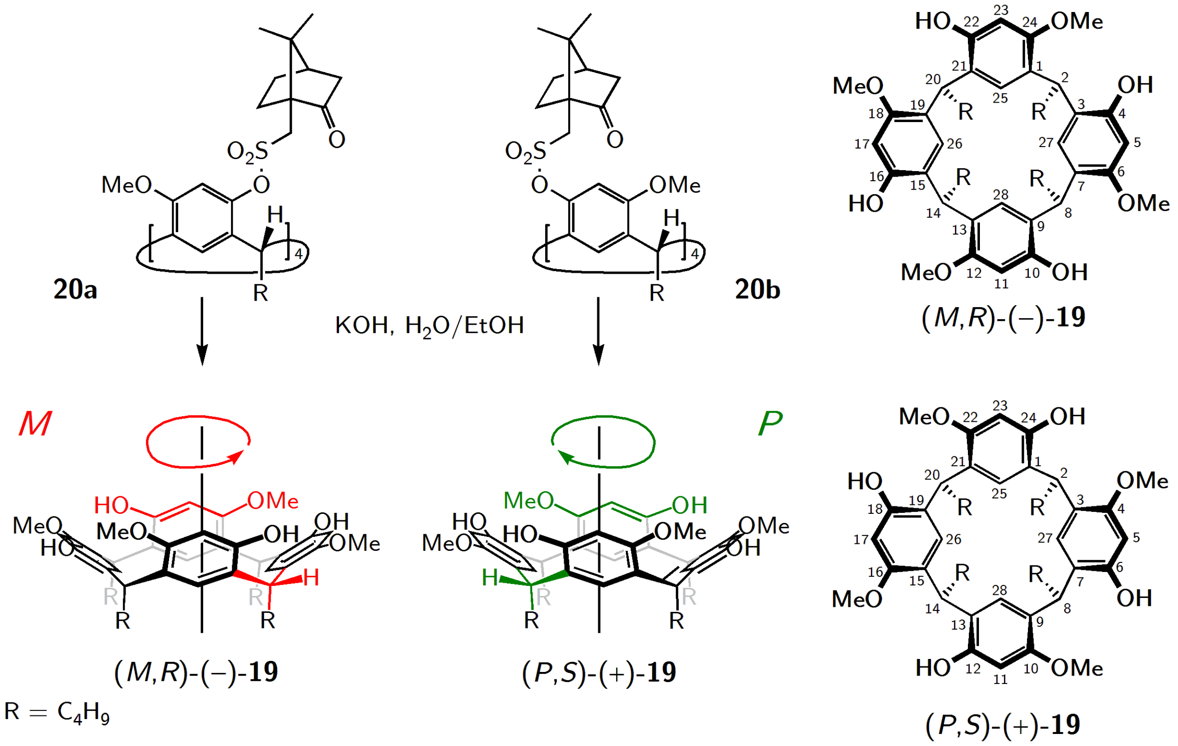
20a
20b
KOH, H2O/EtOH
M
P
(M,R)-(−)-19
(P,S)-(+)-19
R = C4H9
(M,R)-(−)-19
(P,S)-(+)-19
HO
OMe
MeO
OH
R

Figure 2.10: The assignment according to the absolute configuration of tetramethoxyresorcin[4]arene **19**. The alkaline hydrolysis of **20a** and **20b** gives (*M*,*R*)-(−)-**19** and (*P*,*S*)-(+)-**19**, respectively.

Up to date, there are only few cavity extended resorcinarenes known build up from the inherently chiral scaffold. During this work, ODGEN *et al.* presented the racemic pyridine-functionalized inherently chiral resorcinarene **21** (Figure 2.11 a) that build up diastereomeric complexes with (*S*)-(+)-10-camphorsulfonic acid in chloroform.[46] In NMR studies significantly shifted resonances for both the pyridyl moiety and the chiral guest were observed upon complexation. But the resolution of the racemic macrocycles by formation and crystallization of a diastereomeric salt was not successful. The resolution of the precursor resorcinarenes with covalently attached auxiliaries as described in the previous section and a subsequent reaction to the pyridyl resorcinarenes was not carried out.

The *O*-alkylated resorcinarenes[47] were used by RISSANEN as platforms to build up Fréchet-type dendrimers.[48] In Figure 2.11 b the dendrimer **22** of generation 1 is displayed. The macromolecular compounds were synthesised up to generation 3 with the purpose to generate a chiral core. But until now, the enantiomers of the dendrimer compound **22** have not been resolved.

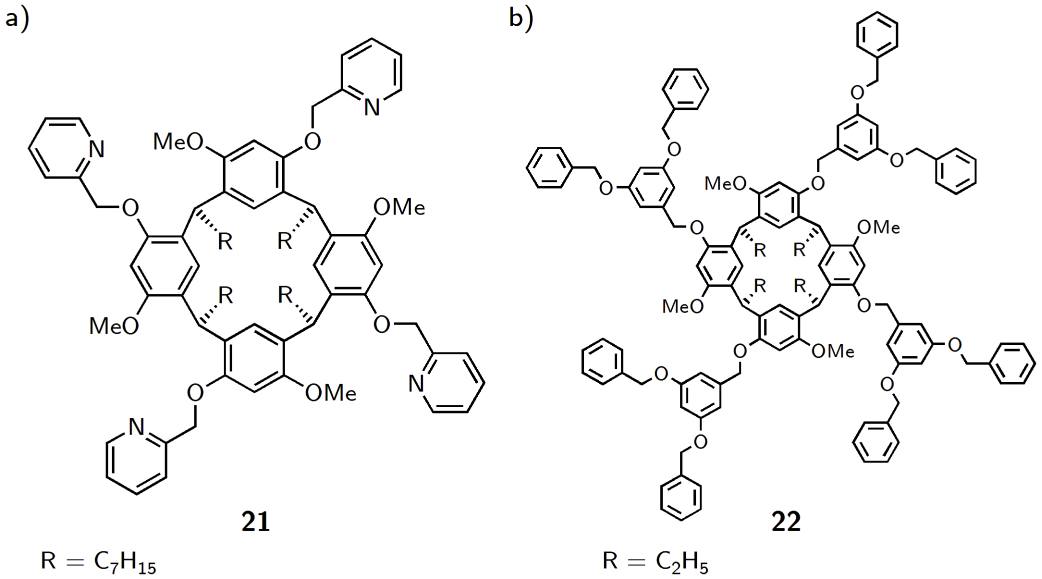

21

R = C_7H_{15}

22

R = C_2H_5

Figure 2.11: (a) Racemic, inherently chiral resorcinarene with pyridyl residues and (b) a Fréchet-type dendrimer of generation 1 based on a resorcinarene scaffold.

2.3 Chiral Artificial Receptors

In molecular recognition processes, specific interactions between a substrate and a receptor are responsible for the strength of the binding and the discrimination of different substrates. The steric fit and complementary arranged binding sites are based on the spatial arrangement of the functional groups. The configuration of a substitution pattern is the intrinsic chiral information in a supramolecular entity.

Stereodiscrimination of artificial receptors has been studied by several techniques like NMR,[49] ITC[50] and MS.[51] In the following, five examples of different classes of receptors are given; 1) crown ethers, 2) trianglamines, 3) resorcinarenes, 4) cyclic tetraamides and 5) calixarenes. The first macrocycle belongs to the class of chiral crown ethers. SAWADA *et al.* investigated compound **23** with a series of amino acid esters by MS with the enantiomer labeling method.[52,53] The chiral guests are added as *quasi*-racemate (see Glossary, p. 107) with one enantiomer deuterium labeled. The diastereomeric complexes of (*R*)-phenylalanine methyl ester (**24**) and **23** appeared in a 4.37-fold higher intensity than the complex of deuterium-labeled (*S*)-phenylalanine methyl ester (**25**).[52] But the relative intensities of the charged complexes depend on the ionisation source; for fast atom bombardement (FAB) and electrospray ionisation (ESI) the *IRIS*-values (ratio of the intensities of the *R*-guest and the *S*-guest complexes) differ strongly. With the ESI-MS method the homochiral diastereomer appears only in 1.8-fold excess.[53] Therefore the ionisation process itself alters the measured thermodynamic selectivity.

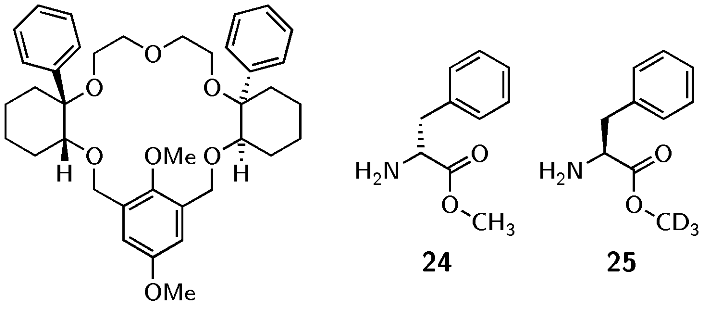

23

Figure 2.12: Chiral crown ether and one of the guest compounds investigated by SAWADA.[52]

KUHNERT *et al.* presented a complete set of all *quasi*-enantiomers of unlabelled (*all*-(*R*)-**26** and *all*-(*S*)-**26**) and labelled (*all*-(*R*)-**27**-d_6 and *all*-(*S*)-**27**-d_6) trianglamines in 2007 (Figure 2.13).[54] The self-association in ESI-generated complexes of *quasi*-enantiomeric mixtures was investigated in the gas phase by MS and the self-aggregation in solution by diffusion NMR techniques. The diastereoselectivity of trianglamines was shown to be of 20%. Host guest complexes were not investigated.

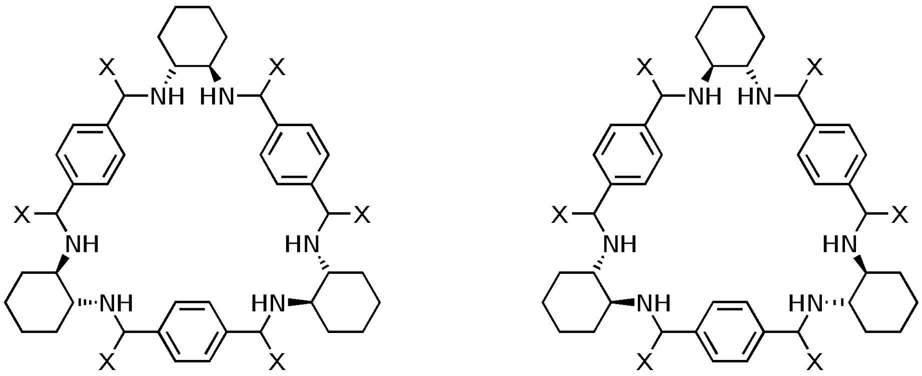

X = H (2*R*, 3*R*, 12*R*, 13*R*, 22*R*, 23*R*)-**26** X = H (2*S*, 3*S*, 12*S*, 13*S*, 22*S*, 23*S*)-**26**
X = D (2*R*, 3*R*, 12*R*, 13*R*, 22*R*, 23*R*)-**27**-d_6 X = D (2*S*, 3*S*, 12*S*, 13*S*, 22*S*, 23*S*)-**27**-d_6

Figure 2.13: Enantiomers of trianglamines **26** and their labelled isotopomers **27**-d_6.

The third example is a resorcinarene scaffold with chiral lateral chains. The very flexible resorcinarene **28** can easily adopt chiral cavities of different size and shape (Figure 2.14 a)[28,31] whereas the cyclic basket **29** shown in Figure 2.14 b is far more rigid.[29] BOTTA and SPERANZA *et al.* investigated the enantioselectivity of these chiral hosts in complexes with a series of amino acid derivatives and amphetamine in reactions with achiral and chiral amines. The ligand exchange reactions were performed as true gas phase experiments that are independent from the ionisation method. The reaction of **28** in complex with (*S*)-tyrosine methyl ester (**30**) with (*S*)-2-butylamine proceeded in the homochiral twice as fast as in the heterochiral. On the other hand, the homochiral complex of the basket compound **29** and (*S*)-tyrosine methyl ester reacted 0.78±0.04 times as fast as the heterochiral one; that is more slowly than the heterochiral one.

The tetraamidic macrocycle **31** with four phenyl residues in *R* configuration forms three body complexes with two host molecules and protonated (*S*)-naphthlyalanine ethyl ester (**32**) as enclosed, charged guest.[55] In kinetic enantioselectivity measurements in the gas phase by MS techniques, the heterochiral complex was found to react 66 times faster with (*S*)-2-butylamine than the homochiral adduct. This is an extraordinary high selectivity compared to those of the resorcinarenes with chiral lateral chains **28**.

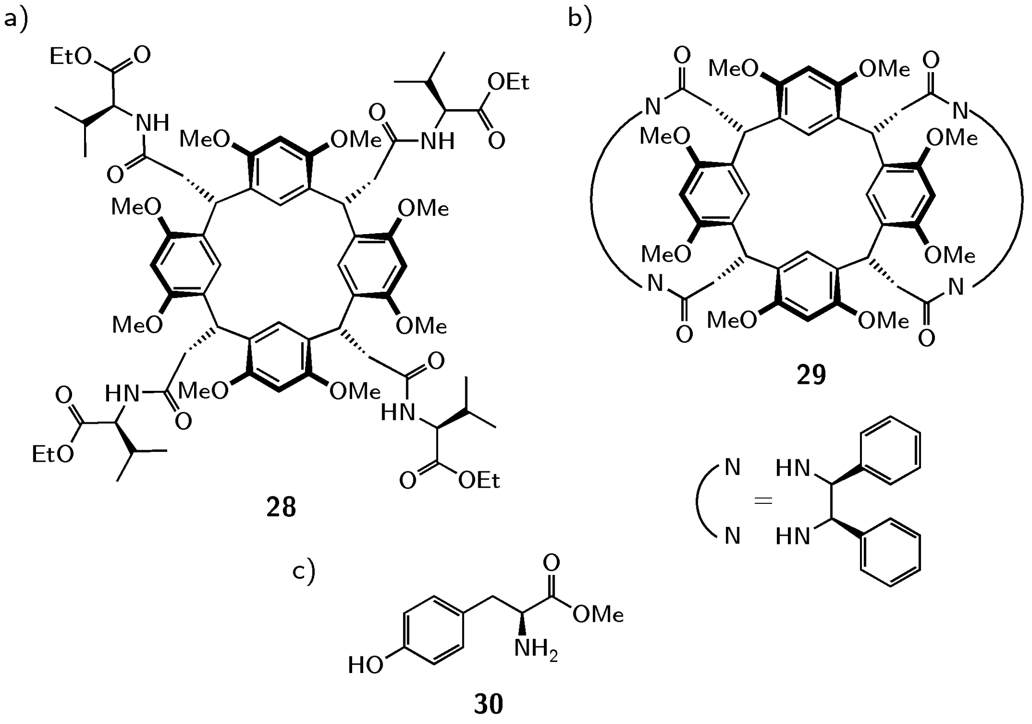

28 **29** **30**

Figure 2.14: (a) Amido[4]resorcinarenes with four (*S*)-valine ethyl ester residues and (b) a basket resorcin[4]arene with two chiral bridging units at the *lower rim*. (c) (*S*)-Tyrosinol methyl ester was the investigated guest in MS experiments.

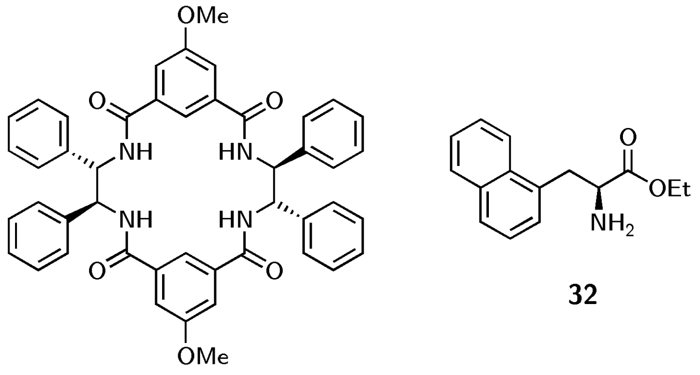

31 **32**

Figure 2.15: Chiral tetraamidic macrocycle and the investigated guest (*S*)-naphthylalanine ethyl ester.

The fifth example of a chiral sensor is a calixarene based macrocycle **33** with a (*S*)-1,1′-bi-2-naphthol moiety at the *lower rim*. In complexation experiments with phenylglycinol (**34**) as chiral guest the absorption properties are characteristically shifted. In ethanol the homochiral complex displays a purple colour and heterochiral complex is of blue colour.

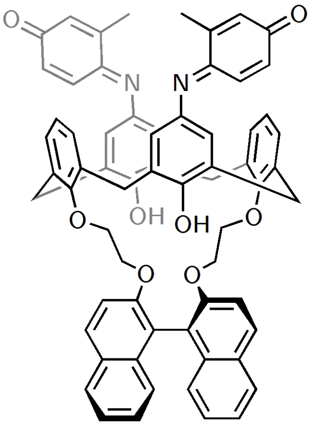

33

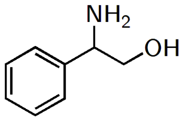

34

Figure 2.16: Chiral calixarene **33** with (*S*)-1,1´-bi-2-naphthol as bridging unit. The enantiomers of phenylglycinol (**34**) were investigated.

3 Objective

The chiral substitution pattern and the shape of inherently chiral resorcinarenes are ideally appropriate for host-guest complexation experiments. The discrimination of chiral substrates arises from the different non-covalent interactions with the chiral surface with donor and acceptor binding sites in a certain spatial arrangement. Cavity-extended chiral resorcinarenes are valuable building blocks in studies of chiral discrimination effects; a large binding pocket is able to enclose a guest entirely. The synthesis of a chiral scaffold stable in its configuration under moderate basic and acidic conditions is of considerable interest. The achiral and chiral resorcinarenes may both serve as platform for further derivatisation reactions.

Unlike the high flexibility in *lower rim* functionalised resorcinarenes, the attachment of chiral moieties at the *upper rim* offers enhanced control of flexibility. In cavitands and resorcinarenes many functional groups can be introduced at the *upper rim* for functionalisation purposes. With short linkers the conformational flexibility is constrained resulting in a well-defined, preorganised hollow space. A synthetic route to chiral resorcinarenes with adjustable conformational properties is of major interest.

Inherently chiral resorcinarenes are a class of chiral building blocks with an unidirectional substitution pattern. Starting from the chiral scaffold with known absolute configuration, a general synthetic route for extension of the cavity is desirable for further derivatisations. The cyclochirality should be preserved in the synthesis.

Thermodynamic stereodiscrimination investigations of labelled and non-labelled guests by MS gave a first hint on the potential of resorcinarenes as chiral receptors.[56] The design and synthesis of a system for further MS experiments is of interest. As the guest labelling of one enantiomer has shown a significant influence of the labelling itself on the complexation properties, a host labelling method should expel this effect. The synthesis and resolution of inherently chiral resorcinarenes and their labelled counterparts provide a suitable host system for chiral recognition experiments.

4 Amidoresorcinarenes

Chiral resorcinarenes can be generated from achiral macrocylic precursors and chiral building blocks that are introduced in the scaffold. The flexibility of the resorcinarene cavity influences significantly the conformation of the pendant moieties. For the purpose to study the distinct impact of the host flexibility on the complexation behaviour, resorcinarenes and cavitands with carboxylic acid functionalities at the *upper rim* were prepared. As small chiral entities amino acids were chosen and the *C*- or *N*-protected enantiomers were attached covalently as amides. The enantiomerically pure macrocycles were characterised by CD spectroscopy.

4.1 Synthesis of Resorcinarenes Functionalised with Amino Acids

From the achiral resorcinarene with pendant isobutyl chains the methylated resorcinarene and the cavitand with carboxylic acid functionalities were prepared. The macrocyclic building blocks were synthesised according to literature procedures (Figure 4.1).[57–61] The scaffold **35** was obtained from the condensation reaction of resorcinol and 2-methylbutanal under acidic conditions. In a subsequent bromination reaction with NBS in chloroform the terabromoresorcinarene **36** was obtained. The methylation reaction was performed in DMF with NaH as the base and MeI as alkylation reagent. This tetrabromo compound **37** was reacted with *n*-BuLi and then with methyl chloroformate to yield the tetracarboxylic acid methylester **38**. After alkaline hydrolysis of **38**, the tetracarboxylic acid **39** was obtained in high yield.

The cavitand **40** was provided by reaction of bromochloromethane in DMF and K_2CO_3 as the base and transferred into tetracarboxylic acid cavitand **42** according to the procedures described for the methylated resorcinarene **39**.

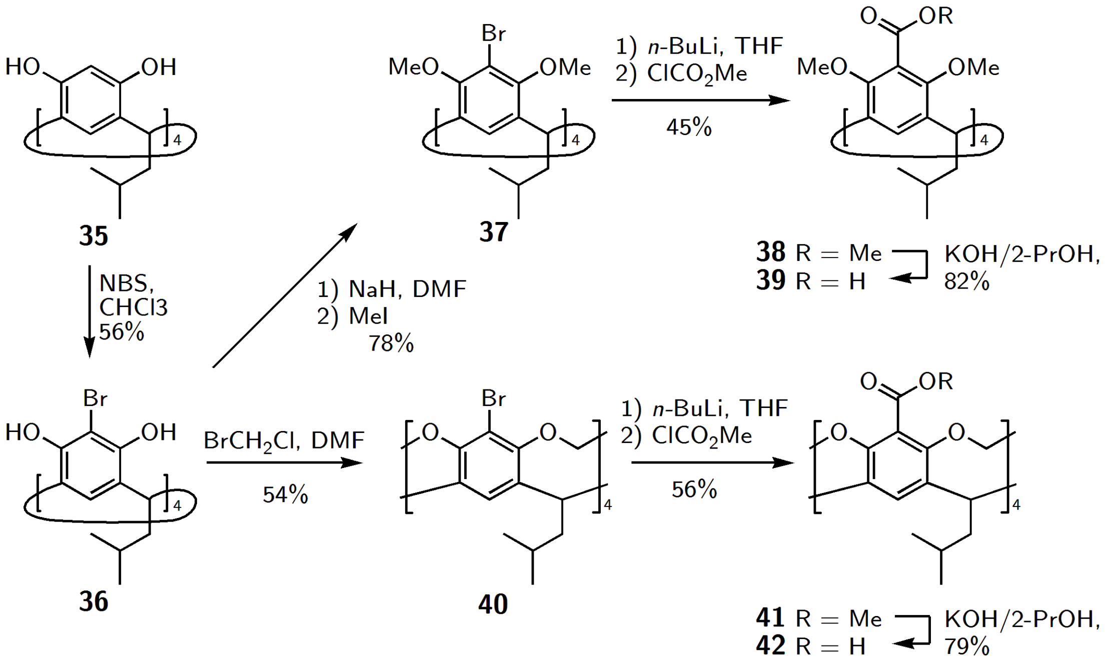
HO
OH
4
35
NBS,
CHCl3
56%
Br
MeO
OMe
4
37
1) NaH, DMF
2) MeI
78%
1) n-BuLi, THF
2) ClCO2Me
45%
O
OR
MeO
OMe
4
38 R = Me
39 R = H
KOH/2-PrOH,
82%
Br
HO
OH
4
36
BrCH2Cl, DMF
54%
Br
O
O
4
40
1) n-BuLi, THF
2) ClCO2Me
56%
O
OR
O
O
4
41 R = Me
42 R = H
KOH/2-PrOH,
79%

Figure 4.1: Preparation of the tetracarboxylic acid precursors **39** and **42**.

The amide formation was performed with TBTU as the activating agent[62] in combination with HOBt and triethylamine as the base. The reaction conditions were chosen according to peptide chemistry procedures[63] giving a racemisation free amide bond formation. After activation of the resorcinarene carboxy component **39** in DCM, 4.8 equivalents of (*S*)-phenylalanine methyl ester were added as hydrochloride salt under cooling with an ice bath. The extent of the reaction was monitored by MALDI-ToF MS.

Usually, the carboxy compound is used in an excess of 1.1 to 1.3 equivalents per functionality to ensure the completeness of the reaction. In this case the tetracarboxylic acid resorcinarene was reacted with an excess of amino component (Figure 4.2). This led to a statistical mixture of mono- and diamide residues at each carboxy functionality. The side products bore overall up to six residues as shown for **43** (Figure 4.3). With an equimolar amount of the carboxyl protected amino acid per carboxyl group **39** was reacted successfully to the tetrakisamido resorcinarene **44** (Figure 4.2).

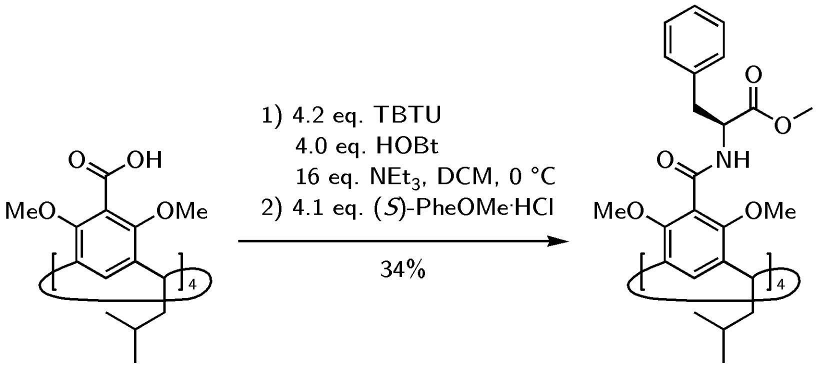
O
OH
MeO
OMe
4
1) 4.2 eq. TBTU
4.0 eq. HOBt
16 eq. NEt3, DCM, 0 °C
2) 4.1 eq. (S)-PheOMe·HCl
34%
O
O
O
NH
MeO
OMe
4

39 **44**

Figure 4.2: Resorcinarenes with amino acids.

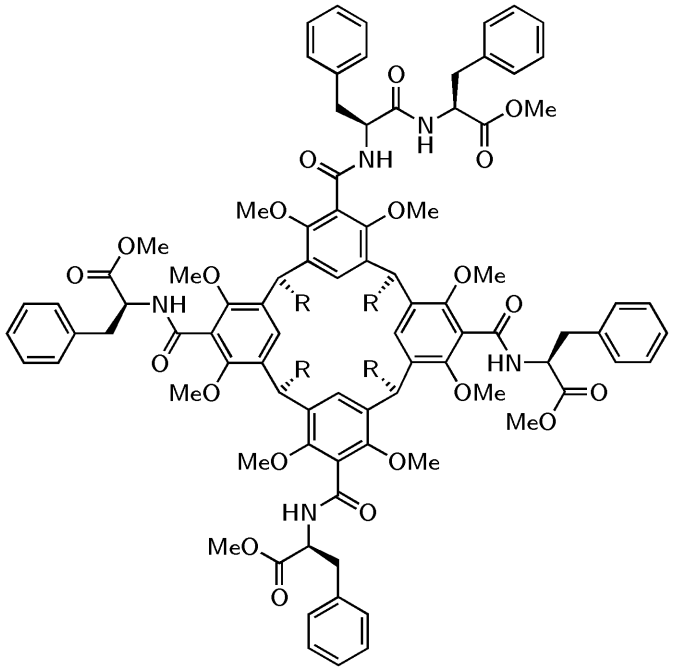
O
N
H
OMe
O
O
NH
MeO
OMe
OMe
O
MeO
NH
O
MeO
R
R
R
R
OMe
O
HN
OMe
O
MeO
MeO
OMe
HN
O
MeO
O

$R = C_4H_9$ **43**

Figure 4.3: Side product in the amide formation reaction with one additional (*S*)-phenylalanine residues.

The crude mixture was filtered through silica gel and the tetrakis-(*S*)-phenylalanine resorcinarene **44** was purified by HPLC. The enantiomer **45** was provided by the analogue reaction of **39** with (*R*)-phenylalanine methyl ester hydrochloride. Compounds **44** and **45** were obtained in moderate yields of 24% and 18%, respectively. The cavitand based resorcinarenes were synthesised according to the same protocol in yields of 34% for **46** with the (*S*)-phenylalanine residues and 22% for its enantiomer **47**. All prepared resorcinarenes and cavitands are displayed in Figure 4.4. Although the resorcinarenes and cavitands are sterically demanding, the chiral macrocycles were prepared in moderate yields. This opens up the way to peptidoresorcinarene conjugates with a short, rigid linker.

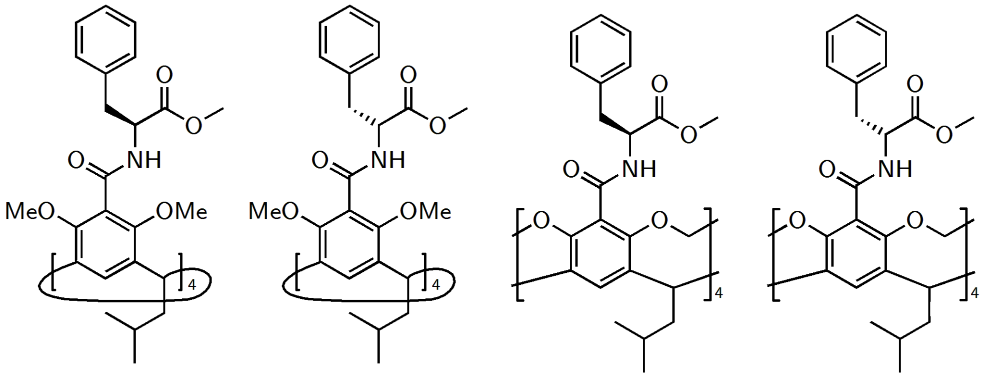

44 **45** **46** **47**

Figure 4.4: Prepared amidoresorcinarenes **44**-**47** from methylated resorcinarenes and cavitands.

The higher conformational flexibility of the resorcinarene compounds **44** and **45** becomes obvious when the NMR spectra in chloroform are compared to those of the cavitands **46** and **47**. On the NMR time scale there is a distinct set of signals for all proton resonances of the cavitand **46** (Figure 4.5 b) and some broad signals for the resorcinarene **44** like those of the methoxy groups H-14 and the aromatic proton H-3 (Figure 4.5 a). The broadened signals at room temperature indicate a slow interconversion between two boat conformations. In the rigid cavitand the protons of the bridging methylene groups H-14 give two doublets due to the anisotropic effect of the cavity at 4.51 and 4.87 ppm for the inner and the outer protons, respectively. The resonances of the phenylalanine residue protons are not shifted significantly if attached to the resorcinarene or to the cavitand (H-8, H-9, H-10-12, H-13), but the signal of the amide protons (H-7) occurring as doublet at 6.36 ppm in **46** does not emerge in the spectrum of the flexible compound **44**. Insight into the conformation of the chiral moieties is given by CD spectra that are discussed in the following section.

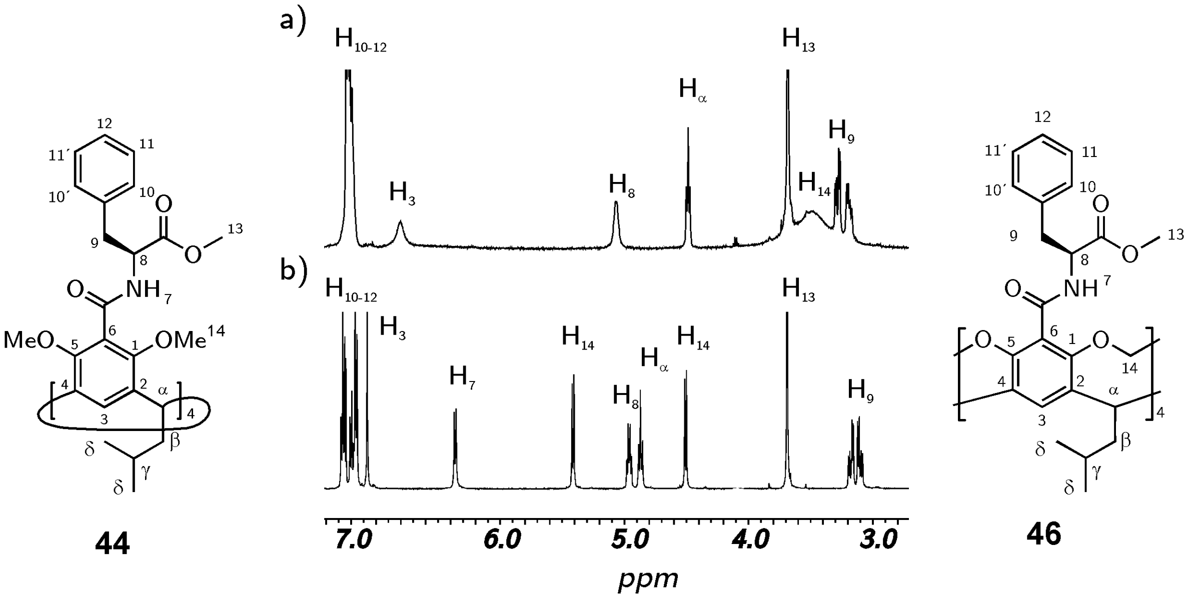

Figure 4.5: Partial ^{H}-NMR spectra (500 MHz) of **44** (a) and **46** (b) in CDCl$_3$.

4.2 Chiroptical Properties of the Amidoresorcinarenes and -Cavitands

The CD spectroscopic studies were carried out in acetonitrile as polar solvent that is transparent $>$ 195 nm and in chloroform that is less polar and transparent $>$ 225 nm. Due to different absorption properties the wavelength region between 200 and 230 nm (see Figures 4.6 and 4.7) cannot be compared. Both enantiomeric pairs of the tetrakisphenlyalanine resorcinarenes (**44** and **45**) and of the tetrakisphenylalanine cavitands (**46** and **47**) show mirror-inverted CD spectra in both solvents (Figures 4.6 and 4.7). The CD signals are overall very weak. Only below 250 nm there are positive absorption coefficients $\Delta\epsilon$ for the (*R*)-phenylalanine containing compounds and negative values for the compounds with moieties of (*S*) configuration that can be ascribed to the amide bond.[64]

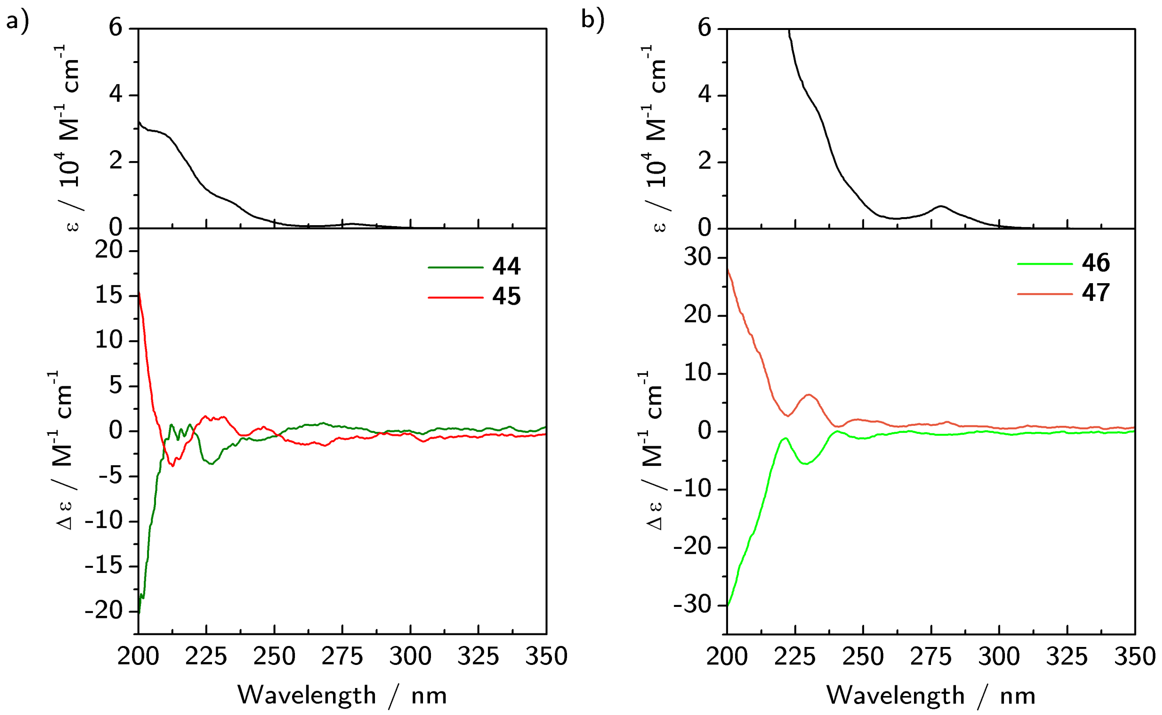

Figure 4.6: UV/Vis and CD spectra of resorcinarenes **44** and **45** (a) and cavitands **46** and **47** (b) in acetonitrile. (1×10^{-4} M).

The CD spectra gave no evidence for intramolecular hydrogen bonding involving the resorcinol units. The strength of the non-covalent interactions between the amide proton and the oxygen atoms of the methoxy groups is expected to be very low. Nevertheless there are very weak bisignate signals of the absorption band of 275 to 325 nm in the apolar chloroform solutions. These could arise from the interaction of the methoxy groups and the methylene bridges in the cavitand, respectively, with the chiral phenylalanine environment.

If the resorcinarene scaffold was influenced strongly by hydrogen bonds like in tetrabenzoxazine (Chapter 2, Section 2.2), the absorption band between 260 and 325 nm (UV/Vis spectra, Figure 2.8, p. 9) would give a significant CD signal. But no increased values for $\Delta\epsilon$ are obtained, neither in acetonitrile nor in chloroform. In an example of oxazine derivatives[39,40] there is an intramolecular hydrogen bonding pattern inducing inherent chirality. The direction is the result of the diastereomeric preference owing to the chiral residues at the upper rim.

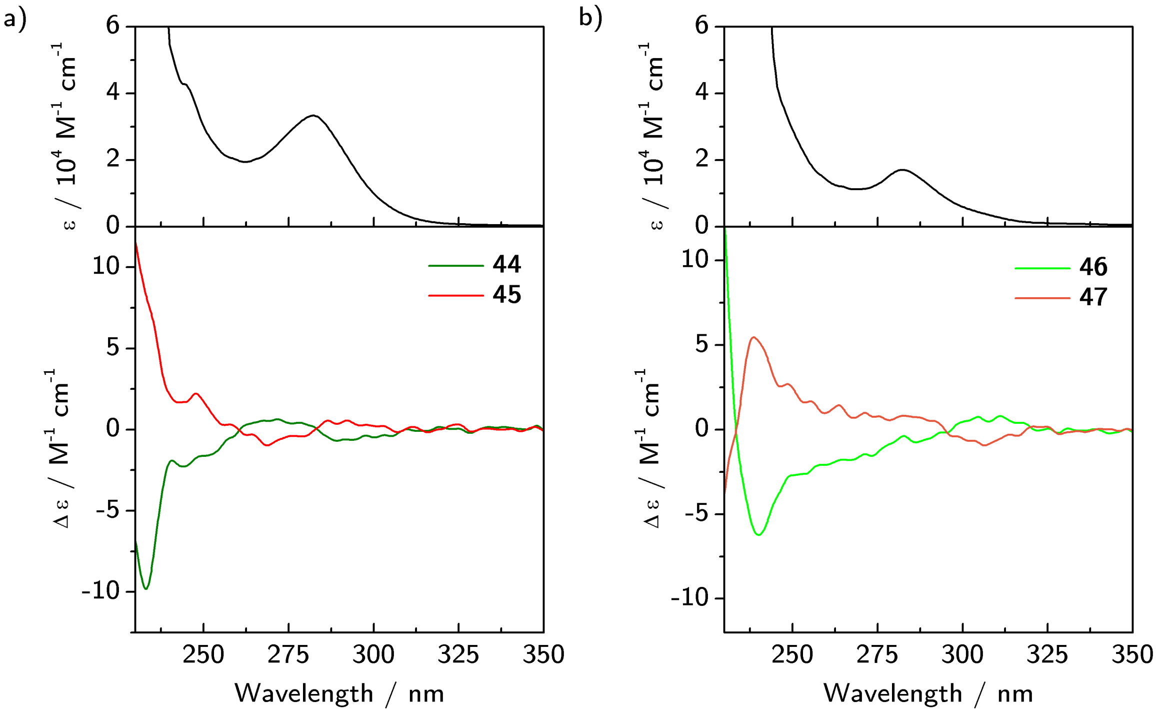

Figure 4.7: UV/Vis and CD spectra of resorcinarenes **44** and **45** (a) and cavitands **46** and **47** (b) in chloroform. (1×10^{-4} M).

The amidoresorcinarenes were shown to be of purely enantiomeric nature without inherent chirality. This is crucial to estimate the geometry in solution that is in these cases not a C_4 symmetric conformation. The CD signal originates from the chiral amino acid moieties. As the spectra are of significantly different shape the conformation changes depending on the solvent polarity.

4.3 Synthesis of Inherently Chiral Resorcinarenes Functionalised with Amino Acids

To the racemic, inherently chiral resorcinarenes four (*S*)-phenylalanine residues were introduced as *N*-Boc-protected esters. TBTU was used as activating agent in combination with HOBt and triethylamine as the base. The amino acid was suspended in DCM and the base was added under cooling with an ice bath. Then TBTU and HOBt were added for activation of the carboxyl group to form an active ester and the mixture was stirred for 1 h. At last, resorcinarene **48** was added dissolved in DCM. In the reaction the tetrakis-(*S*)-phenylalanine is obtained and the tris-esters as byproduct.

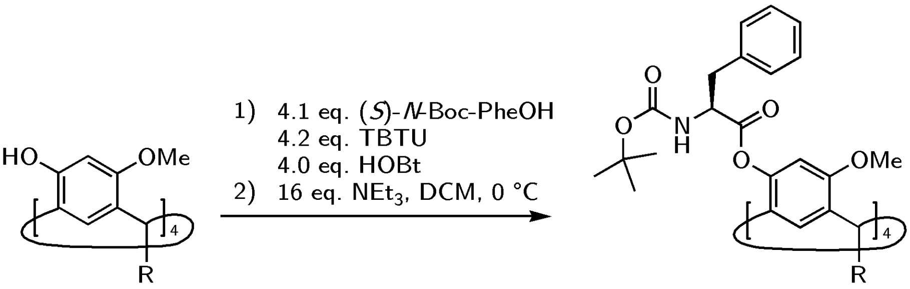

19 R = C_4H_9
48 R = $C_{11}H_{23}$

49a/b R = C_4H_9
50a/b R = $C_{11}H_{23}$

Figure 4.8: Reaction of inherently chiral resorcinarenes **19** and **48** with four (*S*)-*N*-Boc-protected phenylalanine residues. Only one of the diastereomers is displayed.

The tetrakis-(*S*)-phenylalanine diastereomers **50a** and **50b** are separable by HPLC from the tris-(*S*)-phenylalanine resorcinarenes as proved by ESI-MS spectra. Whereas the NMR spectrum shown in Figure 4.9 b indicates that the diastereomers **50a** and **50b** of the fourfold amide were not completely separated as there are minor signals for the H-9, H-7 and H-3 protons (see Figure 4.9 for assignment) that can be ascribed to the second diastereomer. The amide proton occurs as a doublet at δ = 4.98 ppm and at 5.06 ppm as well. From this spectrum the diastereomeric excess was derived as 44%.

For the purpose of a better diastereomer resolution the tetrakis-(*S*)-phenylalanine resorcinarene **49** was prepared with an isobutyl chain. A shorter alkyl chain decreases the solubility in nonpolar solvents like cyclohexane and enhances the separability. With this isobutyl alkyl chain the resolution was significantly improved. The first eluting diastereomer of **49a** and **49b** was enriched up to 85% that corresponds to *de* of 70% as determined by ^{1}H-NMR (Figure 4.9 a).

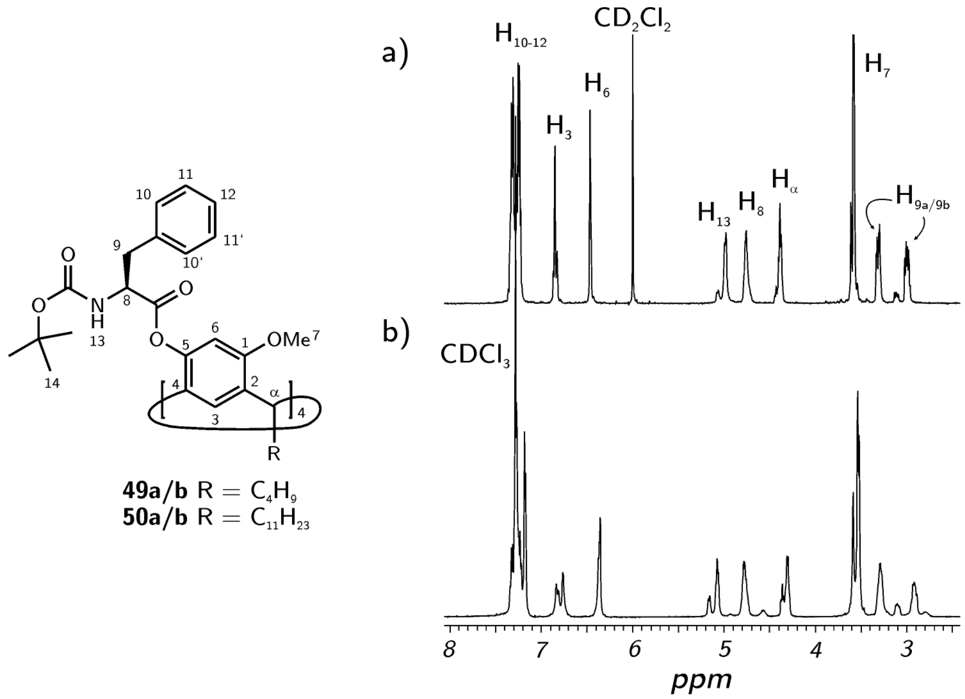

Figure 4.9: Partial ^{1}H NMR spectra (500 MHz) of the diastereomeric mixtures after HPLC separation. (a) **49** in CD_2Cl_2; (b) **50** in $CDCl_3$.

Conclusion and Outlook

Amidoresorcinarenes were prepared from achiral resorcinarene scaffolds with peptide bond formation procedures. The reaction conditions established for single amino acid building blocks may be transferred to reactions with polypeptide compounds. CD spectra of the resorcinarenes and the cavitands display weak Cotton-effects emerging from the phenylalanine residues. In MS experiments the complexation behaviour towards chiral guests will be investigated (see also Chapter 2, Section 2.3). The enantioselectivity of flexible resorcinarenes and the rigid cavitands bearing both the same chiral moiety can be directly compared in ligand exchange reaction measurements due to a mass difference of 64 amu (see also Chapter 6).

5 Cavity-Extended Chiral Resorcinarenes

Racemic, inherently chiral resorcinarenes were first resolved in 2003[44] and the absolute configuration was determined few years later.[43] To serve as artificial receptor, it is of great interest to find a synthetic approach to cavity-extended inherently chiral resorcinarenes with a well-defined shape that are stable towards moderate protic and alkaline conditions for complexation experiments. In this chapter the synthesis and characterisation of resorcinarenes extended with achiral building blocks is presented. The carbon scaffold with known absolute configuration of *rccc*-2,8,14,20-tetraisobutyl-4,10,16,22-tetra-*O*-methylresorcin[4]arene (**19**) was thus extended to a tetrabiaryl ether macrocycle (Section 5.1) *via* an intramolecular Pd-catalysed C-C bond formation. To introduce functional groups as potential binding sites into the chiral macrocycle, a tetrakisbenzyl ether with carboxylic acid ester functionalities was prepared (Section 5.1). The resolved simple tetrabiaryl ether cycloenantiomers were characterised regarding the conformation in solution by NMR- and CD-spectroscopy (Section 5.2, 5.3). The CD spectra were compared to those generated by time-dependent PARISER-PARR-POPLE (TDPPP) calculations based on the X-ray data (Section 5.2).

5.1 Synthesis of a Biaryl Motif

The preparation of a cavity-extended, inherently chiral resorcinarene can be realised starting from the well-characterised resorcinarene **19**. A racemate of the inherently chiral resorcin[4]arene *rac*-**19** was converted into diastereomers for the purpose of resolution. The protocol for this reaction was developed by MATTAY *et al.* for resorcinarenes with isobutyl residues in 2003.[44] In this section the route is only briefly presented as it is already described in literature.* The diastereomers of the monofunctionalised (*S*)-(+)-10-camphorsulfonic esters of the resorcinarenes with isobutyl residues **51a** and **51b** were resolved by silica gel HPLC. The hydrolysis of each diastereomer under strong alkaline conditions gave the enantiomerically pure compounds (*P*,*S*)-(+)-**19** and (*M*,*R*)-(–)-**19**.

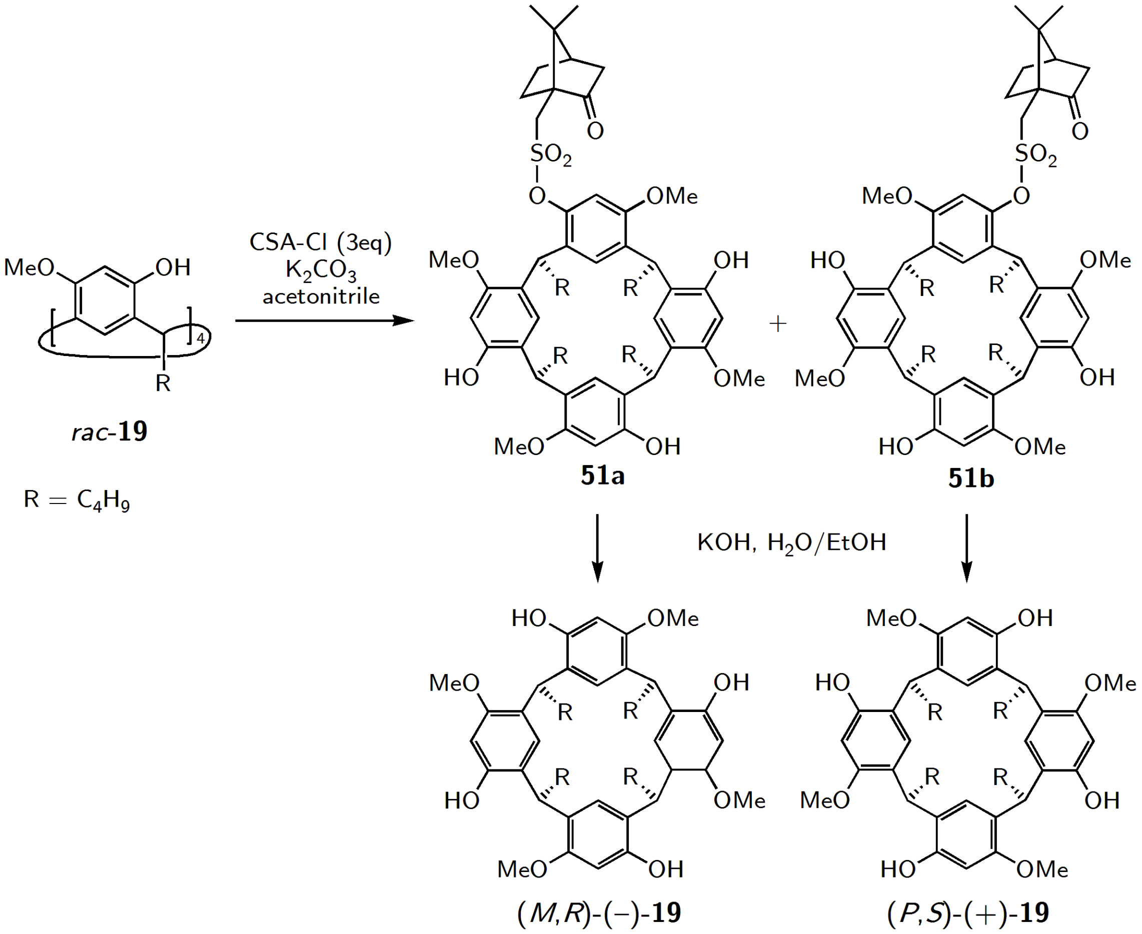
MeO
OH
4
R
rac-**19**
R = C_4H_9
CSA-Cl (3eq)
K_2CO_3
acetonitrile
SO_2
O
OMe
MeO
OH
HO
OMe
MeO
OH
R
51a
+
51b
KOH, H_2O/EtOH
(*M*,*R*)-(–)-**19**
(*P*,*S*)-(+)-**19**

Figure 5.1: Racemic resorcinarene *rac*-**19** was transferred into diastereomers **51a** and **51b** that were separable by HPLC. The auxiliary was removed under strong alkaline conditions to obtain the enantiomerically pure resocinarenes (*P*,*S*)-(+)-**19** and (*M*,*R*)-(–)-**19**.

With these enantiopure precursors in hand, the extended cavity resorcinarenes were built up successively on the base of these well-characterised scaffolds with known absolute configuration.[43] A synthetic challenge was to generate a covalent carbon skeleton within few steps on a smooth way without comprehensive modifications at the upper rim like the introduction of iodine,[57,65] boronic acid[66,67] or ester residues.[68] This can be achieved by an intramolecular direct arylation reaction of simple arenes published by the group of FAGNOU in 2004.[69,70] A preactivation of both arenes is not neccessary; one arene can go without a functional group. (Figure 5.2). According to this concept four bromobenzyl functionalities were introduced into the resorcinarene as 2-bromobenzyl ethers and reacted to the tetrabiaryl compound following the procedures for direct arylation of simple arenes (Figure 5.3). In the following the synthesis of a tetrakis(2´-bromobenzyl) ether resorcinarene and the cyclic tetrabiaryl ether are presented. The reaction conditions were developed for racemic resorcinarenes and then applied to the enantiomerically pure compounds.

---

* For novel inherently chiral resorcinarenes this resolution procedure was likewise applied and is discussed in detail in Chapter 6, Section 6.1.3.

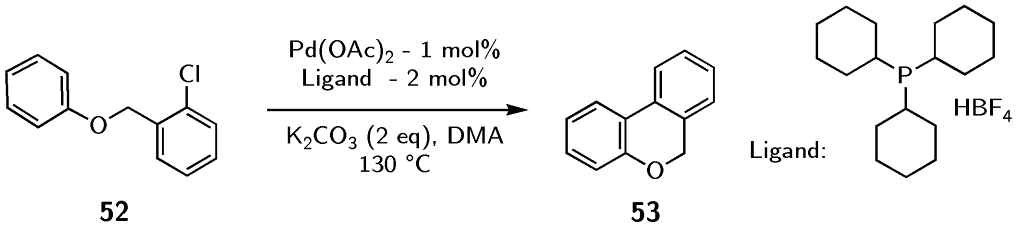

Figure 5.2: Reaction scheme of an intramolecular direct arylation reaction.[69,70]

Tetrakis(2´-bromobenzyl) ether *rac*-**54** was first prepared from *rac*-**19** and 2-bromobenzyl bromide (1.4–1.8 equiv. per functionality) in dry DMF in the presence of K_2CO_3 (8 equiv.) and were separated from the tris(bromobenzyl) ether by column chromatography to give 56% of rac-2. To improve the procedure, racemate *rac*-**19** was deprotonated with NaH (5 equiv. per functionality) in dry DMF to yield the phenolate salt, which was then treated with 2-bromobenzyl bromide (1.07 equiv. per hydroxy group) to give tetrakis(2´-bromobenzyl) ether *rac*-**54** (Figure 5.3). Recrystallisation from chloroform and methanol (4:1, v:v) yielded 84% of pure *rac*-**54**. The enantiomerically pure products were obtained following the same protocol and purified by column chromatography on silica gel to remove the excess amount of 2-bromobenzyl bromide. Compounds (*M*,*R*)-(–)-**54** and (*P*,*S*)-(+)-**54** were obtained in 92% and 72% yield, respectively.

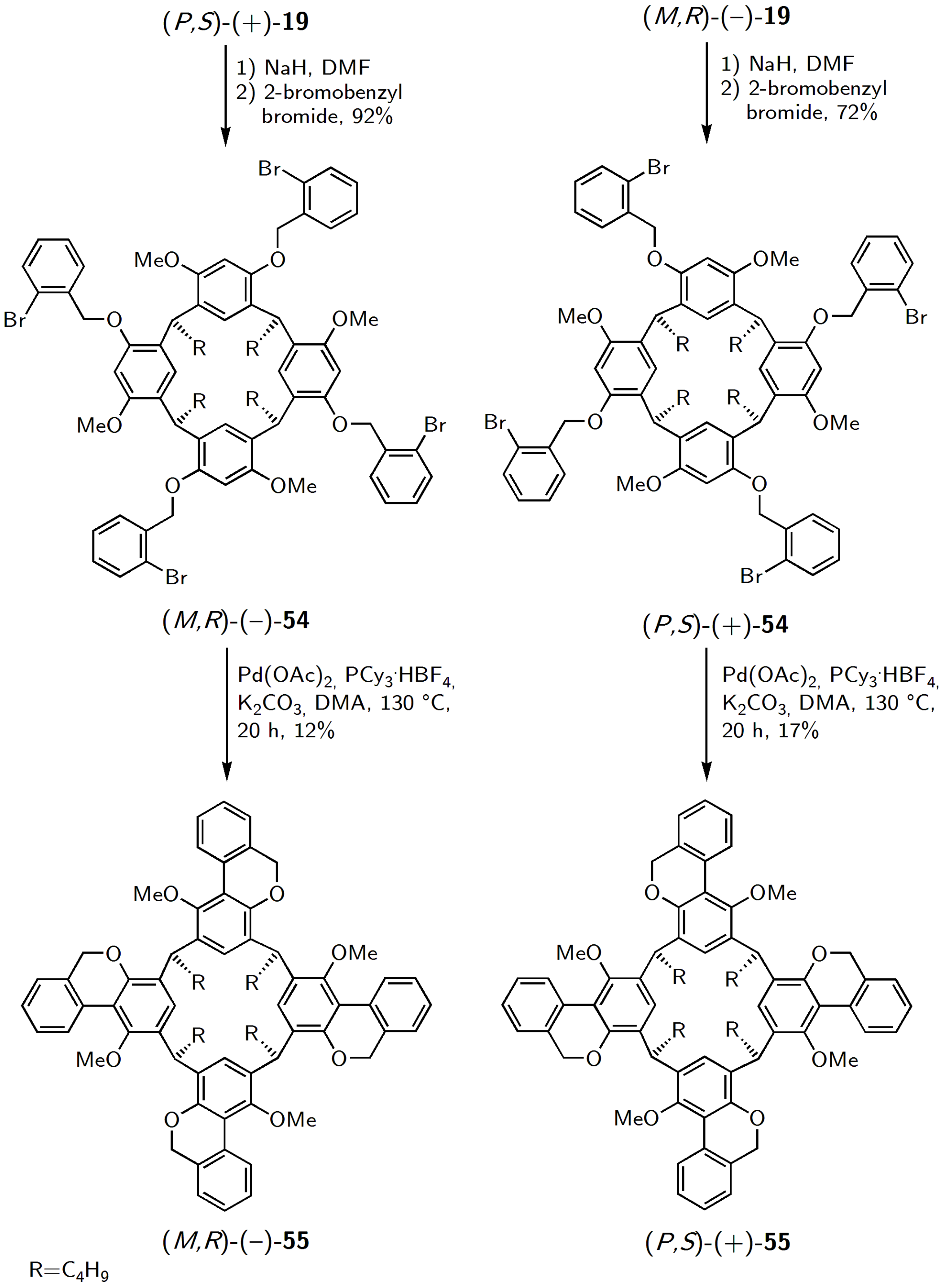
(P,S)-(+)-19
1) NaH, DMF
2) 2-bromobenzyl bromide, 92%
(M,R)-(−)-19
1) NaH, DMF
2) 2-bromobenzyl bromide, 72%
Br
MeO
O
OMe
R
(M,R)-(−)-54
(P,S)-(+)-54
Pd(OAc)2, PCy3·HBF4, K2CO3, DMA, 130 °C, 20 h, 12%
Pd(OAc)2, PCy3·HBF4, K2CO3, DMA, 130 °C, 20 h, 17%
(M,R)-(−)-55
(P,S)-(+)-55
R=C4H9

Figure 5.3: Reaction of **19** to tetrakis(2´-bromobenzyl)ether **54** and the cyclic tetrabiaryl ether **55**.

The subsequent coupling reaction of **54** according to the reaction in Figure 5.2 was firstly applied in the diploma thesis in 2006[71] giving low yields when using $Pd(OAc)_2$, $PCy_3 \cdot HBF_4$ and K_2CO_3 in DMA. To improve the yield the reaction conditions and especially the composition of the catalytic system were varied.

Two reasons for the low yield of the arylation reaction can be assumed; side reactions may occur e.g. with the additives or the macrocycle itself decomposes into smaller fragments. In the first case the phosphane-bound residue may take part in the coupling reaction. For haloarenes without steric hindrance it is known that triphenylphosphane undergoes an aryl-aryl interchange with palladium-bound aryls trough a phosphonium salt as intermediate.[72] This is suppressed by sterically demanding, low-donating substituents causing a slower rate of the oxidative addition.

Among the group of alkyl phosphanes a ligand presented by BUCHWALD[73] (see Figure 5.4) was investigated. The conditions as described above were applied in the reaction of **54**, whereas the BUCHWALD ligand **56** replaced the PCy_3 ligand. But no conversion at all was observed and the starting material **54** was recovered besides a very small amount of partially dehalogenated resorcinarene. The cyclohexyl moieties are relatively small but less donating than phenyl residues and therefore diminish the side reaction of transalkylation. Studies with various amounts of the phosphane ligand and $Pd(OAc)_2$, respectively, were carried out. Beside the peaks with *m/z* ratios corresponding to protonated PCy_3 and the tetrabiaryl product **55** no charged species like alkylated or phosphor substituted resorcinarenes were detected by ESI-MS independent from the ratio of added PCy_3. A transalkylation reaction can therefore be excluded.

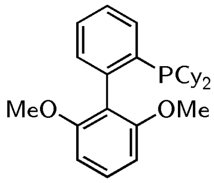

56

Figure 5.4: Ligand **56** developed by BUCHWALD.[73]

In the second case the influence of the counterion BF_4^- on the reaction was investigated, when PCy_3 was added as protonated phosphonium salt. The tetrafluoro borate ion could have led to decomposition of the resorcinarene by a Lewis acid catalysed reaction because of the reversibility of the formation reaction (see Chapter 2, Section 2.2). Surprisingly, no fragments of a decomposed tetramer were isolated and there was no difference in the yield adding the ligand PCy_3 as free phosphane or as HBF_4 salt. The low yield of the arylation reaction cannot be justified yet. The advantage of the $PCy_3 \cdot BF_4$ salt is the far better handling than that of PCy_3, as it is not hygroscopic and airstable towards oxidation.

As the catalytic system, $Pd(OAc)_2$ and PCy_3 (2 equiv.) were chosen; an amount of 30 mol-% per functionality was necessary to complete the reaction and K_2CO_3 (2 equiv. per functionality) was added as the base (Figure 5.3). The progress of conversion was followed by MALDI-ToF-MS. The gradual formation of the product was observed as a mixture of the mono, di, tri and tetrabiaryl compounds. After 20 h of heating at 130 °C in DMA, the only indicated *m/z* signals were 1122 $[M + H]^+$ and 1144 $[M + Na]^+$, which could be ascribed to tetrabiaryl ether *rac*-**55**. In the following, the motif that was build up is shortly denoted as biaryl ether. Resorcinarene *rac*-**55** was purified by column chromatography on silica gel (cyclohexane/ethyl acetate 95:5 (v:v)) to remove inorganic salts and catalyst residues. After recrystallisation from chloroform and methanol (4:1, v:v) the yield was 18% of the racemate; the enantiomerically pure resorcinarenes were obtained on the same reaction route in 12% and 17%.

Starting from compounds (*M*,*R*)-(–)-**19** and (*P*,*S*)-(+)-**19**, the absolute configurations of the scaffolds of (+)-**54** and (–)-**54** had changed owing to the introduction of the 2-bromobenzyl residues, which have a higher priority according to the CAHN-INGOLD-PRELOG rules (see Figure 5.3). Thus, the configurations of (+)-**54** and (–)-**54** were determined as (*P*,*S*) and (*M*,*R*), respectively, and in analogy, those of (+)-**55** and (–)-**55** were determined as (*P*,*S*) and (*M*,*R*).

The synthetic pathway described above offered a new approach to inherently chiral scaffolds. In order to introduce functionalities suitable for complexation experiments a derivative with carboxylic acid methyl ester residues was synthesised. The ester functionalities can be easily transferred into a tetracarboxylic acid.

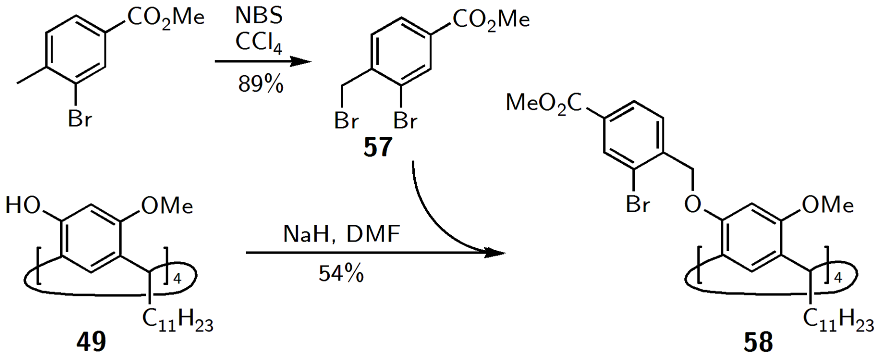

Figure 5.5: Reaction of the inherently chiral resorcinarene with methyl 3-bromo-4-(bromomethyl)benzoate.

For this purpose benzyl ether **58** was synthesised (Figure 5.5), containing a carboxy methyl ester functionality in the 4-position and a bromo substituent in 2-position. The benzoic ester precursor was prepared from methyl 3-bromo-4-methylbenzoate that was reacted with NBS to give **57** in high yield.[74] A subsequent coupling reaction was accomplished under the same conditions as described for tetrabiaryl ether **55**, but without any conversion to a cross-coupling product. The starting material was recovered and traces of the carboxylic acid were detected by MALDI-ToF-MS in the negative ionisation mode. The conditions were systematically altered with regard to the composition of the catalytic system, the base and the solvent. An extended resorcinarene of the cyclic biaryl type with four ester functionalities was not obtained.

A second approach to cavity-extended resorcinarenes with functional groups follows a completely different synthetic route. The scaffold of the extended resorcinarene is not build up successively, but directly from a resorcinol monoalkyl ether (Route I, Figure 5.6) or a cyclic biaryl ether as monomer building block (Route II). A C_4-symmetric skeleton is prepared in a $BF_3 \cdot Et_2O$ catalysed cyclisation of monoalkyl resorcinols like 3-(benzyloxy)phenol and an aldehyde.[42] (see Section 2.2). Here in this case, the analogon 3-(2-bromobenzyloxy)phenol (**59**) was reacted with either an aldehyde or a dimethyl acetal but providing no reasonable yields of a macrocycle.

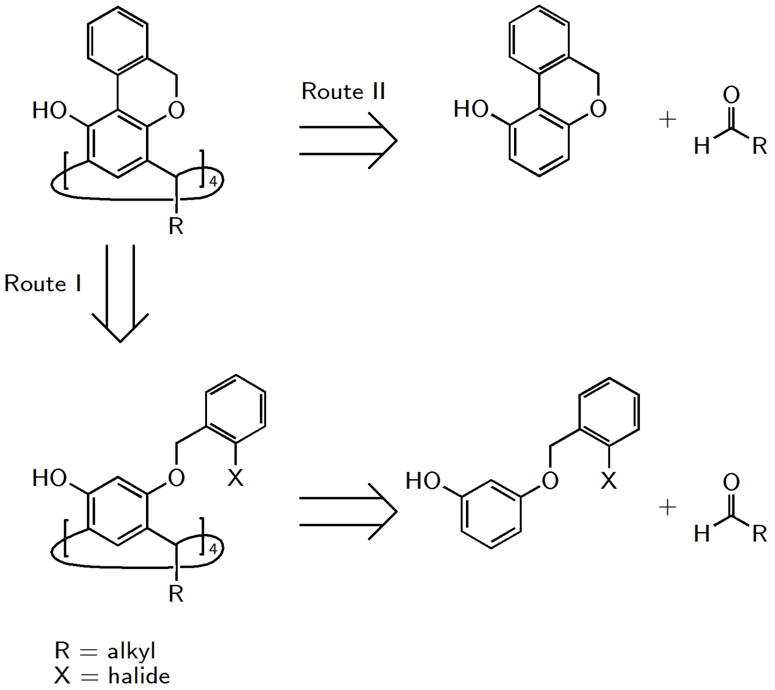

Figure 5.6: Retro synthetic scheme of biarylether formation reactions.

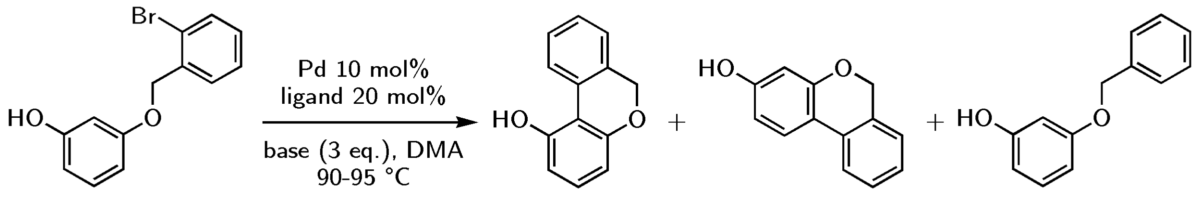

59 **60** **61** **62**

Figure 5.7: Intramolecular coupling reaction of 3-(2-bromobenzyloxy)phenol (**59**) (DMA, 90-95 °C, 18 h). The palladium salt (10 mol%), the ligand (20 mol%) and the base (3 eq.) were varied as described in Table 5.1.

The cyclisation reaction of a biaryl system as monomeric compound is possibly a different way to a tetrabiaryl ether resorcinarene. Up to date there are no examples in literature. For this purpose a monomeric biaryl ether was generated. A simple biaryl system is 3-hydroxy-6-benzo[*c*]chromen (**60**) obtained by the palladium catalysed coupling reaction of 3-(2-bromobenzyloxy)phenol (**59**) (Figure 5.7). The reaction conditions were originally published by RAWAL[75] and were modified in test runs as described in Table 5.1. The relative conversion of all test runs was analysed by gas chromatography. The phenol **59** is deprotonated by the base leading to a preferential carbon-carbon bond formation in the *ortho* and *para* position to the hydroxy group, providing **60** and **61**, respectively (Figure 5.7). A side reaction is the dehalogenation of the bromo moiety (**62**), especially occurring when the hygroscopic base *t*-BuOK was used (Table 5.1, Entries 3, 4, 6). Both reaction conditions of Entries 7 and 9 gave the 3-hydroxy-6-benzo[*c*]chromen **60** in 100% conversion and in excellent selectivity. The reaction of Entry 9 was realised on a gram scale.

The monomeric building block **60** was reacted with 2-methylbutanal and with the corresponding dimethyl acetal, respectively. The aim was the formation of a C_4-symmetric resorcinarene as shown in Figure 5.8. The progress of the reaction was monitored by TLC. All spots on the thin layer chromatogram were analysed by MALDI-ToF-MS. For several spots with different retention factors the same m/z ratios were recorded that correspond to the mass of a protonated, tetrameric compound $[M+H]^+$. That points to the formation of several isomers with different constitutions. These tetrameric isomers are probably of 1,2-*alternate*, 1,3-*alternate*, *chair* and *crown* conformation (see Figure 2.1 in Section 2.1, ??). The asymmetric substitution pattern of the resorcinol monomer **60** gives rise to the formation of regioisomers, likewise existing in the mentioned conformations. All the isomers were not separable by chromatographic methods. The cyclisation reaction is therefore not suitable for the preparation of a

Entry	Cat.	Ligand	Base	**59**	**62**	**60**	**61**
1	$Pd(OAc)_2$	$PCy_3{\cdot}HBF_4$	K_2CO_3		3	68	29
2	$Pd(OAc)_2$	PPh_3	K_2CO_3			37	63
3	$Pd(OAc)_2$	$PCy_3{\cdot}HBF_4$	*t*-BuOK		20	80	
4	$Pd(OAc)_2$	PPh_3	*t*-BuOK		32	58	10
5	$Pd(PPh_3)_4$	-	K_2CO_3	68	2	30	
6	$Pd(PPh_3)_4$	-	*t*-BuOK		39	54	7
7	$Pd(OAc)_2$	**56**	K_3PO_4			100	
8	$Pd(OAc)_2$	**56**	K_2CO_3	66	4	23	7
9	$Pd(OAc)_2$	$PCy_3{\cdot}HBF_4$	K_3PO_4			100	
10	$Pd(OAc)_2$	**56**	*t*-BuOK		8	92	

Table 5.1: Test runs carried out in DMA at 90-95 °C, 18 h. The reactions were quenched with water and acidified to pH 2; the aqueous layers were extracted with Et_2O and the conversion was analysed by gas chromatography.

C_4-symmetric tetramer from **60**.

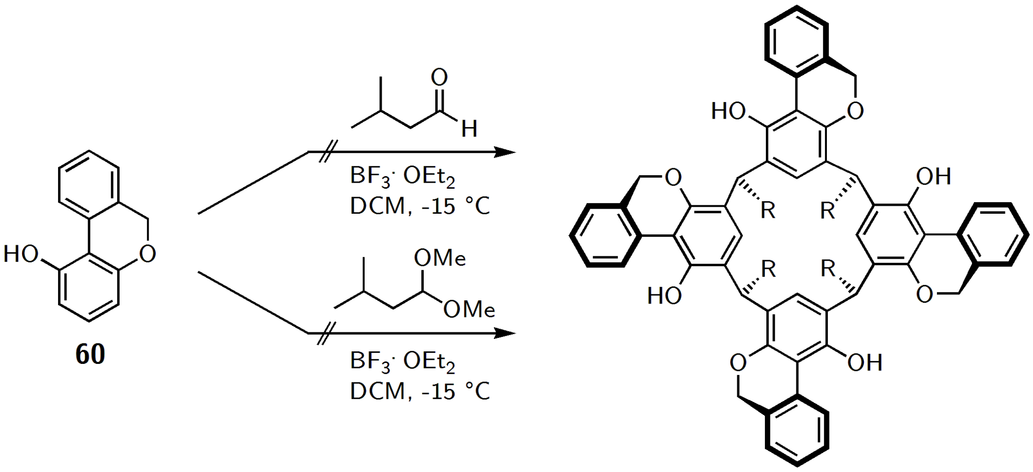

60

R = C_4H_9 **63**

Figure 5.8: Attempts of a cyclisation reaction according to the synthesis of C_4-symmetric resorcinarenes.[41,42]

In conclusion, the sterically demanding resorcinarene **54** was successfully reacted to a tetra-biaryl resorcinarene **55** by direct arylation. Four new carbon-carbon bonds with new chiral axes were generated simultaneously. The configuration of these axes in both enantiomers was elucidated by X-ray analysis, NMR spectroscopy and CD spectroscopy as described in the following sections.

5.2 Crystal Structures and Conformational Analysis

The crystal structure of **55** shows the extended resorcin[4]arene in the boat conformation of the resorcinol scaffold (Figure 5.9). The triclinic crystals of the racemic P$\overline{1}$ space group comprise the two cycloenantiomers. This differs from the enantiomerically pure compounds precipitating each not as single crystalline compounds.

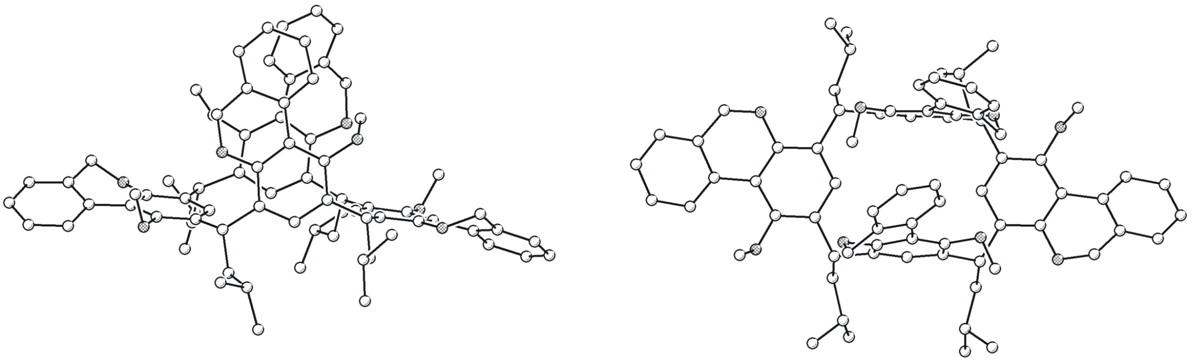

Figure 5.9: Crystal structure of tetrabiaryl ether resorcin[4]arene (*M*,*M*,*M*,*P*)-(*M*,*R*)-(–)-**55**. View along the chiral axis of the inherently chiral scaffold. Carbon atoms are shown as colourless circles and oxygen atoms as hatched circles. Hydrogen atoms are omitted for clarity.

The biaryl ether scaffold builds up four new atropisomeric units, which leads to the potential diastereomeric nature of **55**. In the solid state, the dibenzopyran units are twisted between 19.6° and 22.3° owing to the nonplanar ether bridges that have dihedral angles between 54.5° and 58.4°. On the basis of the configuration of the methylene bridges of **19**, the relative configuration can be derived as (*M*,*M*,*M*,*P*) for (*M*,*R*)-(–)-**55** and as (*P*,*P*,*P*,*M*) for (*P*,*S*)-(+)-**55**. The biaryl ethers with opposite axial chirality are located in the parallel arranged resorcinol residues. Each methoxy group points in the same direction as the methylene ether bridges of the dibenzopyran units.

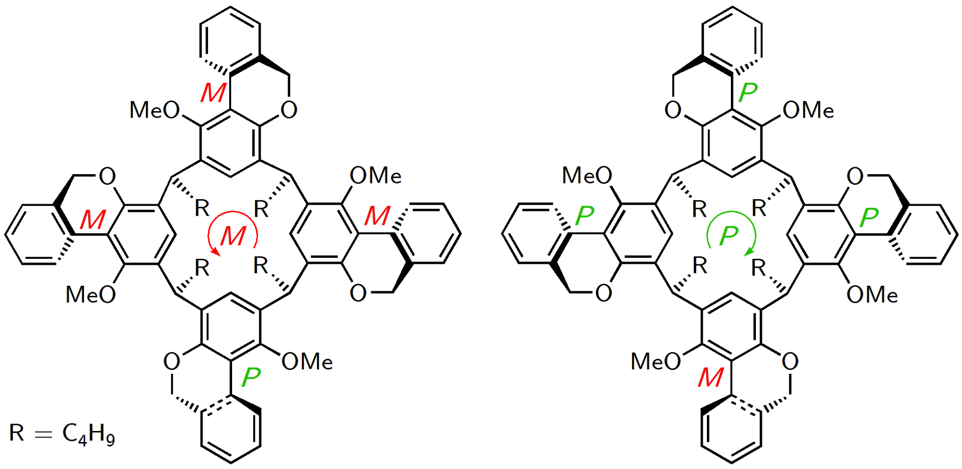

(*M*,*M*,*M*,*P*)-(*M*,*R*)-(−)-**55** (*P*,*P*,*P*,*M*)-(*P*,*S*)-(+)-**55**

Figure 5.10: Assignment of the new stereocenters in **55** according to the X-ray structure.

Compound **55** containing four stereogenic bridging carbon atoms and four atropisomeric biaryl units was hence found to be of enantiomeric character. The boat conformation should give rise to two sets of resonance signals for the aromatic protons in the ^{1}H NMR spectrum; however, the cavity of **55** is not fixed in this conformation in solution. Instead, the C_4 symmetry of **55** can only be assumed on the basis of an averaged data set on the NMR timescale (Figure 5.11). The ^{1}H and ^{13}C NMR resonance signals were assigned by means of 1D and 2D NMR experiments (COSY, HMBC) (Figure 5.11).

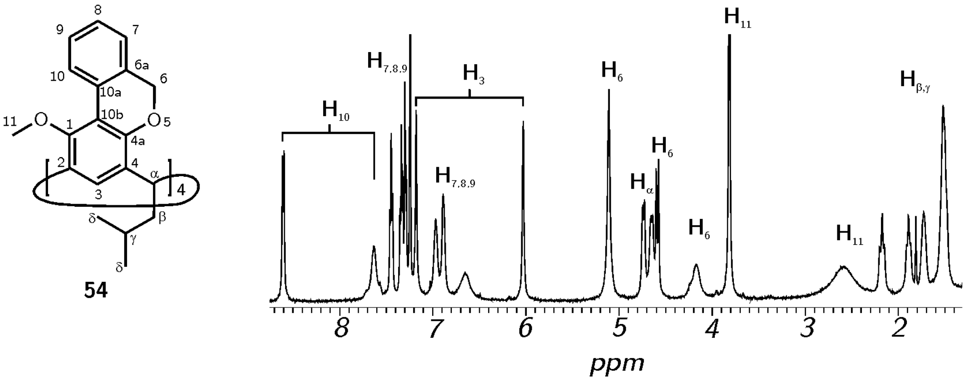

Figure 5.11: The designation of the carbon and hydrogen atoms of **55** for NMR spectroscopic studies. Partial ^{1}H-NMR spectrum (500 MHz) of biaryl ether resorcinarene **55** at 213 K in $CDCl_3$.

At room temperature, the signals are slightly broadened and the multiplets are not resolved properly (Figure 5.12 a, assignments see Figure 5.11). With increasing temperature up to 330 K (Figure 5.12 b-d), the resonances convert into definite singlets or multiplets, as can be seen for the methoxy groups at δ = 3.26 ppm, the ether bridge protons at δ = 4.63 and 4.84 ppm, the aryl protons at δ = 6.73 ppm and 8.13 ppm and the diastereotopic protons of the methylene unit of the alkyl chain at δ = 1.78 and 1.84 ppm (Figure 5.11). The ether bridges show two doublets for each proton at δ = 4.85 and 4.64 ppm, respectively, which was already observed for the diastereotopic protons of 2 at δ = 5.03 and 4.82 ppm. Hence, for the observed doublets of **55**, there are two possible effects on the benzylic protons resulting in that motif. Either the anisotropic effect of the inherently chiral cavity is very strong and helimerisation of the biaryl units is too weak for monitoring by NMR spectroscopic techniques or the ether bridge is configurationally stable and consequently no interconversion occurs. The methoxy group is sterically demanding and the high grade of substitution prohibits free rotation around the C_{Ar}-O-bond. The stability of the chiral axes in cyclic ether atropisomers is known for several benzonaphthopyran compounds.[76] At higher temperature, the doublets are resolved sharply, which supports the assumption of a strong anisotropic effect. Fast helimerisation should lead to a broadened signal for each proton. Low-temperature NMR spectroscopic studies were carried out in 1:1.5 mixtures of $CDCl_3$ and CD_2Cl_2 due to solubility of the sample. The NMR spectrum shown in Figure 5.12 was measured in deuterated chloroform. The interconversion of the two boat conformers becomes slow and a coalescence point is observed at T_c = 263 K. Below this temperature, signals separate into two sets that can be ascribed to the fixed boat conformation. The resonance signals were assigned by NOESY experiments at 203 K. The free enthalpy $\Delta G^{\ddagger}_{c}$ for this interconversion was calculated by the following equation, where $\Delta\nu$ is the resonance shift difference in Hz.[77]

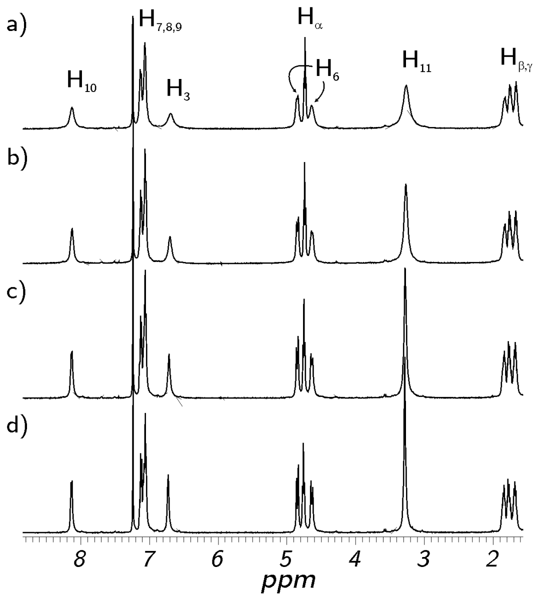

Figure 5.12: Partial 1H NMR spectra (500 MHz) of biaryl ether resorcinarene **55** at (a) 300 K; (b) 310 K; (c) 320 K; and (d) 330 K in $CDCl_3$.

$$\Delta G^{\ddagger}_{c} = 19.1\ T_c\ (9.97 + \log T_c - \log \Delta\nu)$$

The complete freezing of the dynamics may not have been reached, and therefore, the shift difference maxima of the aromatic 3-H and 10-H protons and of the methoxy groups were used. The energy barrier $\Delta G_c^\ddagger$ was calculated to be 48.4 kJ mol^{-1}. A very slow interconversion of the boat conformations at low temperature minimises the anisotropy for the coplanar arene units; however, the NMR spectroscopic experiments did not allow an unambiguous interpretation of the resonance signals for the protons of the ether bridge between 5.2 and 4.1 ppm and for those of the *ortho* aryl position, which is referred to as diastereoisomerism of the nonplanar pyran units. In conclusion, the anisotropic effect of the inherently chiral scaffold is adopted as the main cause for the different resonance signals, whereas a stable configuration of the atropisomers cannot be excluded.

5.3 Chiroptical Properties of the Tetrabiaryl Ether

The UV and CD spectra of the enantiomeric pair of **55** were measured in the nonpolar solvent cyclohexane and show almost perfect mirror images (Figure 5.13). The absolute configuration of the macrocyclic scaffold can be deduced from the starting material, but the introduced chiral axes may change their configuration of the atropisomeric axes in solution depending on the temperature. The mirror images are a first hint on their enantiomeric nature. If there were different axial configurations, the diastereomers would possibly give shifted absorption maxima. Only little is known about rotational barriers of cyclic biaryl ethers of the pyran type.[76] The racemisation of the atropisomers can take place within hours at room temperature depending on the *ortho* substituents, or it can be completely suppressed.

The configurations of the biaryl units in solution are not known and the simulation of the CD spectra was performed by STEFAN GRIMME on the basis of the X-ray data. The CD spectra of (*M*,*R*)-(−)-**55** with the (*M*,*M*,*M*,*P*)-configuration were generated by means of time-dependent PARISER-PARR-POPLE (TDPPP) calculations,[78,79] which included only the π-electrons of the basic biaryl ethers (Figure 5.3).

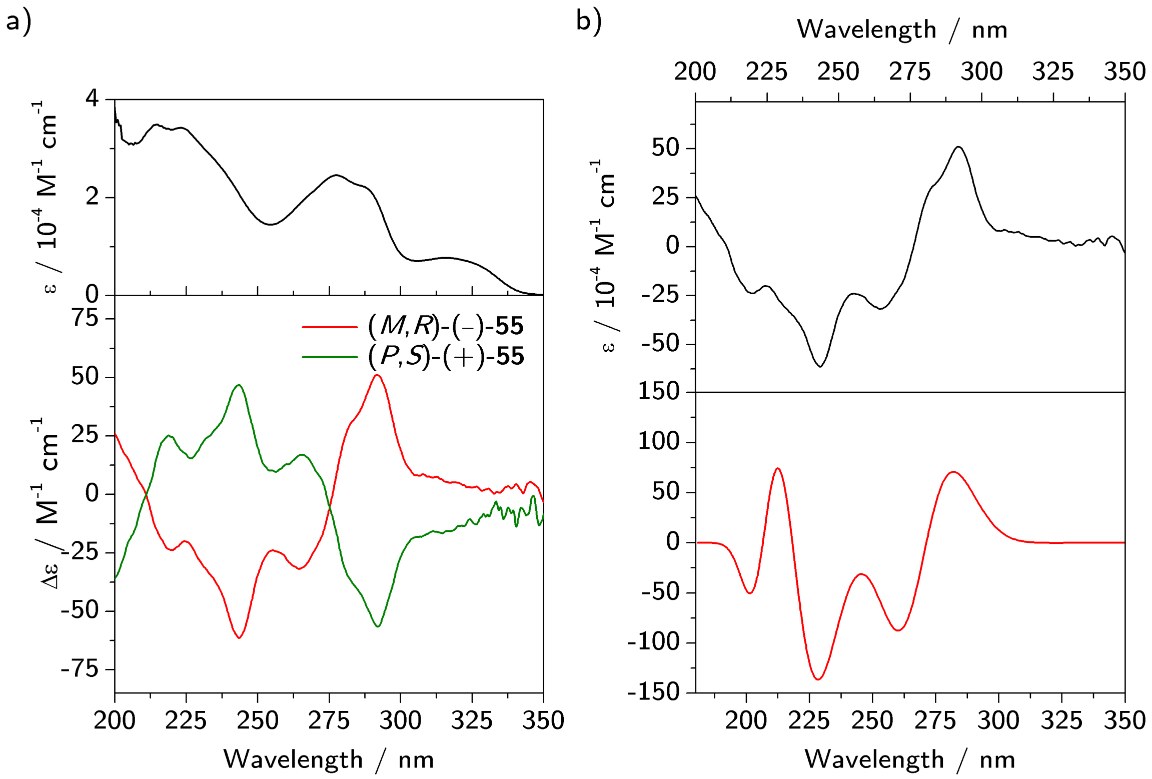

Figure 5.13: UV/Vis (top) and CD spectra (bottom) of *rac*-**55** and enantiomerically pure tetrabiaryl ether resorcin[4]arenes (*M*,*R*)-(−)-**55** and (*P*,*S*)-(+)-**55**, respectively (a). The measurements were carried out in cyclohexane at ambient temperature. CD spectrum (b) of (*M*,*M*,*M*,*P*)-(*M*,*R*)-(−)-**55** generated by TDPPP calculations (black line) and the experimentally obtained spectrum (red line).

TDPPP calculations gave very good reproduction of the experimental data. Compared to the experimental spectrum, the theoretical excitation energies merely seem to be slightly shifted to shorter wavelengths. This may originate from different average structures of the experimental spectra and the X-ray data; the CD spectra were recorded at room temperature and the diffraction data are recorded at 100 K. Analogous simulations of the CD signal with different dibenzopyran and methoxy configurations resulted in significantly differing spectra. As compounds (*M*,*R*)-(−)-**55** and (*P*,*S*)-(+)-**55** are enantiomers in the crystal structure and show mirror images in their CD spectra, they are denoted as cycloenantiomers.

Conclusion

The biaryl motif was build up on the scaffold of the inherently chiral resorcinarene *via* an intramolecular cross-coupling reaction, generating four new chiral axes. The relative configuration of the biaryl axes was determined based on the absolute configuration of the scaffold. CD spectra, NMR investigations and a theoretical simulation of the CD signal gave insight into the configuration of all stereogenic centers in the macrocycle and the resorcinarenes were disclosed as cycloenantiomers.

6 Chiral Resorcinarenes as Receptors for Chiral Molecular Recognition

As a suitable system to investigate the kinetic enantioselectivity in the gas phase, a labelled and non-labelled pair of resorcinarene enantiomers (*quasi*-enantiomers, for explanation see Glossary, p. 107) was chosen. The labelled resorcinarene was prepared from a terminally deuterated, aliphatic aldehyde (Section 6.1). The chromatographic resolution of the macrocycles as diastereomers with the auxiliary (*S*)-(+)-10-camphorsulfonic acid and the chiroptical properties of the enantiomers are presented in Sections 6.1.3 and 6.2. *Quasi*-diastereomeric adducts were generated by ESI from solutions containing the *quasi*-racemate and the chiral guest. The true gas phase replacement experiments were performed in an ICR cell with several amines as reacting gas. The enantioselectivities are discussed in Section 6.3. In NMR studies in solution, two host-guest systems were investigated regarding their complexation properties (Section 6.4). The coordination complexes of the resorcinarene and tyrosinol were analysed by DFT calculations (Section 6.5).

6.1 Synthesis of Chiral Resorcinarenes

To investigate kinetic enantioselectivity by means of mass spectrometry, inherently chiral resorcinarenes were prepared with different molecular masses. The gas phase experiments require a mass difference giving a sufficiently resolved isotope pattern of the two enantiomers. Due to the deuterium-labelling of one enantiomer, its mirror image is non-superimposable with the other enantiomer. These chiral entities are denoted as *quasi*-enantiomers if one of them is physically different, e.g. in the isotope constitution (see Glossary, p. 107).[54,80] The structural constitution, the size and the surface of the involved binding sites in a complexation process should be affected only by a minimum upon deuteration.

The proposed binding sites of inherently chiral resorcinarenes in complexes with chiral and achiral charged guests are the four hydroxy and the four methoxy groups as well as the cavity itself establishing cation-π-interactions.The orientation of the guests on the upper aromatic cavity is further favored by the presence of very long aliphatic alkyl chains on the opposite side which constitute a second, but apolar cavity. Apart from the upper rim the lateral chains are appropriate to introduce a terminally labelled group (Figure 6.1).

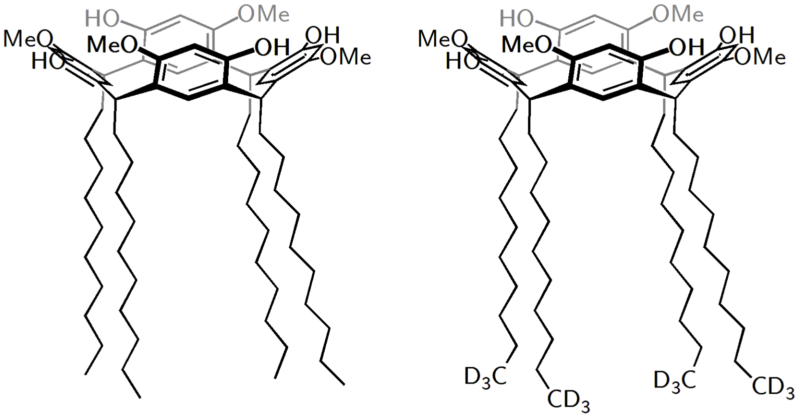

Figure 6.1: labelled and non-labelled resorcinarenes with aliphatic lateral chains.

As described in Chapter 2, Section 2.2 the resorcinarenes are synthesised from 3-methoxyphenol and an aliphatic aldehyde that introduces the lateral chains. The alkyl chain was terminally functionalised with a deuterated methyl group. The mass difference sums up to 12 atomic mass units of the tetramer and allows the simultaneous measurement of the reactivity of the *quasi*-diastereomeric complexes with a given chiral guest in the absence of any significant isotope effects. The length of the alkyl chain depends on the suitable starting material as there are propanal as shortest and undecanal as longest aldehyde reported in literature.[41,42]

6.1.1 Synthesis of a Labelled Aldehyde

In an aliphatic, labelled aldehyde there are two functionalities necessary to build up the target molecule. The aldehyde group can be obtained from a selective reduction of an ester with e.g. DIBAL-H, or an oxidation of an alcohol or an alkene functionality (Figure 6.2). A protecting group for the aldehyde functionality is e.g. a dialkyl acetale. The second functional group serves as precursor for a labelled alkyl residue. The strategy was to generate a terminally labelled alkyl residue *via* an alkyl-alkyl cross-coupling reaction. This can either be achieved in a substitution reaction or in a catalysed reaction of alkyl halides. The reagent of choice was MeMgI-d_3 that is commercially available as solution in Et_2O.

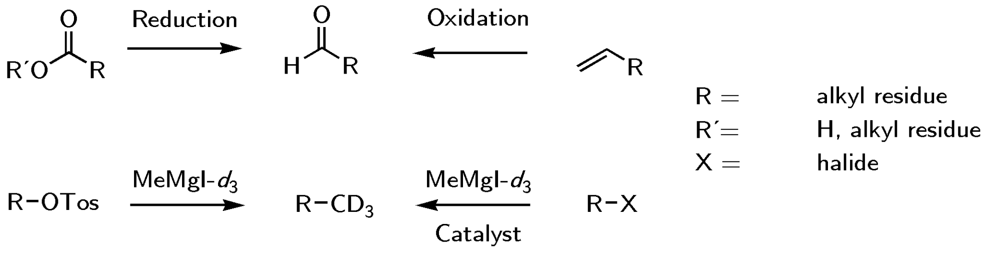

Figure 6.2: Scheme of the synthetic key steps in the preparation of a terminally labelled aldehyde.

In first attempts, the preparation of terminally deuterated heptanal was started from ϵ-caprolactone (**64**). The lactone was reacted in methanol to methyl 6-hydroxyhexanoate (**65**) under acidic conditions. The free hydroxyl group was transferred into tosylester **67** and into methyl 6-bromohexanoate (**66**), respectively. In a following step bromoester **66** was reduced to the corresponding aldehyde **69** with DIBAL-H at -90 °C in Et_2O and DCM in good yield. The additive $MgBr_2 \cdot Et_2O$ was originally used as chelating agent in a regioselective reduction of malic acid derivatives.[81] Although in **66** there are only the ester and the bromoalkane functionalities, the salt is necessary to run the reaction to completeness and to obtain the aldehyde free of side products. The aldehyde **69** was transferred into the dimethyl acetale **70** by standard procedures. From the subsequent reaction step to an aldehyde with MeMgI-d_3 solution in Et_2O the starting material was recovered and no other products were detected by GC-MS.

The tosylate **67** was reacted with MeMgI-d_3 solution in Et_2O as well as with MeLi-solution on a second route. In both cases the tosyl group was substituted by iodide (**68**); in the first reaction this is not surprising as the GRIGNARD reagent contains a magnesium complex with iodide. In the latter case the carbanion was generated from MeI and lithium. The halide anion that is still in the solution was more reactive than the alkyl anion. If the methyl group was introduced, the ester would have been reduced with DIBAL-H according to the literature procedure.[81]

Besides the synthesis of labelled heptanal a synthesis for labelled undecanal was developed. The strategy was to transfer a functionalised alkene into a terminally labelled alkene *via* an alkyl-alkyl cross-coupling reaction. For labelled dodecene the synthesis was previously reported

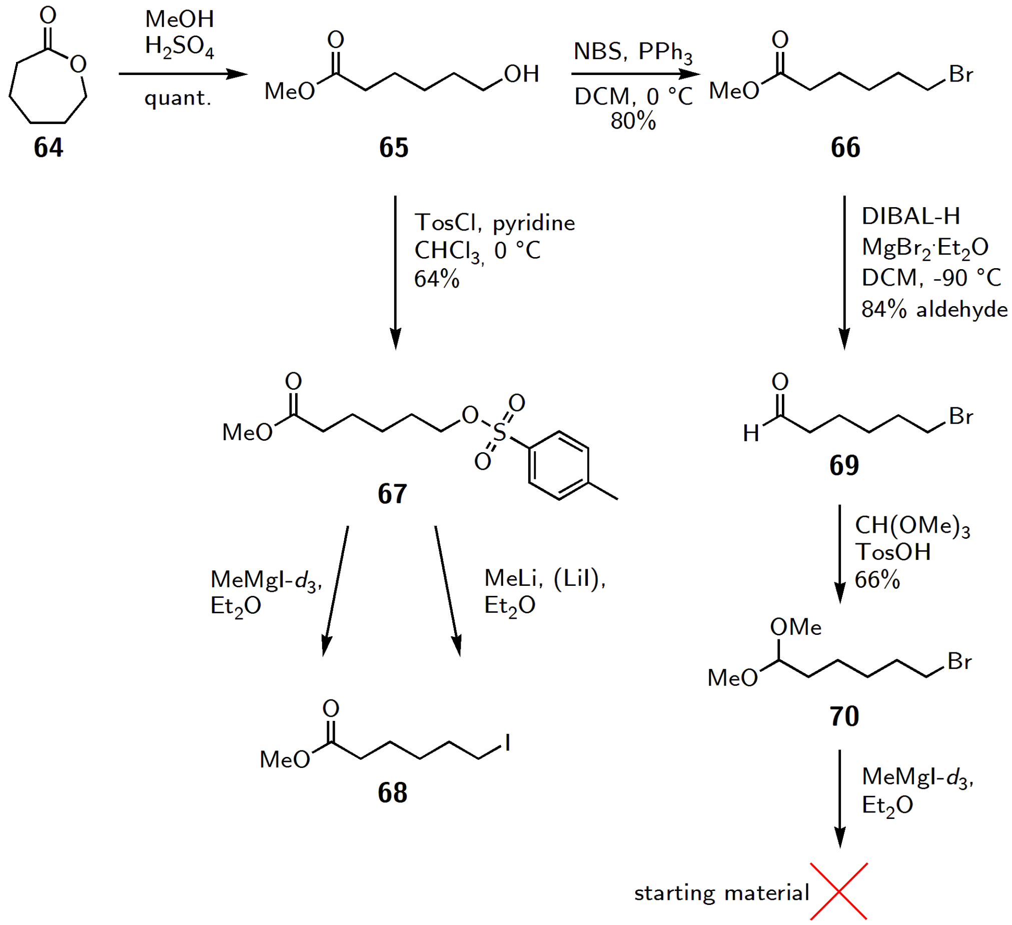
MeOH
H_2SO_4
quant.
NBS, PPh_3
DCM, 0 °C
80%
TosCl, pyridine
$CHCl_3$, 0 °C
64%
DIBAL-H
$MgBr_2 \cdot Et_2O$
DCM, -90 °C
84% aldehyde
$CH(OMe)_3$
TosOH
66%
MeMgI-d_3,
Et_2O
MeLi, (LiI),
Et_2O
MeMgI-d_3,
Et_2O
starting material
64
65
66
67
68
69
70
MeO
OH
Br
I
H
OMe

Figure 6.3: Attempts to synthesise terminally deuterated heptanal. The bromodimethylacetale **70** and the tosylate **67** were not successfully converted into labelled compounds.

but without experimental data[82] or in a many-step synthesis.[83] A short route is therefore favourable. Dodecene can be oxidised in a subsequent reaction to provide the aldehyde.

Starting form 1-undecenol (**71**) the bromo alkene **72** was prepared with NBS and PPh_3. 1-Bromo-10-undecene (**72**) was reacted with MeMgI-d_3 and Li_2CuCl_4 as catalyst. The catalysed GRIGNARD reaction was published by CHANTEGREL[84] for the preparation of labelled heptanal, but in test runs no conversion occurred. In 2007 TERAO published a copper-catalysed alkyl-alkyl cross-coupling reaction of bromoalkenes with GRIGNARD reagents.[85] The catalyst consists of $CuCl_2$ and 1-phenyl propyne as additive. According to this procedure 1-bromo-10-undecene (**72**) was converted into 44% 1-dodecene-12,12,12-d_3 (**73**) and 25% 1-iodo-10-undecene (**74**). TERAO *et al.* examined only bromo and chloro containing GRIGNARD reagents, so that the halide influence of iodine on the reaction was not investigated. The strategy of the synthesis was revised and the labelled compound was prepared starting from the more reactive 10-undecenyl tosylate (**75**) that was transferred into 1-dodecene-12,12,12-d_3 (**73**). The reaction with MeMgI-d_3 solution, 3 mol% $CuCl_2$ and 12 mol% 1-phenyl propyne in THF gave the alkene **76** in excellent yield (Figure 6.4).[85] The oxidation of the dodecene-d_3 (**73**) with $NaIO_4$ was catalysed by ruthenium added as $RuCl_3{\cdot}3H_2O$ to a mixture of acetonitrile and water to yield the aldehyde **76** (91%) and traces of the 1,2-diol in 6% and the carboxylic acid in 3%.[86] Differing from the published protocol, the content of water in the solvent mixture had to be diminished from 15% to 8% in acetonitrile and $NaIO_4$ was added in a 1.5-fold excess. The alkene was completely converted as determined by gas chromatography. The side products were removed by column chromatography. For a determination of the deuteration

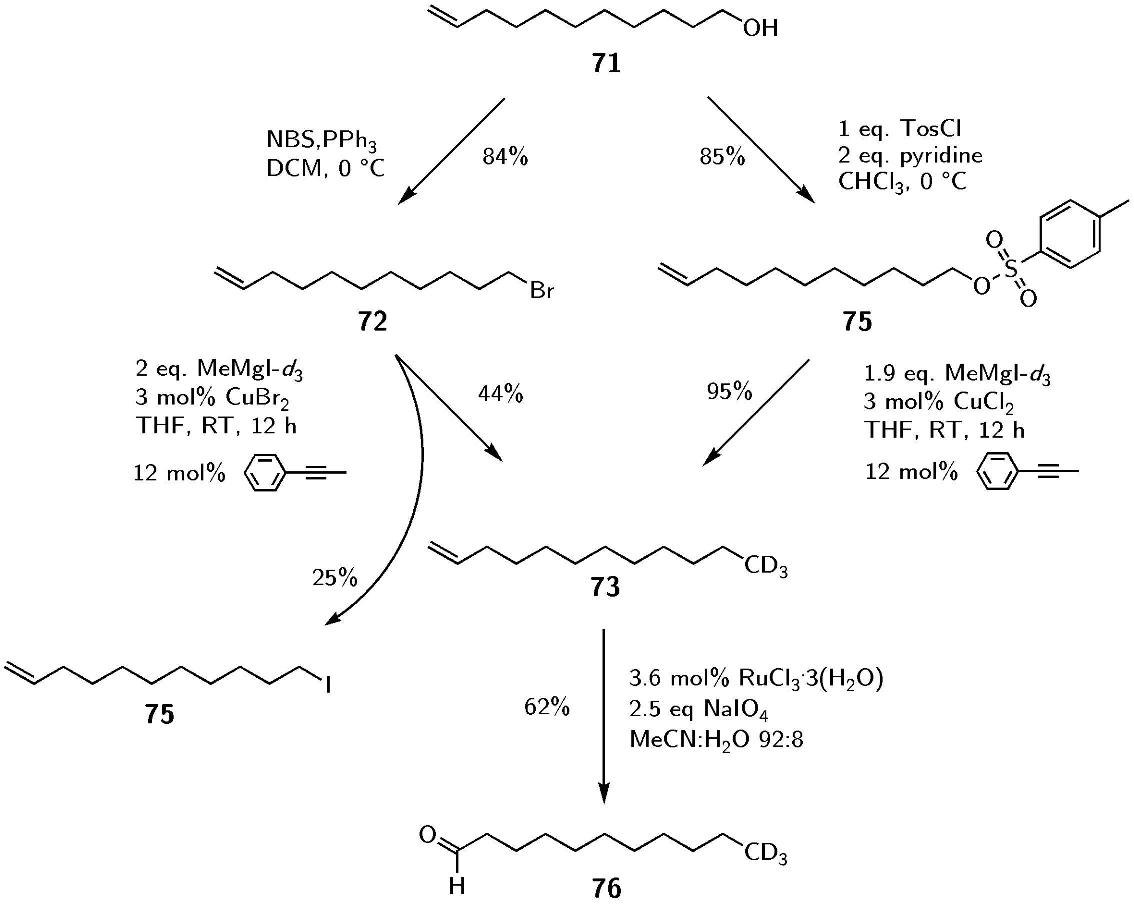
OH
71
NBS,PPh$_3$
DCM, 0 °C
84%
85%
1 eq. TosCl
2 eq. pyridine
CHCl$_3$, 0 °C
Br
72
O
S
O
O
75
2 eq. MeMgI-d_3
3 mol% CuBr$_2$
THF, RT, 12 h
12 mol%
44%
95%
1.9 eq. MeMgI-d_3
3 mol% CuCl$_2$
THF, RT, 12 h
12 mol%
25%
CD$_3$
73
I
75
62%
3.6 mol% RuCl$_3$·3(H$_2$O)
2.5 eq NaIO$_4$
MeCN:H$_2$O 92:8
O
H
CD$_3$
76

Figure 6.4: Synthesis of labelled 1-undecanal-11,11,11-d_3 *via* a copper catalysed reaction of MeMgI-d_3 with tosylate **75**. Alkene **73** was oxidised with $NaIO_4$ to aldehyde **76**. The reaction of bromoalkene **72** yielded **73** and 1-iodo-10-undecene (**75**) as side product.

level by mass spectrometric analysis, the obtained aldehyde **76** was transferred quantitatively with the Girard T reagent[87] into salt **77** under acidic conditions (Figure 6.5). The charged hydrazone has a deuteration level of >99% as determined by EI-MS.

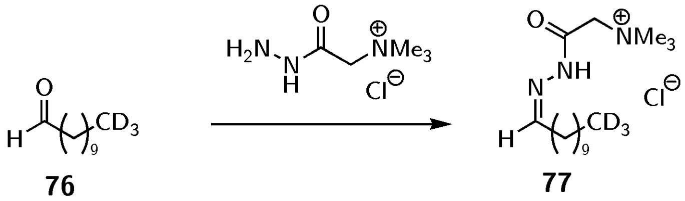

Figure 6.5: Aldehyde **76** functionalised with the Girard T reagent under acidic conditions.

6.1.2 Synthesis of Racemic, Inherently Chiral Resorcinarenes

The racemates of the C_4-symmetric macrocycles were synthesised according to literature procedures.[41] 3-Methoxyphenol and the corresponding aldehyde, 1-undecanal (**78**) and 1-undecanal-11,11,11-d_3 (**76**), respectively, were reacted under Lewis acid catalysis to the racemic resorcin[4]arenes **79** and **80** in moderate yields (Figure 6.6). The residues R are marked with the indices H and D for the unlabelled and the labelled alkyl chain.

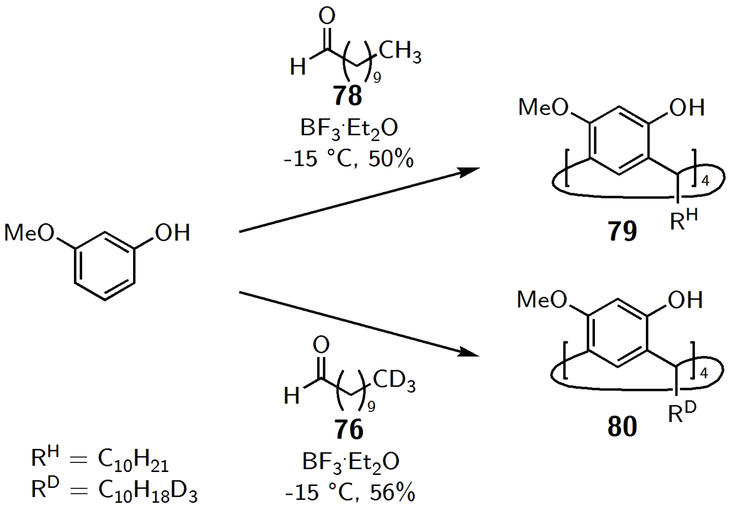

Figure 6.6: Reaction of 3-methoxyphenol and the corresponding aldehyde to the racemates **79** and **80**.

In the ^{1}H-NMR spectra (Figure 6.7 a, c) the terminal methyl group in **79** occurs as a triplet at $\delta = 0.87$ ppm and it is missing in the spectrum of compound **80**. Due to the technical preparation of the Grignard reagent from MeI-d_3, the ratio of the ^{13}C carbon isotope in the CD_3 group is extremely low. The isotopomers of MeI-d_3 as there are e.g. $^{13}CD_3I$, $^{13}CHD_2I$, $^{12}CD_3I$ or $^{12}CHD_2I$, are seperated by distillation and the ^{13}C isotope is depleted. In the ^{13}C-NMR spectra of the labelled alkene **73** and the labelled aldehyde **76**, respectively, the signals of the methyl groups are not higher than the background signals. In Figure 6.7 b this is shown in the partial ^{13}C-NMR spectrum of the resorcinarene **80**. The signal of the deuterated methyl group is a poorly resolved multiplet of very weak intensity between 13.05 and 13.35 ppm. The resonance of the terminal CH_3 group in **79** is slightly downfield shifted to 14.11 ppm. The influence extends to the vicinal methylene group whose ^{13}C resonance signal occurs at 22.41 ppm in the labelled resocinarene compared to 22.70 ppm in the spectrum of the unlabelled one.

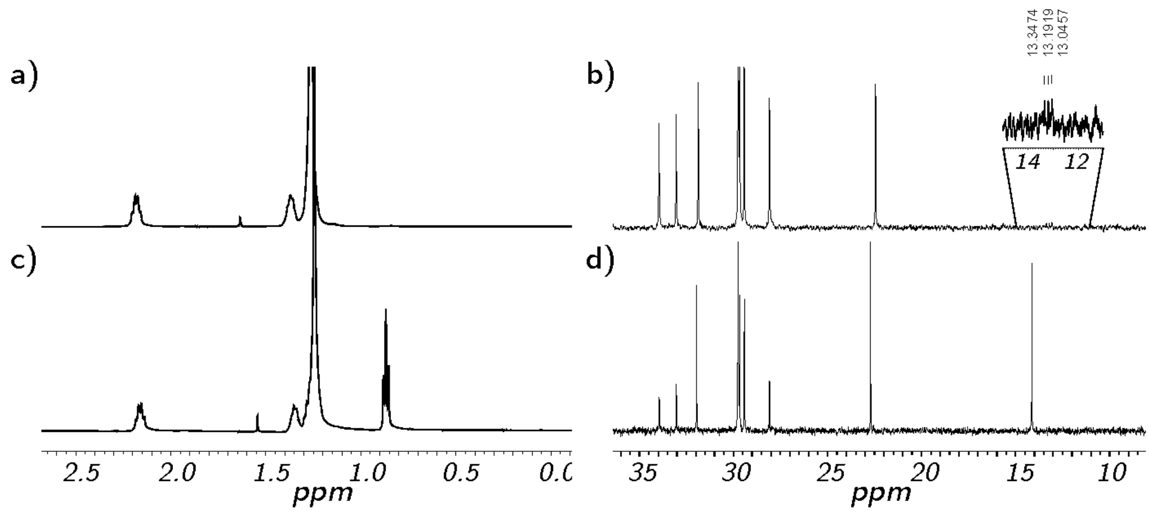

Figure 6.7: Partial ^{1}H- and ^{13}C-NMR spectra of *rac*-**80** (a, b) and *rac*-**79** (c, d) at 500 MHz and 125 MHz, respectively, in $CDCl_3$.

6.1.3 Enantiomer Resolution of Inherently Chiral Resorcinarenes

For resolution of the cycloenantiomers the auxiliary (*S*)-(+)-10-camphorsulfonic acid is attached covalently to the inherently chiral resorcinarenes **79** and **80** forming the corresponding diastereomers as described in literature procedures.[43,44] The inherently chiral enantiomers were transferred into monofunctionalised camphorsulfonic esters with freshly prepared (*S*)-(+)-10-camphorsulfonyl chloride, K_2CO_3 and DMAP (Figure 6.8). Due to the solubility properties of long pendant alkyl chains the experimental procedure with the (*S*)-(+)-10-camphorsulfonic acid was modified regarding the solvent mixture.[43,44] In the earlier publication,[44] the reaction was carried out in THF and the resorcinarenes were treated with *n*-BuLi as the base. The racemates of **79** and **80** were dissolved in THF and acetonitrile was added (2:3 v:v). Preliminary experiments with K_2CO_3, (*S*)-(+)-10-camphorsulfonyl chloride and DMAP in pure THF and in pure acetonitrile, respectively, failed to provide an ester formation within a reasonable time. The ether THF is necessary to dissolve the resorcinarenes as the solubility in acetonitrile is rather low, but the presence of acetonitrile is crucial for the proceeding of the reaction.

The monofunctionalisation gives a statistical mixture of the starting material, the monoester and traces of the dicamphorsulfonic esters. The diastereomeric pairs of **81** and **82** (Figure 6.8), respectively, were purified by flash column chromatography; both the starting material and the diesters were recovered. The diastereomers were separable by silica gel HPLC. The eluting solvents were cyclohexane and ethyl acetate in a ratio of 81:19 (v:v). A run of 140 min duration gave a sufficient resolution of the (+)- and the (–)-diastereomer with retention times of 93 min and 102 min, respectively. The nonlabelled racemate of **79** was resolved following the same procedure. The stereogenic centers were assigned following the suggestion of HEANEY *et al.*[88] (see also Section 2.2). The auxiliary is designated by the first descriptor (1), the stereogenic centers of the resorcinarene are derived from the view along the axis (2-5). They are listed starting from the methylene bridge in vicinity of the camphorsulfonic ester group and continue along the macrocycle following that direction (see Figure 6.8).

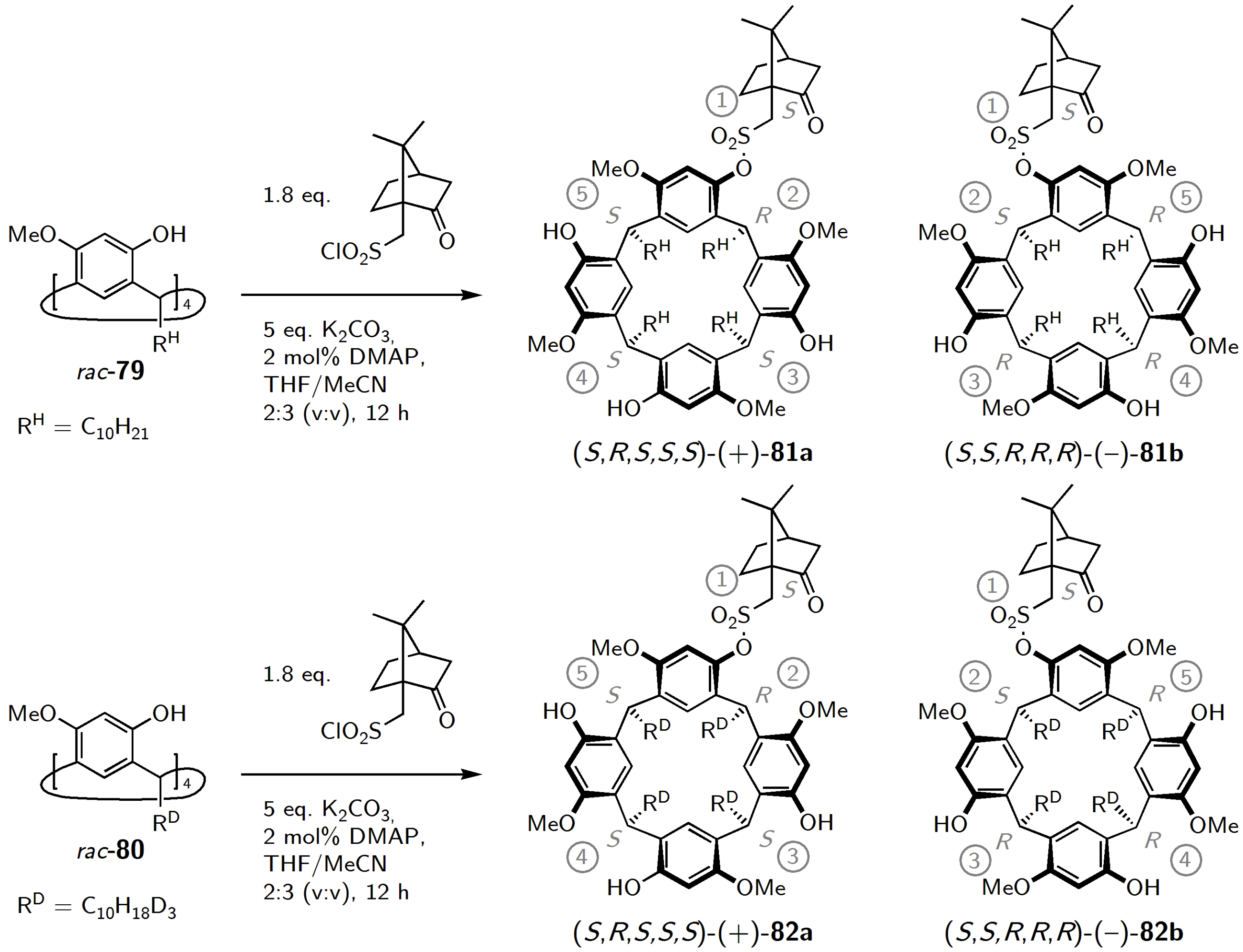
rac-79
$R^H = C_{10}H_{21}$
1.8 eq.
ClO_2S
5 eq. K_2CO_3,
2 mol% DMAP,
THF/MeCN
2:3 (v:v), 12 h
(S,R,S,S,S)-(+)-81a
(S,S,R,R,R)-(−)-81b
rac-80
$R^D = C_{10}H_{18}D_3$
1.8 eq.
ClO_2S
5 eq. K_2CO_3,
2 mol% DMAP,
THF/MeCN
2:3 (v:v), 12 h
(S,R,S,S,S)-(+)-82a
(S,S,R,R,R)-(−)-82b
①
②
③
④
⑤
S
R
MeO
OH
HO
OMe
O_2S
O
R^H
R^D

Figure 6.8: Synthesis of the diastereomers **81** and **82**; the corresponding descriptors are displayed in grey.

The NMR-spectra of the C_1-symmetric resorcinarenes differ characteristically from each other as described in the following (Figure 6.9). Between $\delta = 4.20$ and 4.73 ppm are the resonances of the methylene bridges (Figure 6.8, stereogenic centers 3-5), the downfield shifted triplet displays the methylene proton close to the ester functionality (2). Upon esterification the resonances of the methoxy groups split into three signals between 3.70 and 3.89 ppm for **82a** and four signals between 3.72 and 3.91 ppm for **82b**, respectively. The difference becomes most obvious in the resonances of the methylene group vicinal to the sulfonic ester. For both protons a doublet occurs at 3.82 ppm and 3.29 ppm in diastereomer **82a** with coupling constants of 14.8 and 14.9 Hz, respectively. In the second eluting diastereomer **82b** the upfield shifted dublett is clearly resolved at 3.25 ppm, and the downfield shifted doublet is superimposed by the methoxy signals. From this NMR analysis the diastereomeric excess was determined as *de* >99%.

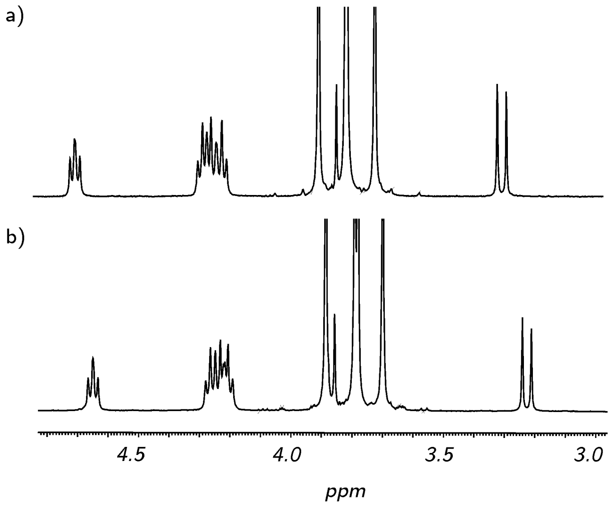

Figure 6.9: Partial ^{1}H-NMR spectra (500 MHz) of diastereomers (a) **82a** and (b) **82b** in $CDCl_3$.

In contrast to the different NMR spectra the CD spectra of the diastereomers **81a** and **81b** are perfect mirror images of each other (Figure 6.10). The camphor moiety does not affect the Cotton effect[79] originating from the chromophoric resorcinol units, but interrupts the intramolecular hydrogen bonding at the *upper rim*. This phenomenon is discussed for the enantiomerically pure scaffolds in detail in Section 6.2.

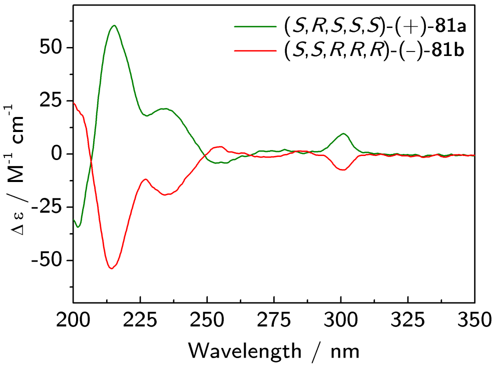

Figure 6.10: CD-spectra of the diastereomers **81a** and **81b** in cyclohexane (c = 5×10^{-5} M).

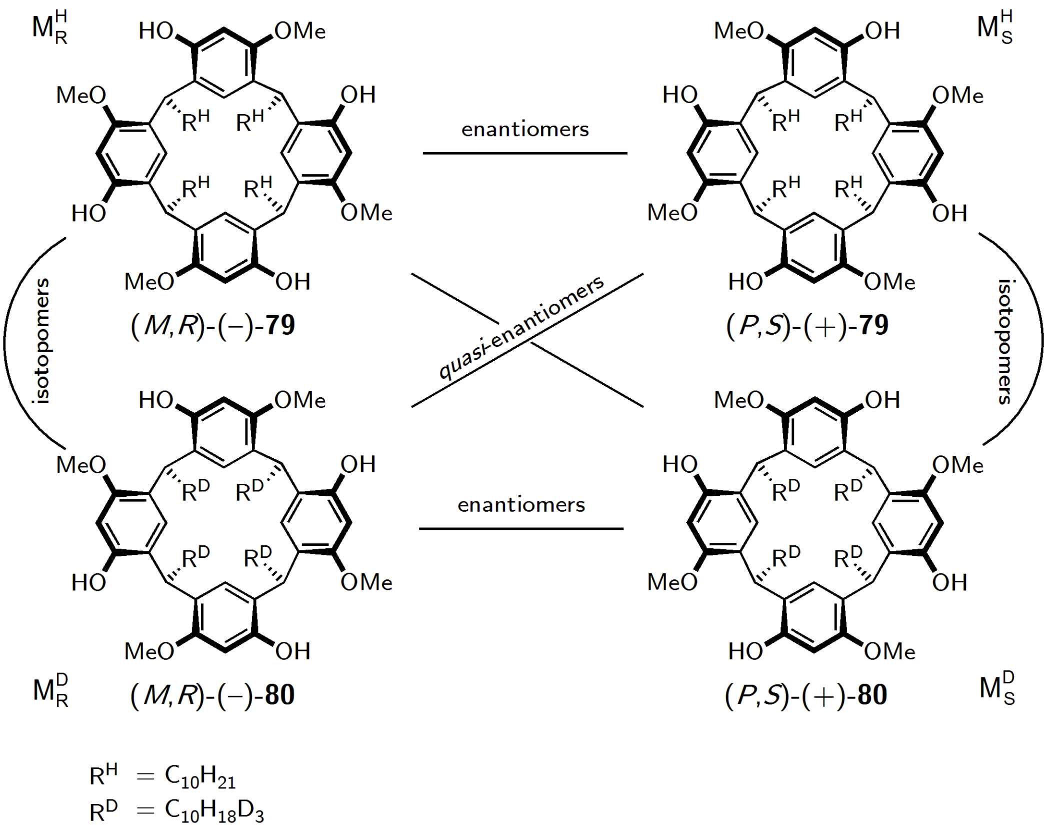

Figure 6.11: All the C_4-symmetric inherently chiral resorcin[4]arenes with terminally labelled and unlabelled alkyl chains in the *crown* conformation. For explanation of the terms see also Glossary, p. 107.

The diastereomers were transferred under alkaline conditions into the enantiomerically pure resorcin[4]arenes. After removal of the auxiliary the (+)-diastereomers **81a** and **82a** provided (*P*,*S*)-(+)-**79** and its deuterated isotopomer (see Glossary, p. 107) (*P*,*S*)-(+)-**80**, respectively, and the (−)-diastereomers **81b** and **82b** gave (*M*,*R*)-(−)-**79** and (*M*,*R*)-(−)-**80**, respectively (Figure 6.11). The absolute configuration of inherently chiral resorcinarenes is known from earlier studies carried out by HEANEY *et al.*[43] (see also Chapter 2, Section 2.2). The resorcinarenes are designated as M and the indices H and D for the isotope labelling, and *S* and *R* for the chirality sense. The *M* and *P* descriptors are applied to inherently chiral resorcinarenes to describe the axial chirality additionally to the *R*/*S* notation for the stereogenic centers (following the CAHN-INGOLD-PRELOG rules).[88] The relation between these four compounds is shown in Figure 6.11. The term *quasi*-enantiomer describes a compound with opposite configuration whose mirror image is not superimposable with the referred enantiomeric compound due to a physical difference, here the labelled alkyl chain (see also Glossary, p. 107). The resorcinarenes (*P*,*S*)-(+)-**79** and (*P*,*S*)-(+)-**80** are isotopomers as one is the isotopically enriched analogue of the other. For the MS experiments the four enantiomerically pure resorcinarenes (see Figure 6.11) were prepared. The pairs of the *quasi*-enantiomers (*M*,*R*)-(–)-**79** and (*P*,*S*)-(+)-**80** and their isotopomers (*M*,*R*)-(–)-**80** and (*P*,*S*)-(+)-**79** give the *quasi*-racemats **I** and **II**, respectively, with a mass difference of 12 amu. The deuteration grade of the racemic and the resolved enantiomers of **80** was determined by HRMS as >99%.

This is the first set of all *quasi*-enantiomeric, isotopically labelled, inherently chiral resorcinarenes. The only other complete set of isotopically labelled *quasi*-enantiomers of host systems was reported for trianglamine macrocycles by KUHNERT *et al.* (Chapter 2, Section 2.3).[54] The lateral chains in **80** are stable in protic and basic conditions that no H/D exchange reaction may occur. All experiments can be performed with both *quasi*-racemates to determine the stereodiscrimination reliably regarding any isotope effects and measuring errors. This chiral cross-check and the simultaneous measurement of the enantioselectivity of both host enantiomers under the same experimental conditions allow a very distinct characterisation of the stereodiscrimination power.

6.1.4 Achiral, Labelled Resorcinarenes

For the MS studies an achiral reference system was synthesised as well. Four achiral resorcinarenes were prepared with unlabelled and labelled alkyl chains (Figure 6.12). The octahydroxy resorcinarene scaffold was build up with resorcinol and the corresponding aldehyde according to literature procedures.[89] The labelled aldehyde was synthesised as described in Section 6.1.1. Resorcinol and aldehyde **76** and **78**, respectively, were condensed under acidic conditions to the tetramers **83** and **84** in low yields. Probably, the reaction time of 3 h was insufficient.

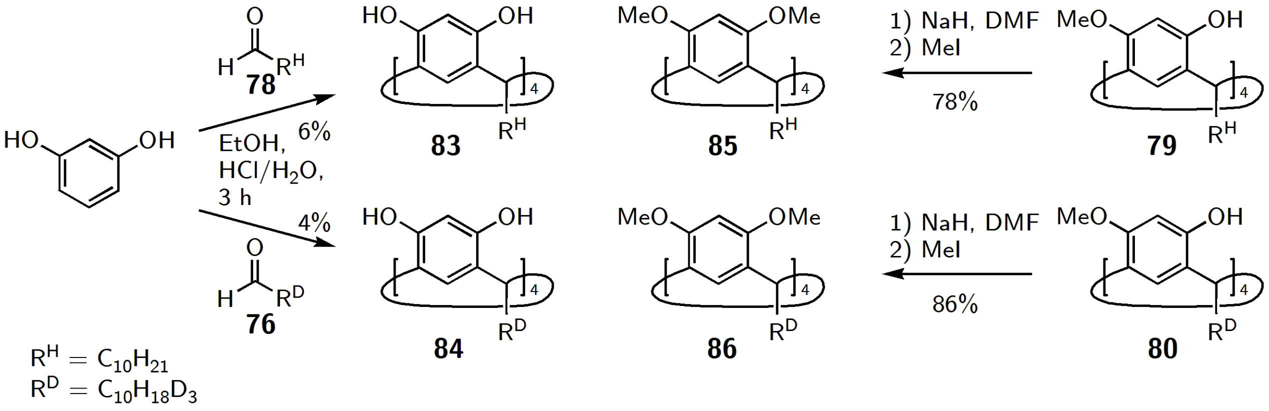

Figure 6.12: Synthesised labelled and unlabelled, achiral resorcinarenes.

The methylated compounds **85** and **86** were generated from the inherently chiral racemate of **79**. The hydroxyl groups were deprotonated by NaH in DMF, and reacted with MeI. These successfully prepared compounds show that the deuterated aldehyde offers a general route to labelled macrocycles and to MS experiments of sophisticated systems like large container molecules.

6.2 Chiroptical Properties of the Enantiomers

The CD-spectra of the enantiomeric pairs of **79** and **80** show mirror images of each other in cyclohexane as well as in methanol (Figure 6.14). Thus the enantiomers of **79** and their labelled isotopomers of **80** show their *quasi*-enantiomeric nature without influence of the labelled groups on the absorption properties. The optical rotation values are equal for the isotopomeric compounds within the errors of the measurement (Table 6.1).

Enantiomer	$[\alpha]_D^{25}$ 10^{-1} cm^2 g^{-1}	Conc. g 100 mL^{-1}
(*P*,*S*)-(+)-**79**	+48.5	1.0
(*M*,*R*)-(−)-**79**	-47.4	1.0
(*P*,*S*)-(+)-**80**	+49.2	1.0
(*M*,*R*)-(−)-**80**	-48.0	1.0

Table 6.1: Optical rotation values.

In literature there are few examples for significantly divergent chiroptical properties of isotopomers. EAMES *et al.*[90] reported a specific optical rotation of deuterium-containing isotopomers. The labelled isotopomers of 2-dimethylaminocyclohexyl-1-trimethylammonium iodide were systematically investigated towards their optical rotation properties. With increased degree of labelling the specific rotation is lowered moreover the impact of the molecular mass. Slightly lowered $\Delta\epsilon$-value were observed in CD-spectra of labelled camphor compared to the unlabelled derivatives[91] as well as for labelled trianglamines.[54]

The conformation of inherently chiral resorcinarenes in solution was investigated by CD spectroscopy and quantum chemical calculations at the DFT level.[92] The presumed configuration in the beginning of 2006 was corrected in september 2006 by HEANEY *et al.*[43] Herein the correct assignment of the absolute stereochemistry is applied and the corresponding CD spectra are presented.

In cyclohexane the Cotton effects are bisignate and in methanol monosignate. The absorption band in the range of 260 and 310 nm can be ascribed to the L_b transitions of the unsymmetrical resorcinol units. In cyclohexane as aprotic solvent a bisignate Cotton effect occurs arising from a C_4 symmetric crown conformation stabilised by intramolecular hydrogen bonding. The solvent methanol is able to disrupt that network and an intermolecular hydrogen bonding occurs. Two opposite arenes (Figure 6.13, conformation I, 1 and 3) are oriented upwards and the other two arene units (2 and 4) are oriented outwards. This C_2-symmetric boat conformation is in a fast dynamic equilibrium with the boat conformation II overall a monosignate Cotton effect is displayed.

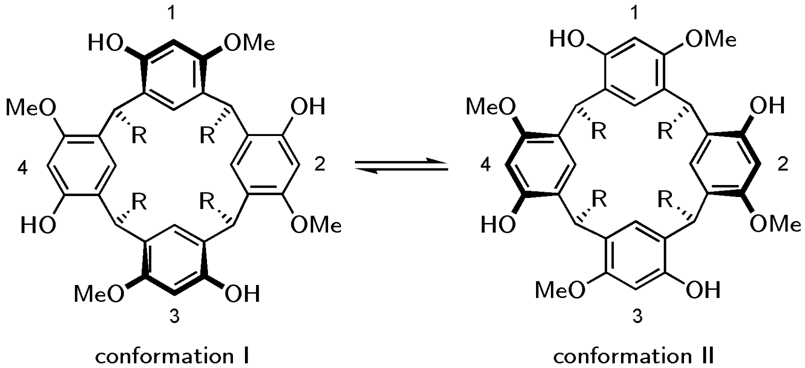

Figure 6.13: Conformations of both C_2-symmetries. R represents an alkyl chain.

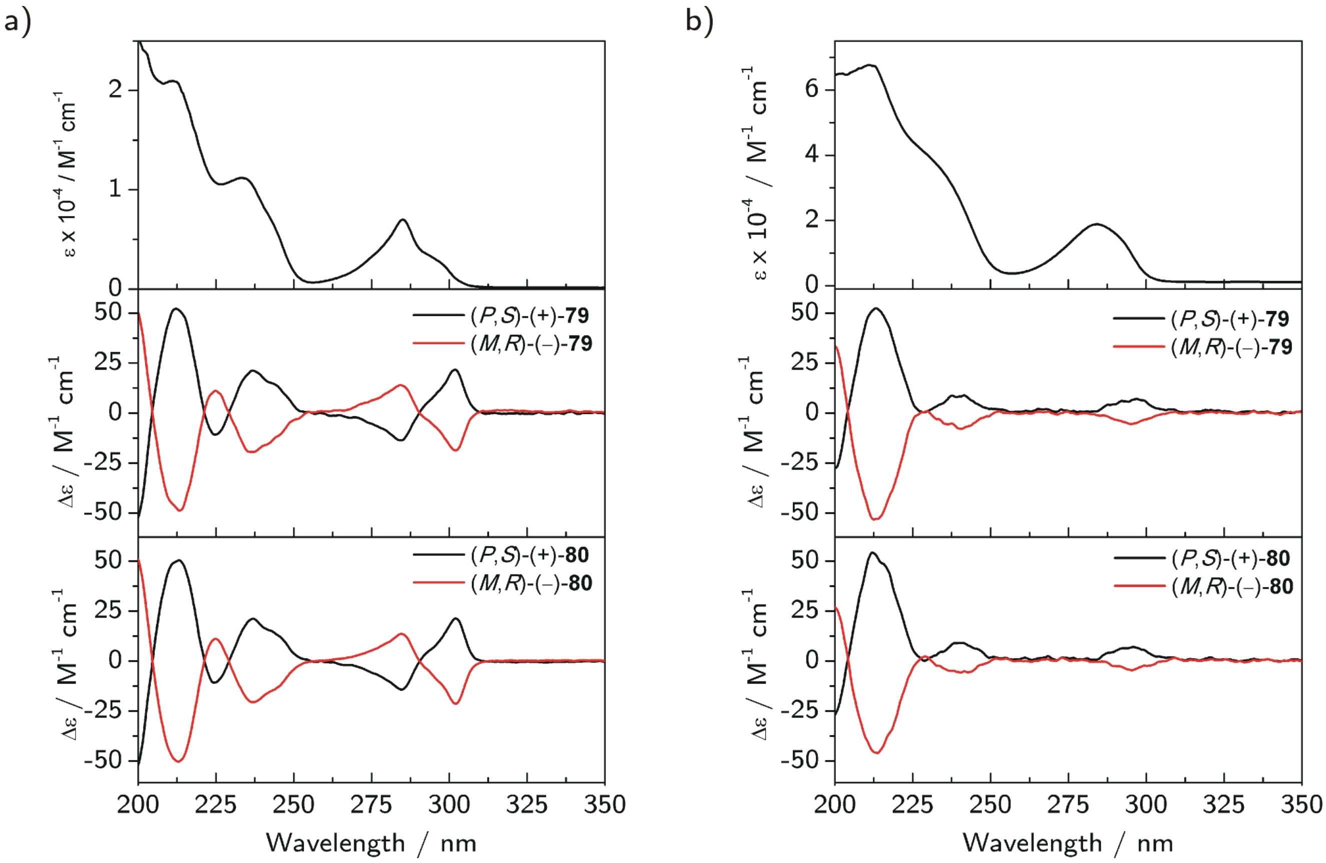

Figure 6.14: UV/Vis and CD-spectra in (a) cyclohexane and (b) methanol (5×10^{-5} M).

In protic solvents like methanol one can assume an intermolecular hydrogen bonding with the solvent molecules with *boat* conformation of the resorcinarene scaffold. DFT calculations of the desolvated macrocycle predict a *crown* conformation at the *upper rim*.[92] Up to date, the conformation dependence upon complexation with achiral or chiral guests in solution was not investigated.

6.3 Enantioselectivity of Inherently Chiral Resorcinarenes

Enantioselective recognition in supramolecular systems involves the aggregation of a chiral receptor and a chiral guest.[93] If there is a pair of hosts with opposite configuration, two diastereomeric adducts are formed held together by noncovalent interactions. The spatial arrangement causes a difference in these short-range forces, e.g. in the strength of interactions and in the sterical fit. This leads to a preferential binding of a chiral guest by one host over another. The complexes are characterised by a different stability (thermodynamic enantioselectivity, equilibrium constant K) and reactivity towards an exchanging guest B (kinetic enantioselectivity, reaction rate k). The chiral host is marked as M and the guest as G (Figure 6.15); the indices *S* and *R* denote the configuration.

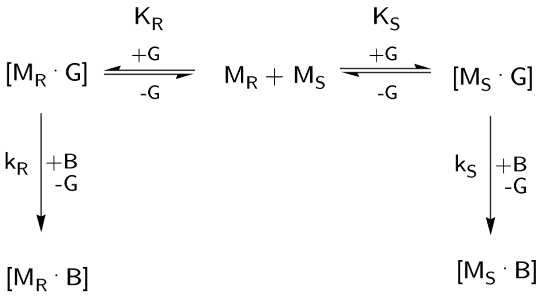

Figure 6.15: Scheme of thermodynamics and kinetics in chiral complexes.

The investigation of non-covalent interactions by mass spectrometric analysis is well known for supramolecular systems,[94–96] especially for molecular recognition of chiral interactions.[97,98] The reactions can be performed with a low amount of the chiral target molecule. Between the two diastereomeric adducts of the labelled and the unlabelled resorcinarene of opposite chirality and the chiral amino guest there is a difference of $\Delta\Delta G$ in their stability indicated by the free Gibbs energies (Figure 6.16). In exchange reactions with an achiral amino base there are different acivation barriers $\Delta G^{\ddagger}_S$ and $\Delta G^{\ddagger}_R$ resulting in a faster reaction rate if the barrier is lower than that of the other adduct or in a slower reaction rate when the barrier is higher. The height of the activation energy barrier $\Delta G^{\ddagger}$ and $\Delta G^{\ddagger}_R$ resulting in a faster reaction rate depends on the (thermodynamic) stability of the diastereomeric adduct and the transition state structure.

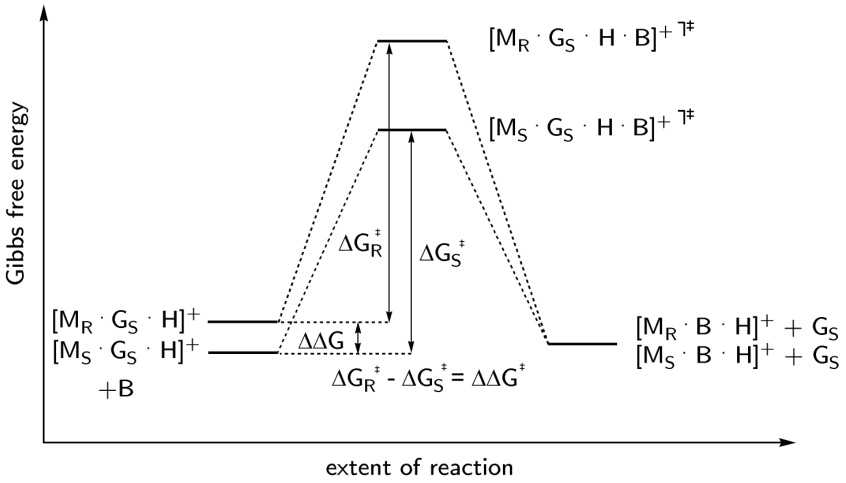
Gibbs free energy
extent of reaction
[M_R · G_S · H · B]+ ‡
[M_S · G_S · H · B]+ ‡
[M_R · G_S · H]+
[M_S · G_S · H]+
+B
ΔG_R‡
ΔG_S‡
ΔΔG
ΔG_R‡ - ΔG_S‡ = ΔΔG‡
[M_R · B · H]+ + G_S
[M_S · B · H]+ + G_S

Figure 6.16: Energy scheme of the diastereomeric adducts, the transition states and the products that are equal in energy.

In earlier MS studies on the enantioselectivity of inherently chiral resorcinarenes published by MATTAY *et al.*[56] the enantiomer labelling method[52,99,100] was applied to the chiral guest compounds (Figure 6.17). Enantiomerically pure amines were reacted with MeI and MeI-d_3, respectively, giving the quarternary ammonium ions. The two *quasi*-diastereomeric adducts formed from the C_4-symmetric host and the *quasi*-enantiomers of the guest appear as two signals with different *m/z* ratios of $\Delta m = 9$ amu.

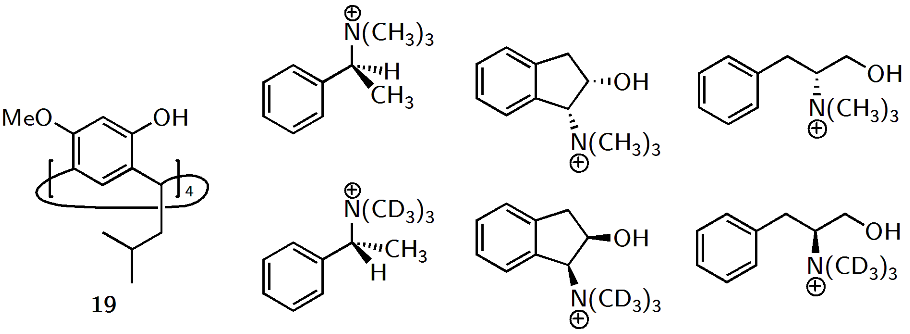
MeO
OH
4
19
N(CH3)3
H
CH3
N(CD3)3
CH3
H
OH
N(CH3)3
OH
N(CD3)3
OH
N(CH3)3
OH
N(CD3)3

Figure 6.17: labelled and unlabelled guests investigated by MATTAY *et al.*[56] in a previous ESI-MS study.

The complexes were generated by the electrospray ionisation method (ESI) and the resulting adducts of resorcinarene **19** and guests (see Figure 6.17) were investigated by mass spectrometry regarding their relative peak intensities.[56] The investigation by ESI-MS gave the ratio of the (thermodynamically) formed *quasi*-diastereomeric complexes. The difference in ion abundance results from the chiral effect on the one hand and the isotope effect on the other hand. The latter effect was determined from experiments with the host antipode under the same conditions. The discrimination effects are significant with a diastereomeric excess of 10.6% ± 1.3% for the homochiral complex; but this is rather low compared to the isotope effect of 10-20%. In this case the size of labelled and unlabelled methyl groups attached to the binding site may contribute to the complexation behaviour of the guest ion.

For gas phase experiments, charged host/guest adducts are generated by several possible ionisation processes as there are e. g. the fast atom bombardement (FAB),[101] matrix assisted laser desorption/ionisation (MALDI)[102] or electrospray ionisation (ESI).[103] They all have in common to generate charged adducts from a mixture in the solid state or in a solution. But the ionisation process itself alters the ratio of the adducts that are present in the solution and the derived diastereoselectivities are distorted. The ionisation source has indeed an influence on the relative abundance of a diastereomeric ionic complex as known for crown ethers.[52,99,100]

In this study, true gas-phase experiments were performed to measure the enantioselectivity ρ in reactions of diastereomeric adducts with primary amino bases (Figure 6.18). Aim of the study was to determine the intrinsic factors governing the enantiorecognition. In a solvent free environment like the gas phase, the ionic or ion-dipole interactions are stronger than in solution and e.g. hydrophobic interactions are destabilised in the absence of solvent. The reactivity of a complex in the gaseous phase is independent from the relative peak intensities of the generated diastereomeric adducts.

$$\begin{array}{ll}
[M_S \cdot H \cdot G_S]^+ \xrightarrow[+\,B\,-\,G_S]{k_{homo}} [M_S \cdot H \cdot B]^+ + G_S & \\
 & \dfrac{k_{homo}}{k_{hetero}} = \rho \\
[M_R \cdot H \cdot G_S]^+ \xrightarrow[+\,B\,-\,G_S]{k_{hetero}} [M_R \cdot H \cdot B]^+ + G_S &
\end{array}$$

Figure 6.18: Reaction rates (k) for the homochiral and the heterochiral adducts. The enantioselectivity ρ is the ratio of these reaction rates.

The complexes of the resorcinarene (M), a proton (H) and a chiral guest (G) were generated in a nano-ESI source from a *quasi*-racemic solution of the host (**79** and **80**) each in a concentration of 1×10^{-5} M and containing a threefold excess of the selected guest G (6×10^{-5} M) in $CH_3OH/CHCl_3$ (10:1). The resorcinarene hosts are those shown in Figure 6.11, denoted by the indices *S* and *R* for their chirality sense and H and D to indicate the mass difference upon deuteration, D is the labelled resorcinarene. The chiral guests (Figure 6.19) are devided into three groups: 1) amino acids, A; 2) amino acid esters, E; 3) amino alcohols, N. All of them bearing an amino functionality and at least one further group like hydroxyl, carboxylic acid or aromatic imino functionalities. Glycine ethyl ester is the achiral reference E_0.

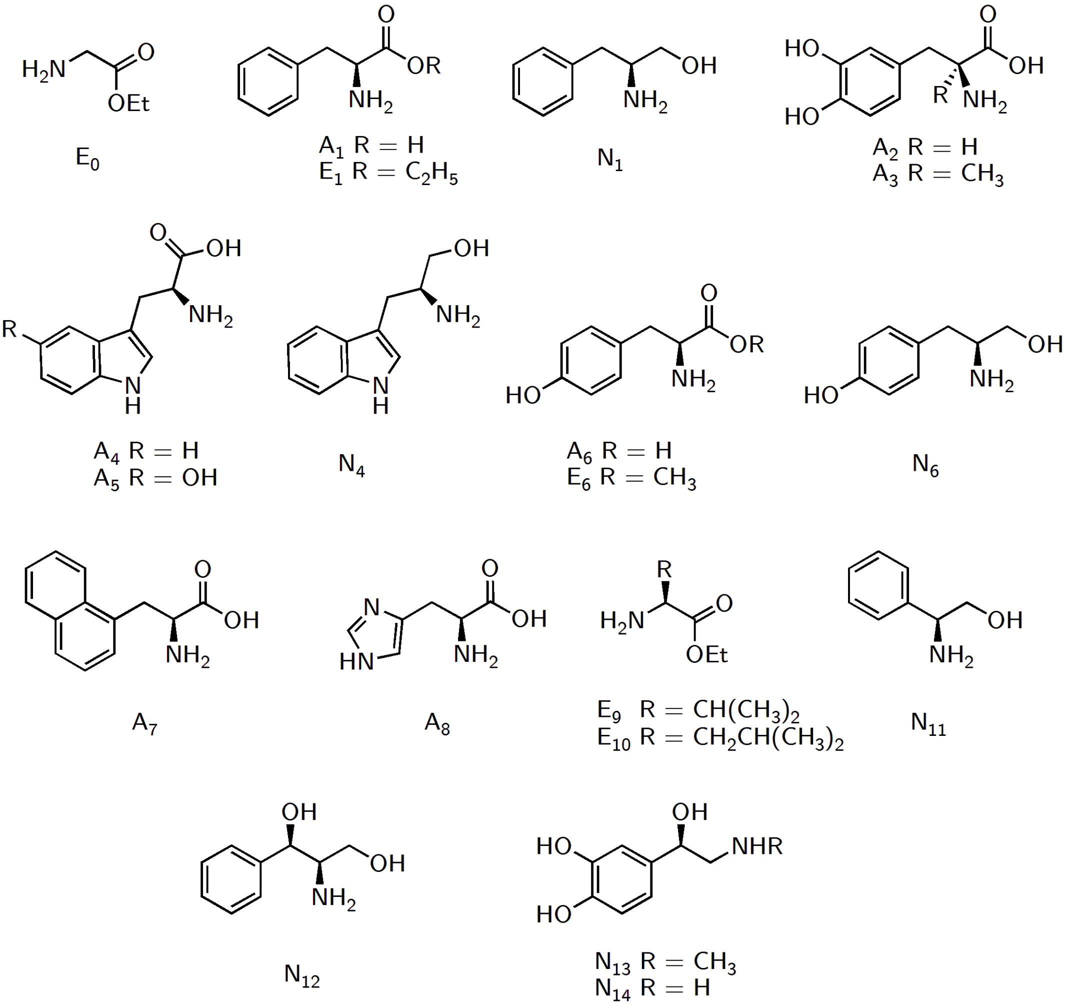
E_0
A_1 R = H
E_1 R = C_2H_5
N_1
A_2 R = H
A_3 R = CH_3
A_4 R = H
A_5 R = OH
N_4
A_6 R = H
E_6 R = CH_3
N_6
A_7
A_8
E_9 R = $CH(CH_3)_2$
E_{10} R = $CH_2CH(CH_3)_2$
N_{11}
N_{12}
N_{13} R = CH_3
N_{14} R = H

Figure 6.19: The chiral guests G investigated by mass spectrometry. A: amino acids, E: amino acid esters, N: amino alcohols.

The isolated adducts were reacted with chiral and achiral primary amines (B, ethylamine, 2-propylamine and 2-butylamine) (Figure 6.18). The enantioselectivity ρ is the ratio of the rate constants obtained for the homochiral diastereomeric complex k_{homo} and the heterochiral complex k_{hetero}.

Reaction 1

$$\begin{array}{ll} [M_S^{H} \cdot H \cdot G_S]^+ \xrightarrow[+\,B\,-\,G_S]{k_{homo}} [M_S^{H} \cdot H \cdot B]^+ + G_S & \\ & \dfrac{k_{homo}}{k_{hetero}} = \rho_1 \\ [M_R^{D} \cdot H \cdot G_S]^+ \xrightarrow[+\,B\,-\,G_S]{k_{hetero}} [M_R^{D} \cdot H \cdot B]^+ + G_S & \end{array}$$

Reaction 2

$$\begin{array}{ll} [M_S^{D} \cdot H \cdot G_S]^+ \xrightarrow[+\,B\,-\,G_S]{k_{homo}} [M_S^{D} \cdot H \cdot B]^+ + G_S & \\ & \dfrac{k_{homo}}{k_{hetero}} = \rho_2 \\ [M_R^{H} \cdot H \cdot G_S]^+ \xrightarrow[+\,B\,-\,G_S]{k_{hetero}} [M_R^{H} \cdot H \cdot B]^+ + G_S & \end{array}$$

Figure 6.20: Reactions of the *quasi*-racemates 1 (reaction 1) and the opposite labelled *quasi*-racemate 2 (reaction 2) with an achiral base B.

The ESI-FT-ICR measurements and analysis of the results were performed by CATERINA FRASCHETTI. An example of the measurements is given in Figure 6.21. The relative intensities of the reacting diastereomer and the product complex are shown (see also Figure 6.20).

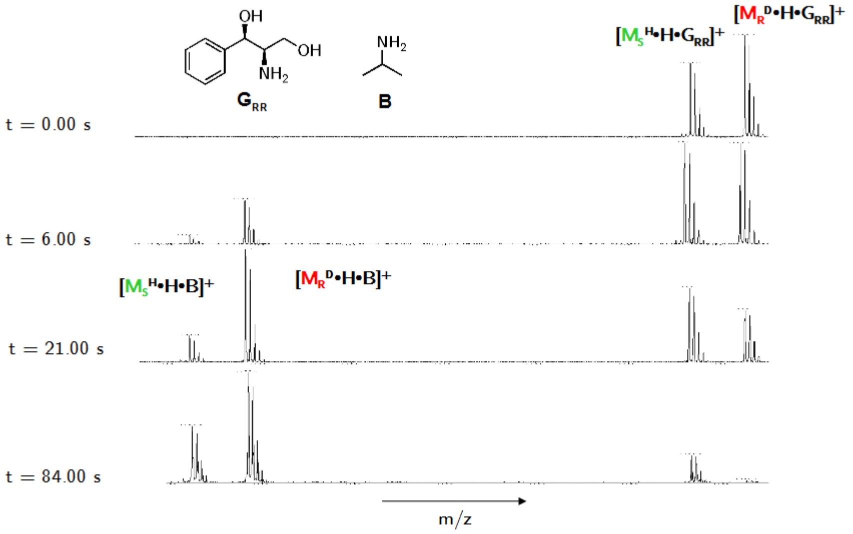

Figure 6.21: Reaction of *quasi*-racemate 1 in complex with (1*R*,2*R*)-2-amino-1-phenylpropane-1,3-diol (N_{12}). The reacting gas is 2-propylamine, the proceeding of the reaction is shown from the beginning (t = 0) to t = 84 s.

To estimate any hypothetical isotope effect, the reactions were performed as cross-check experiments with both *quasi*-racemates of the resorcinarenes in Reaction 1 and Reaction 2 (Figure 6.20). The kinetic results were analysed by plotting the log($[M\cdot H\cdot G]_t^+$/ $[M\cdot H\cdot G]_0^+$) versus the reaction time, where $[M\cdot H\cdot G]_t^+$ is the precursor ionic abundance at time t and $[M\cdot H\cdot G]_0^+$ is the sum of the $[M\cdot H\cdot G]_t^+$ and the $[M\cdot H\cdot B]^+$ product. The reaction rates and the enantioselectivities are reported in the Appendix, Tables 8.1 - 8.3. The enantioselectivities towards 2-propylamine as the base (PA=220.8 kcal mol^{-1}) are summarized in Figure 6.22. The dotted line indicates no reaction enantioselectivity (ρ=1). The farther the values are from unity the higher the degree of chiral distinction. If the enantioselectivity is below ρ = 1, the heterochiral complex reacts faster than the homochiral one. With the achiral glycine ethyl ester a control experiment was performed. In this case no appreciable deviation from unity was obtained ($[M^H_S\cdot H\cdot G]^+/[M^D_R\cdot H\cdot G]^+$ ρ = 0.98±0.06 and $[M^D_S\cdot H\cdot G]^+/[M^H_R\cdot H\cdot G]^+$ ρ = 1.00±0.06). Most of the enantioselectivities in Figure 6.22 are below the unity. The exceptions are complexes of 5-hydroxy-tryptophane (A_5, ρ = 2.20±0.13), (1*R*,2*R*)-2-amino-1-phenylpropane-1,3-diol (N_{12}, 3.88±0.29) and norepinephrine (N_{14}, 1.52±0.09).

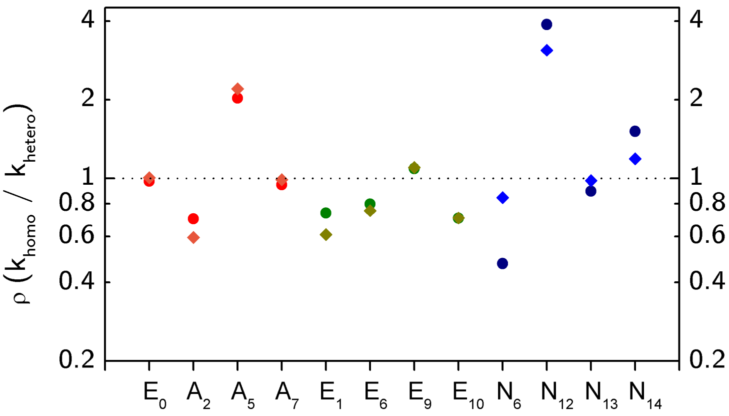

Figure 6.22: Enantioselectivity ρ measured for the exchange reaction of 2-propylamine. The ratios of reaction 1 (ρ_1, cycles) and 2 (ρ_2, rhombi) are displayed.

To ascertain whether the enantioselectivities are sensitive to the basicity of the amine, the study has been extended to the comparatively less basic ethylamine (PA = 218.0 kcal mol^{-1}) and to the more basic *S*)-2-butylamine and *R*)-2-butylamine (PA=222.2 kcal mol^{-1}). The relevant kinetic results are summarised in Figures 6.23, 6.24 and 6.25, respectively.

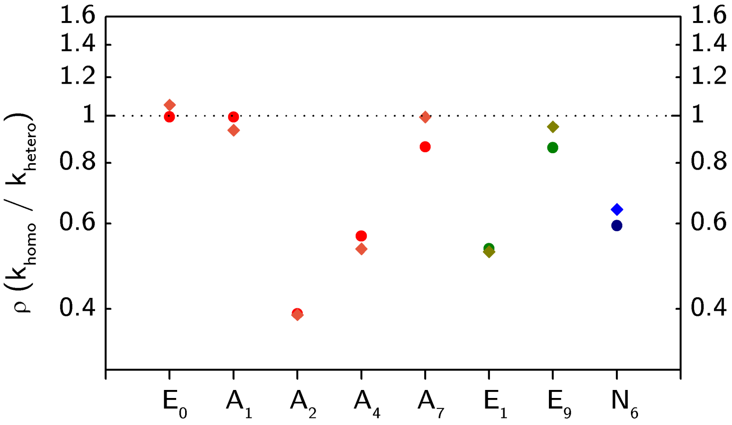

Figure 6.23: Enantioselectivity ρ measured for the exchange reaction of ethylamine. The ratios of reaction 1 (ρ_1, cycles) and 2 (ρ_2, rhombi) are displayed.

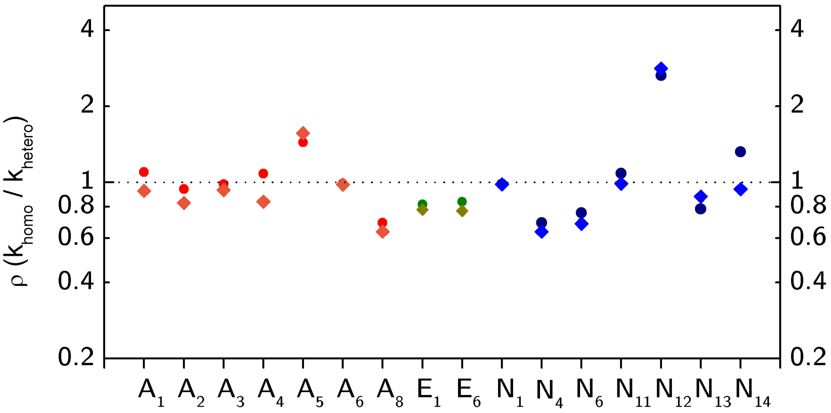

Figure 6.24: Enantioselectivity ρ measured for the exchange reaction of (S)-2-butylamine. The ratios of reaction 1 (ρ_1, cycles) and 2 (ρ_2, rhombi) are displayed.

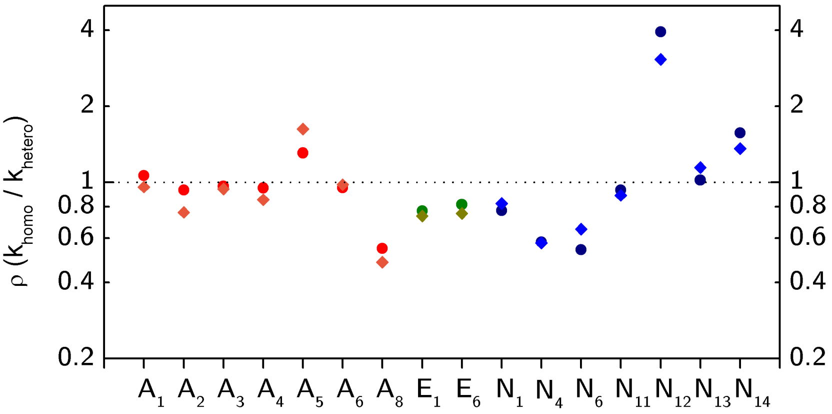

Figure 6.25: Enantioselectivity ρ measured for the exchange reaction of (R)-2-butylamine. The ratios of reaction 1 (ρ_1, cycles) and 2 (ρ_2, rhombi) are displayed.

In all the considered experiments the reactions of the aminoalcohol complexes are the most selective ($0.47 \pm 0.02 < \rho < 3.89 \pm 0.29$). The highest selectivity was measured with (1*R*,2*R*)-2-amino-1-phenylpropane-1,3-diol (N_{12}) as guest; the homochiral complex reacted four times faster than the heterochiral adduct. The amino acids and the amino esters show a lower enantioselectivity. The homochiral complex of (*S*)-5-hydroxy-tryptophane (A_5) reacts 2.03±0.11 times faster with 2-propylamine than the heterochiral complex. All other amino acids show selectivities between 0.40±0.02 and 1.10±0.08. The amino esters have moderate selectivities ($0.70 \pm 0.03 < \rho < 1.09 \pm 0.07$). In most of the reactions the heterochiral complexes react faster than their homochiral counterparts, except the complexes of A_5, N_{12} and N_{14}.

The reactions were all performed with the *quasi*-racemates 1 and 2. The experimental uncertainty associated with the measured kinetics does not exceed ±10%, the comparison of the $[M_S^H{\cdot}H{\cdot}G]^+/[M_R^D{\cdot}H{\cdot}G]^+$ and $[M_S^D{\cdot}H{\cdot}G]^+/[M_R^H{\cdot}H{\cdot}G]^+$ pairs confirms the expectation that H/D isotopic effects do not affect appreciably the relevant reaction kinetics. The kinetic isotope effects (K_{IE}) are between 0.84 and 1.14. The only exception in all considered reactions is the tyrosinol complex (N_6) reacting with 2-propylamine ($K_{IE} = 0.74$). The exchange rates differ significantly for the labelled and the unlabelled adducts. Therefore the isotopomers M_S^H and M_S^D were investigated simultaneously with other bases of similar proton affinity as shown in Table 6.2. The reacting gases were 2-propylamine, 1-propylamine, 1-pentylamine and morpholine. In further experiments the achiral resorcinarenes were investigated as well. The achiral adducts with the octamethylated resorcinarenes (index A denotes the resorcinarenes as

Base	Proton Affinity[a]	Host	cm^3 s^{-1} · molecule × 10^{11}	K_{IE}
2-propylamine	220.8	M^{H}_{S}	0.0639	0.76
		M^{D}_{S}	0.0844	
2-propylamine	220.8	M^{H}_{R}	0.1000	0.74
		M^{D}_{R}	0.1354	
2-propylamine	220.8	M^{H}_{A}	0.00450	0.91
		M^{D}_{A}	0.00495	
1-propylamine	219.4	M^{H}_{S}	0.0249	0.95
		M^{D}_{S}	0.0263	
1-pentylamine	220.7	M^{H}_{S}	0.2549	1.06
		M^{D}_{S}	0.2410	
morpholine	220.9	M^{H}_{S}	0.1120	0.99
		M^{D}_{S}	0.1130	

Table 6.2: Reaction rates of the complexes [M·H·(*S*)-tyrosinol]$^+$ with different amines.
[a] Proton affinities are given in kcal mol^{-1}.

achiral) reacted overall more slowly than the chiral complexes (Table 6.2). But the labelled and the unlabelled resorcinarenes M^{D}_{A} and M^{H}_{A}, respectively, with the same pace. A significant kinetic isotope effect was observed only in the reaction of tyrosinol complexes with inherently chiral resorcinarenes in reaction with 2-propylamine.

For resorcinarenes and methylated resorcinarenes a series of MS studies and calculations is known in the literature.[104,105] In all cases the aliphatic lateral chains do not interact with charged guests. This lead to further investigations of the involved binding sites. With NMR techniques the complexes of tyrosinol (N_6) and (1*R*,2*R*)-2-amino-1-phenylpropane-1,3-diol (N_{12}) were investigated (Section 6.4). A further inside into the complexation modi gave DFT-based calculations of the tyrosinol adducts (Section 6.5).

If the guest interacts with the chiral surface of the host, the exchange reaction with a chiral amino base should also be affected by the configuration of the neutral base B. The enantioselectivity in this case is expressed as ξ by the reaction rates of a complex towards (*S*)- and (*R*)-2-butylamine. Differing from the previously discussed experiments, the reaction rates of two different experiments for each complex are compared. This enantioselectivity is expressed by the $\xi = k_R/k_S$ ratios of the reactions shown in Figure 6.26. The enantioselectivities of adduct [M^{H}_{S}·H·G]$^+$ are displayed as $\xi_S = (k_R)^S/(k_S)^S$ and those of [M^{D}_{R}·H·G]$^+$ are displayed

$$[M_R \cdot H \cdot B_R]^+ \xleftarrow[+\,B_R\,-\,G]{(k_R)^R} [M_R \cdot H \cdot G]^+ \xrightarrow[+\,B_S\,-\,G]{(k_S)^R} [M_R \cdot H \cdot B_S]^+ \qquad \frac{(k_R)^R}{(k_S)^R} = \xi_R$$

$$[M_S \cdot H \cdot B_R]^+ \xleftarrow[+\,B_R\,-\,G]{(k_R)^S} [M_S \cdot H \cdot G]^+ \xrightarrow[+\,B_S\,-\,G]{(k_S)^S} [M_S \cdot H \cdot B_S]^+ \qquad \frac{(k_R)^S}{(k_S)^S} = \xi_S$$

Figure 6.26: Reaction rates (k) for the homochiral and the heterochiral adducts with a chiral amino base B. The enantioselectivity ξ is the ratio of reaction rates.

as $\xi_R = (k_R)^R/(k_S)^R$, respectively (Figure 6.27).

The enantioselectivities ξ diverge significantly from each other, thus the configuration of the reacting base has a rather high influence on the reactivity. During the proton transfer from the proton-bound complex to the neutral amine that replaces the guest, there is an effective interaction with the chiral *upper rim* of the resorcinarene.

The enantioselectivity ρ values of all considered reactions (Figures 6.22-6.25) may be attributed to purely thermodynamic factors due to different stabilities of the diastereomeric adducts or kinetic factors due to different transition state structures (see also Figure 6.16). A first hint gives the comparison of the enantioselectivities for diastereomeric complexes reacting with gases of different proton affinities (Figure 6.28). For most of the reactions the enantioselectivity decreases with an increasing proton affinity. The only exception is the reactivity of the epinephrine complex (guest N_{13}) with an overall low enantioselectivity. The

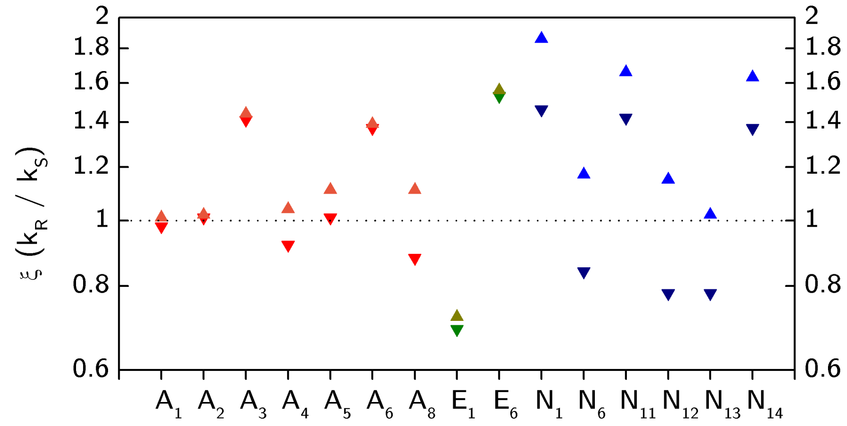

Figure 6.27: Enantioselectivities k_R/k_S of the reactions towards 2-butylamine. Reactions of the $[M_S^H{\cdot}H{\cdot}G]^+$ complexes (triangles downwards) and $[M_R^D{\cdot}H{\cdot}G]^+$ (triangles upwards).

reactions become more exothermic with a more basic amine and is therefore less sensitive to the complexation by the resorcinarene. Thus the measured selectivities arise from a different stability of the transition structures in the reaction of the diastereomeric $[M{\cdot}H{\cdot}G]^+$ complex to the product $[M{\cdot}H{\cdot}B]^+$ complex instead of simply reflecting the thermodynamic stability of the diastereomeric adducts. The highest enantioselectivity was measured for guests bearing at least two hydroxyl groups and an amino group as there are (1*R*,2*R*)-2-amino-1-phenylpropane-1,3-diol (N_{12}) and (*S*)-5-hydroxy-tryptophane (A_5). The hydroxyl groups may interact with the upper rim of the resorcinarene and the basic amino group keeps the charge and behaves as the effective hook. The effect of the neutral gas proton affinity on the selectivity clearly indicates that enantioselectivity originates from kinetic factors.

All kinetic plots exhibit a monoexponential decay with an excellent linearity. This indicates that there is one kinetically distinguishable $[M{\cdot}H{\cdot}G]^+$ population reacting with a pseudo-first order rate constant. Furthermore, investigations on the conformation of the resorcinarene are necessary. The complex is either formed in solution before evaporating the nano-ESI nanodroplets in the ion source or during that process. As shown by CD spectroscopy, the preferred conformation of the resorcinarene in methanol is the *boat* conformation (Section 6.2); DFT calculation on the geometry always predict a *crown* conformation.[104,105] In the following section the complex formation in solution (Section 6.4) and DFT calculations of the diastereomeric adducts are discussed (Section 6.5).

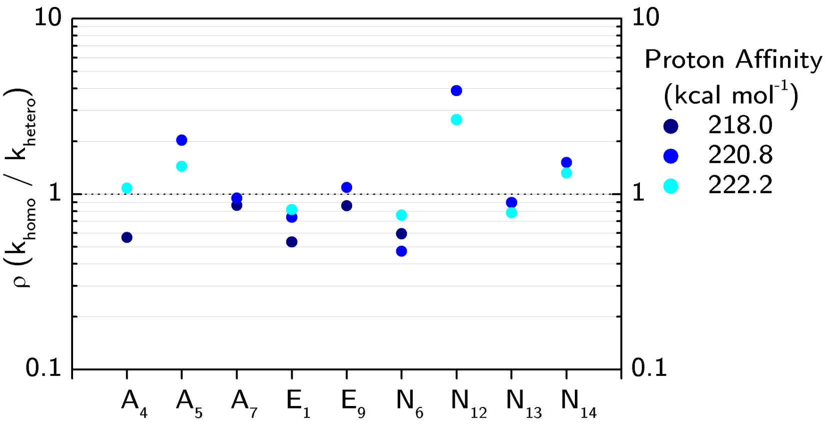

Figure 6.28: Enantioselectivity as the k_{homo}/k_{hetero} ratio with respect to the amine proton affinity of ethylamine (218.0 kcal mol^{-1}), 2-propylamine (220.8 kcal mol^{-1}) and 2-butylamine (222.2 kcal mol^{-1}).

6.4 Diastereomeric Complexes in Solution

The potential of the resorcinarenes as chiral receptors was demonstrated by MS studies in the gas phase. In this section the complex formation in solution is presented. The resorcinarenes were dissolved as racemic mixtures in $CDCl_3$, CD_2Cl_2, MeOH-d_4 or DMSO-d_6, the chiral guests N_6 and N_{12} (Figure 6.29) were added (5 equivalents) in solid form and the suspensions were sonicated. A filtration was necessary and the solutions were investigated by ^1H, ^2H and ^{13}C-NMR spectroscopy. In $CDCl_3$, a complex formation with (1*R*,2*R*)-2-amino-1-phenylpropane-1,3-diol (N_{12}) was observed in a very small amount of less than 1% signal intensities in the ^1H spectrum (Figure 6.30). The new signals could be ascribed to shifted proton resonances of a diastereomeric complex with lower symmetry than the C_4-symmetry of the resorcinarene.

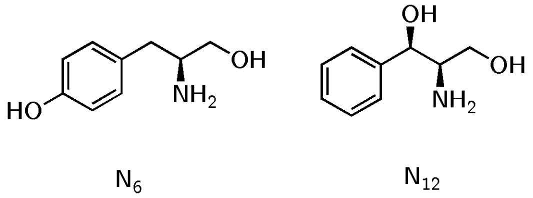

Figure 6.29: Guests (1*R*,2*R*)-2-amino-1-phenylpropane-1,3-diol (N_{12}) and tyrosinol (N_6) for complex formation experiments in solution.

In the absence of a polar solvent the charged amino alcohols were insoluble in $CDCl_3$ or CD_2Cl_2 (Figure 6.31 a). For this purpose reference spectra were recorded from the suspension as well as from the filtrate and no other signals except the solvent residue signals occurred. The complex is formed in a very small amount (Figure 6.31 b) as can be seen in detail in Figure 6.32. After addition of a small amount of DMSO to a non-filtered suspension, only the signals of the free resorcinarene and the chiral amino compound are observed (Figure 6.31 c); the supramolecular interactions between the host and the guest are destroyed by the solvent interactions. In the polar solvent DMSO and in the protic solvent methanol a complex formation does not occur at all (Figure 6.31 d). On the NMR time scale the interconversion between the two boat conformations is too fast to be detected as a set of distinct signals at ambient temperature.

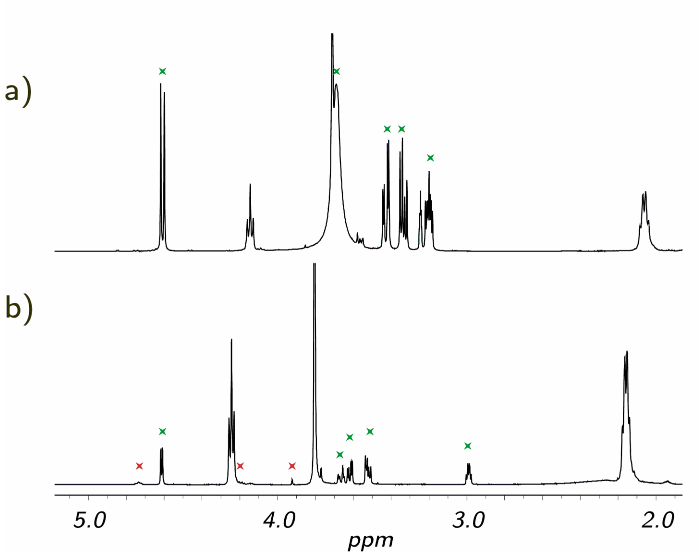

Figure 6.30: ^{1}H-NMR spectra of (a) *rac*-**79** and (1*R*,2*R*)-2-amino-1-phenylpropane-1,3-diol (N_{12}) in MeOH-d_4 and (b) *rac*-**80** and (1*R*,2*R*)-2-amino-1-phenylpropane-1,3-diol in $CDCl_3$. The signals of the free (1*R*,2*R*)-2-amino-1-phenylpropane-1,3-diol are marked with green stars and the signals arising from the complex are marked with red stars.

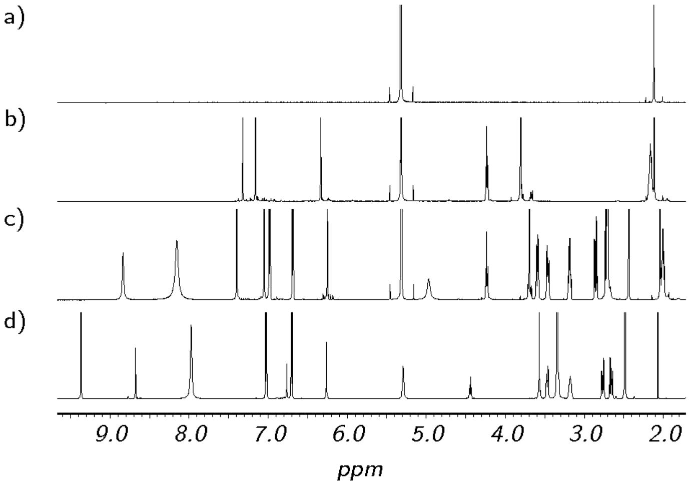

Figure 6.31: ^{1}H-NMR spectra (600 MHz) of (a) tyrosinol in CD_2Cl_2, (b) *rac*-**79** and tyrosinol in CD_2Cl_2, (c) *rac*-**79** and tyrosinol in CD_2Cl_2 and 50μL of DMSO-d_6, (d) *rac*-**79** and tyrosinol in DMSO-d_6.

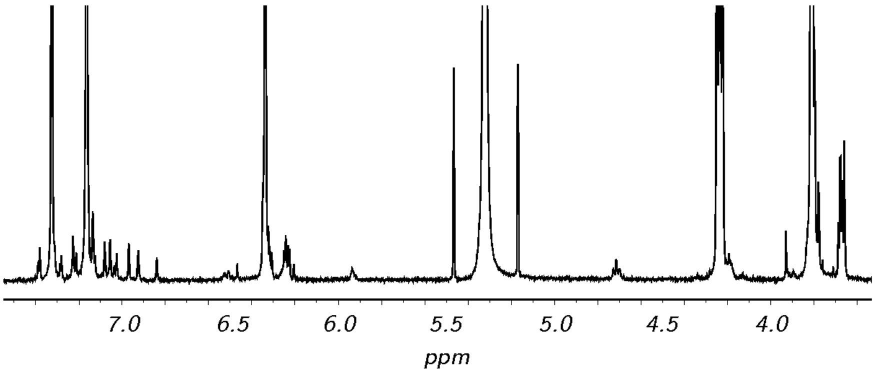

Figure 6.32: Partial ^{1}H-NMR spectra (600 MHz) *rac*-**79** and tyrosinol in CD_2Cl_2.

As there was a kinetic isotope effect observed in the reactions of the diastereomeric adducts, the complexes were investigated by ^{2}H-NMR spectroscopy to elucidate the role of the aliphatic side chain. The ^{2}H-NMR spectrum of *rac*-**80** shows a singlet at 0.84 ppm assigned to the terminal CD_3 group of the alkyl chains (Figure 6.33). Surprisingly, a new signal appears at 1.55 ppm when tyrosinol was added as HCl salt. This result was not obtained when traces of acids like aqueous hydrochloric acid or trifluoroacetic acid were added to the resorcinarene solution in $CDCl_3$. Probably the tyrosinol accelerates the proton/deuterium exchange of water brought into the sample with the tyrosinol. Thus the signal is ascribed to water (D_2O and HDO) and not to terminal methyl groups involved into a complexation process.

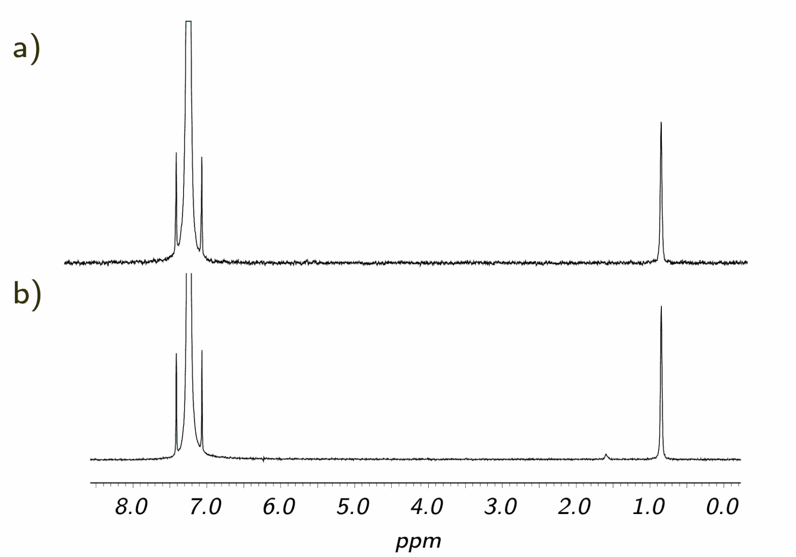

Figure 6.33: Partial ^{2}H-NMR spectra (92 MHz) of (a) *rac*-**80** in $CDCl_3$ and (b) *rac*-**80** and tyrosinol $CDCl_3$.

The yield of the diastereomeric adducts in apolar solution is rather low. The small complex amount besides the free host and guest molecules are not sufficient for detailed investigations concerning e.g. the thermodynamic stability and enantioselectivity in solution. The studies in solution especially those by CD spectroscopy suggest a predominance of the *boat* conformation in protic solvents and in mixtures of a non polar and a hydrogen bonding solvent. In the gas phase the geometry optimisation leads to the C_4-symmetric scaffold of the resorcinarene. Only when adding four methanol molecules the boat conformation is stable.

6.5 DFT-Calculations of the Diastereomeric Complexes

The thermodynamic stability of the diastereomeric complexes of the inherently chiral resorcinarene in *S* configuration and (*R*)- and (*S*)-tyrosinol, respectively, were calculated by DFT means. The long alkyl chains at the *lower rim* were replaced by methyl groups. ALEXANDER ROZHENKO used the RI-BP86 method for geometry optimisation and vibration frequencies calculations. There are two stable conformations A and B close in energy for the diastereomeric adduct shown in Table 6.3.

When associated in the conformation A, the ammonium group and the two hydroxyl groups are coordinated by the resorcinarene. The aromatic part is therefore inside the cavity (Table 6.3 a, b and e, f) and the aromatic hydroxyl group takes part in the complexation. In the conformation B only the ammonium and the vicinal hydroxyl functionalities are coordinated. The aromatic moiety points outside the cavity (Table 6.3 c, d and g, h). For both guest configurations the energies are very similar.

Regarding the exchange reactions, in all cases the ammonium groups are suggested to be a centre for the nucleophilic attack by the amine molecule. In the conformation B, the ammonium site is shielded by the aromatic rings and other substituents and deeply inside the cavity. The ammonium group is more accessible in the conformation A for the attack by the replacing amine. The total energy, calculated for the most favored conformation for a replacement reaction, the homochiral complex in conformation A (e and f), is significantly higher than that obtained for the corresponding conformation B of the homochiral complex (g, h), and therefore, the adduct exists predominantly in the conformation "ring outside".

In the considered conformations the calculations predict a higher stability for the heterochiral complexes. Hence, if the selectivity of the amino exchange reaction of the heterochiral complex originates only from the thermodynamic stability, the reaction would proceed more slowly than that of the homochiral complex, resulting in an enantioselectivity value above $\rho = 1$. This contradicts the experimental results giving selectivities of $0.47 \pm 0.02 < \rho < 0.84 \pm 0.03$ and supports the assumption that kinetic factors are responsible for the selectivity.

In further studies, molecular dynamic calculations (MD) will be performed on the conformational switch of the resorcinarene. The diastereomers may interconvert between a *crown* and a *boat* conformation, depending on non-covalent interactions stabilising the *boat* conformation that is without coordinating solvent molecules not favoured in the gas phase.[92]

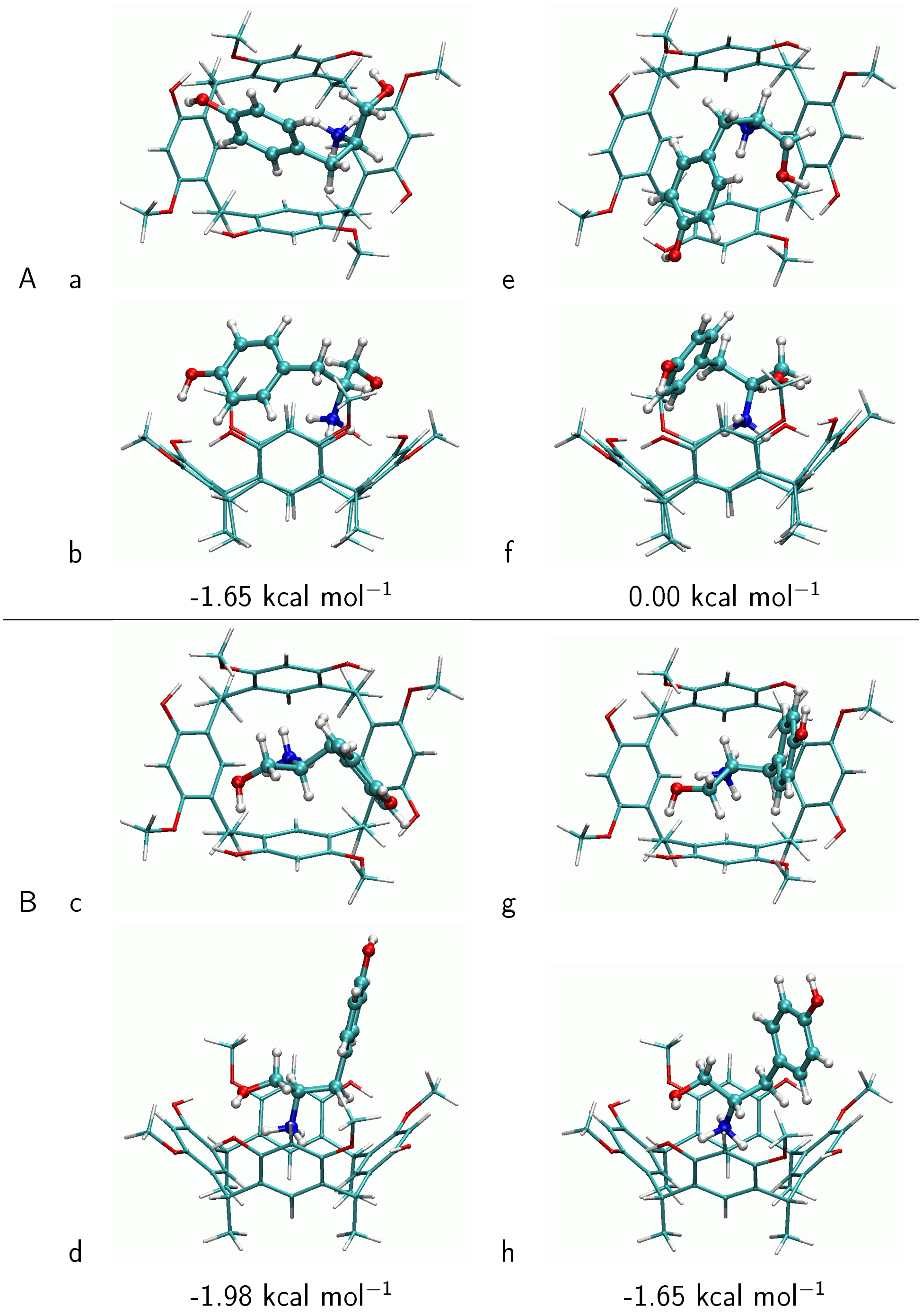
A
a
e
b
f
-1.65 kcal mol^{-1}
0.00 kcal mol^{-1}
B
c
g
d
h
-1.98 kcal mol^{-1}
-1.65 kcal mol^{-1}

Table 6.3: Different adducts of chiral host with (*R*)-tyrosinol in the confomations A (a, b) and B (c, d) and (*S*)-tyrosinol in confomations A (e, f) and B (g, h).

Conclusion

A complete set of inherently chiral resorcinarenes and their *quasi*-enantiomeric counterparts was prepared and the racemates were resolved. The conformations of the enantiomerically pure resorcinarenes in different solvents were characterised by CD spectroscopy with no molecular difference with respect to the labelling. The *quasi*-racemates were investigated by means of the nano-ESI-FT-ICR technique in guest exchange reactions with achiral and chiral amines. The ratio of the reaction rates quantifies the enantioselectivity of the diastereomeric adducts. In most cases the heterochiral complexes react faster than the homochiral (up to 2.5 times for guest 3,4-dihydroxy-(*S*)-phenylalanine, A_2). There are few exceptional cases with opposite enantioselectivity like the complexes of (1*R*,2*R*)-2-amino-1-phenylpropane-1,3-diol (N_{12}) whereas the homochiral complex reacts four times faster than the heterochiral homologue. Further insight into the complex geometry was gained by DFT calculations of (*S*)- and (*R*)-tyrosinol adducts with the resorcinarene of (*S*) chirality. The thermodynamic stability is similar for both complexes, but the heterochiral diastereomer is slightly more stable and should react more slowly. As the experimental results gives the opposite enantioselectivity, it is ascribed mainly to kinetic factors. In solution these complexes have low association constants as shown by NMR studies.

7 Summary

In the first part of this work a general route to prepare amidoresorcinarenes was developed. The achiral resorcinarene precursors were transferred into the methylated scaffold and into the cavitand, respectively. In both macrocycles four carboxylic acid groups were introduced in an overall four steps synthesis. The amidoresorcinarenes **44**-**47** were prepared from tetracarboxylic acids precursors and the corresponding amino acid methylesters. With TBTU, HOBt and triethylamine in DCM the tetrakisphenylalanine macrocycles were synthesised free of racemisation in moderate yields.

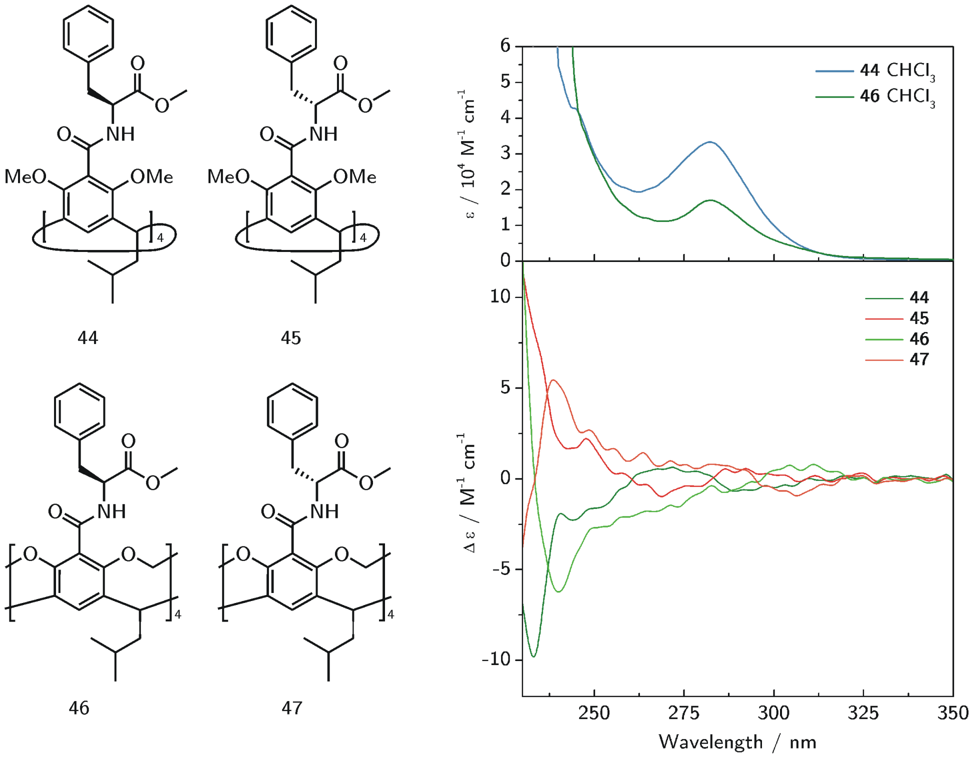

Figure 7.1: Synthesised amidoresorcinarenes and -cavitands. UV/Vis and CD spectra in chloroform.

Both enantiomers generated and their CD spectra indicate the enantiomeric nature of the compounds (Figure 7.1). In solvents of different polarity the structural conformation is slightly changed. In further MS experiments, the influence of the flexibility on enantiodiscriminating processes of the rigid and the more-flexible hosts can be directly compared in their complexation behaviour towards chiral guests.

The cavity-extension of inherently chiral resorcinarenes with a C_4 symmetric substitution pattern was carried out in the second part of this work. Starting from the tetramethoxyresorcinarene with known absolute configuration a tetrabiaryl motif was build up *via* a tetrakis(2´-bromobenzyl) ether **54** as intermediate compound. The successive reaction sequence allows the unambiguous assignment of the configuration at the methine moieties of the macrocycles derived from resorcinarene **19** as shown in Figure 7.2. The four C-C-bonds were formed in a Pd catalysed, intramolecular coupling reaction yielding the tetrabiarylether **55**.

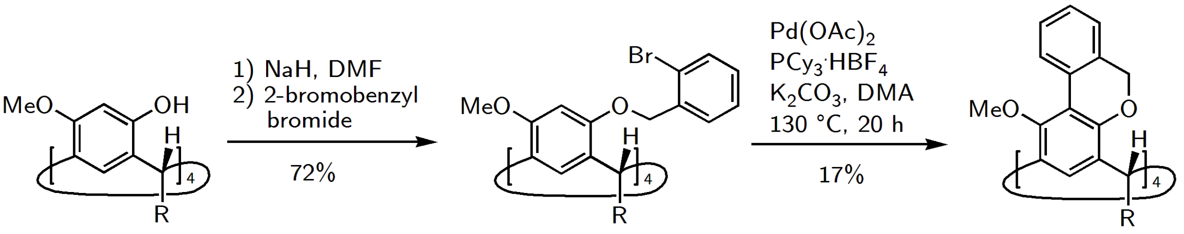

(*M,R*)-(−)-**19**

(*P,S*)-(+)-**54**

(*P,S*)-(+)-**55**

R=C_4H_9

Figure 7.2: Reaction of (*M,R*)-(−)-**19** to tetrakis(2´-bromobenzyl)ether (*P,S*)-(+)-**54** and the cyclic tetrabiaryl ether (*P,S*)-(+)-**55**.

In the biarylether formation reaction four chiral axes as new stereogenic elements are generated. From conformational analysis of tetrabiarylether **55** by NMR spectroscopy the biaryl units are found to be very rigid in solution. The conformation of the atropisomers was elucidated by evaluation of CD spectroscopic data and analysis of the X-ray structure. The CD signal was simulated by TDPPP-calculations for the structure obtained from the X-ray data and matches very well with the experimental CD spectra (Figure 7.3). Biarylethers are stable in their configuration and no helimerisation in the cyclic ether units occurs that could have led to diastereomer formation. The cavity-extended resorcinarenes are of cycloenantiomeric character.

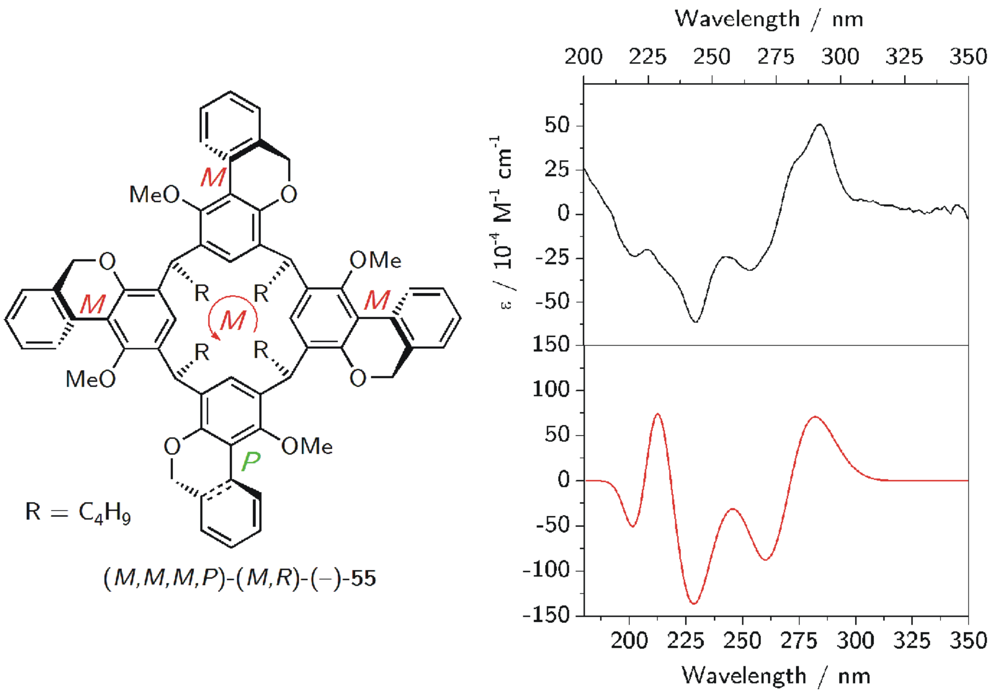

Figure 7.3: Configuration of (*M*,*M*,*M*,*P*)-(*M*,*R*)-(−)-**55** and CD spectra in cyclohexane (red line). The spectrum of (*M*,*M*,*M*,*P*)-(*M*,*R*)-(−)-**55** was generated by TDPPP calculations (black line).

In the third part of the work the synthesis of a system with unlabelled and labelled resorcinarenes was developed. The labelling was introduced in the lateral alkyl chains remote from the binding sites at the *upper rim* to prevent an isotope effect on the binding event in chiral recognition studies by means of MS. In a three step synthesis 1-undecanal-11,11,11-d_3 (**76**) was prepared from 1-undecen-10-ol (**71**) in an overall good yield of 54% (Figure 7.4).

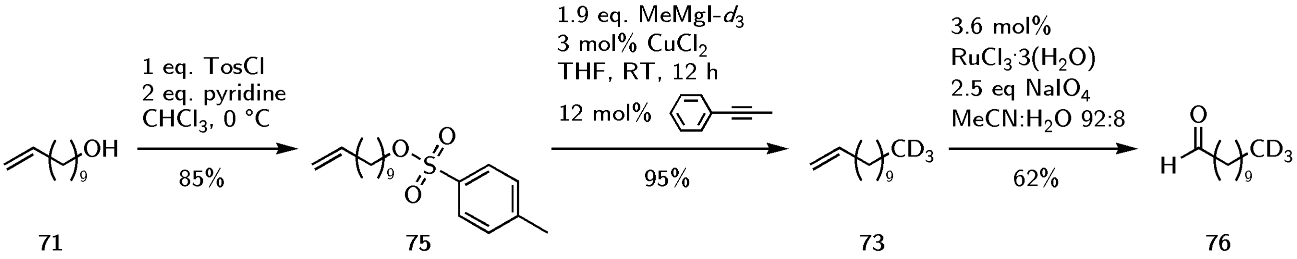
1 eq. TosCl
2 eq. pyridine
CHCl₃, 0 °C
85%
1.9 eq. MeMgI-d₃
3 mol% CuCl₂
THF, RT, 12 h
12 mol%
95%
3.6 mol%
RuCl₃·3(H₂O)
2.5 eq NaIO₄
MeCN:H₂O 92:8
62%
OH
9
O
S
O
O
9
CD₃
9
O
H
CD₃
9
71
75
73
76

Figure 7.4: Synthesis of labelled 1-undecanal-11,11,11-d_3 *via* a copper catalysed reaction of MeMgI-d_3 with tosylate **75**. Alkene **73** was oxidised with $NaIO_4$ to aldehyde **76** in an overall yield of 54%.

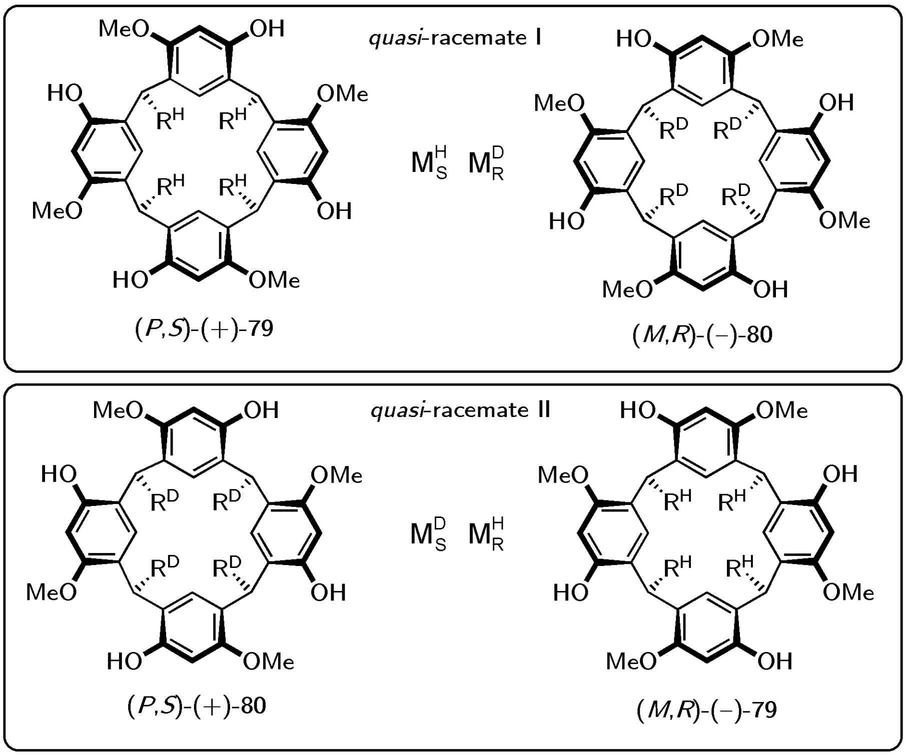

$R^H = C_{10}H_{21}$
$R^D = C_{10}H_{18}D_3$

Figure 7.5: Synthesised *quasi*-racemats of inherently chiral resorcinarenes with lablelled and non-labelled side chains.

The labelled aldehyde **76** was reacted to the racemic resorcinarene *rac*-**80**-d_{12} in a $BF_3{\cdot}Et_2O$ catalysed condensation reaction with 3-methoxyphenol. For the resolution of the enantiomers a synthetic protocol was developed. The monofunctionalisation with (*S*)-(+)-10-camphorsulfonic acid as chiral auxiliary yielded diastereomers that were separable by HPLC. The *quasi*-racemate of the inherently chiral tetramethoxyresorcinarenes were investigated regarding their enantiodiscriminating properties in true gas phase experiments in an ICR cell. The charged *quasi*-diastereomeric complexes with chiral amino alcohols, amino acids and amino acid esters were reacted with volatile amines in exchange reactions. The enantioselectivities were in the range of $0.40 < \rho < 3.89$, whereas the aminodiol guests exhibit a remarkably high enantiorecognition for an artificial system. In most cases the heterochiral diastereomeric adducts react faster than their homochiral analogues. The exceptions are (1*R*,2*R*)-2-amino-1-phenylpropane-1,3-diol (N_{12}), (*S*)-5-hydroxy-tryptophane (A_5) and (*S*)-norepinephrine (N_{14}). The two hydroxyl groups and the amino functionality interact selectively with the *upper rim* hydroxyl groups as shown by DFT calculations of a tyrosinol complex. The enantioselectivity is both sensitive to the proton affinity and to the configuration of the base. These results point at an enantioselectivity mainly due to diastereomeric transition structures and therefore due to kinetic factors.

Table 7.1: Highest measured enantioselectivities of $[M{\cdot}H{\cdot}G]^+$ complexes.

Guest G	enantioselectivity ρ	Base
A_2	ρ_1 0.391±0.014	ethylamine
	ρ_2 0.398±0.015	
A_5	ρ_1 2.029±0.111	2-propylamine
	ρ_2 2.202±0.131	
N_{12}	ρ_1 0.472±0.018	2-propylamine
	ρ_2 0.843±0.032	
N_{12}	ρ_1 3.940±0.233	(*R*)-2-butylamine
	ρ_2 3.065±0.188	

A kinetic isotope effect that was detected in only one reaction of tyrosinol. In reactions with different bases and different hosts, e.g. achiral non-labelled and labelled resorcinarenes (**85** and **86**-d_{12}, Figure 7.6), the isotope effect is absent. To understand the impact of the deuterated chains on the complexation behaviour molecular dynamic calculations are in progress.

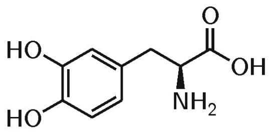
HO
HO
O
OH
NH2

A_2

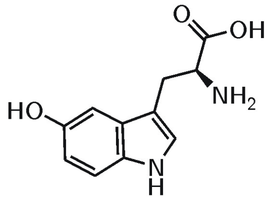
O
OH
NH2
HO
N
H

A_5

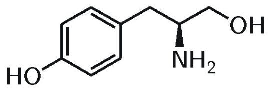

N_6

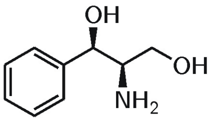

N_{12}

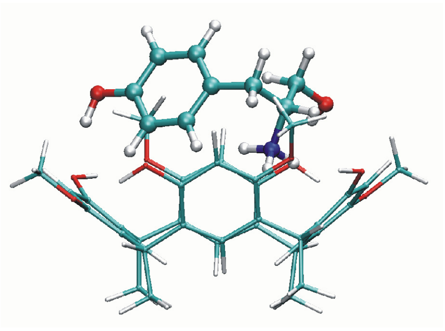

Figure 7.6: Chiral guests that show high enantioselectivities in complexes with inherently chiral resorcinarenes. Tyrosinol on complex with the inherently chiral resorcinarene.

8 Experimental Section

8.1 General Remarks

All solvents used were of an analytically pure quality or purified by distillation. Melting points were determined with a Buchi B-540 apparatus and are uncorrected. NMR spectra were recorded with a Bruker DRX 500 (^{1}H NMR: 500.13 MHz, ^{13}C NMR: 125.77 MHz) or a Bruker Avance 600 (^{1}H NMR: 600.13 MHz, ^{13}C NMR: 150.90 MHz) instrument in $CDCl_3$ with $CHCl_3$ as reference (^{1}H: 7.24 ppm, ^{13}C: 77.0 ppm), in CD_2Cl_2 with CH_2Cl_2 as reference (^{1}H: 5.32 ppm, ^{13}C: 53.8 ppm), in MeOH-d_4 with MeOH as reference (^{1}H: 3.30 and 4.78 ppm, ^{13}C: 49.0 ppm), in DMSO-d_6 with DMSO as reference (^{1}H: 2.49 ppm, ^{13}C: 39.5 ppm). Single-crystal X-ray analyses were carried out at 100(2) K with a Nonius KappaCCD diffractometer by using Mo-K_α radiation of the wavelength 0.71073 Å. The structures were solved and refined with SHELXS-97 with refinements on F^2. The hydrogen atoms were normally calculated to idealised temperature factors and refined as riding atoms. Disordered solvent molecules and pendant alkyl chains were treated isotropically. IR spectra were recorded with a Nicolet 380 infrared spectrophotometer with an ATR cell. HRMS were recorded with a Bruker APEX III with ESI in positive ion mode, and spectra were internally calibrated with HP TuneMix (*m/z* = 622/922/1522). Specific rotations were recorded with a Perkin-Elmer 341 polarimeter. $[\alpha]_\mathrm{D}$ values are given in units of $10^{-1\circ}$cm^2 g^{-1}. CD spectra were recorded in cyclohexane or methanol at room temperature with a JASCO J-810 spectropolarimeter.

8.2 ESI-FT-ICR Experiments

The experiments were performed at room temperature in an APEX III FT-ICR mass spectrometer fitted with an nano-ESI source (Apollo Bruker) and a resonance cell ("infinity cell") located between the poles of a superconducting magnet (7.0 T). The starting $CH_3OH/CHCl_3$

(10:1) solutions contained the cyclochiral hosts M_S^H (1×10^{-5} M), M_R^D (1×10^{-5} M) and a threefold excess of the selected guest G (6×10^{-5} M). The resulting ions were transferred into the resonance cell by use of a system of potentials and lenses and were quenched by collisions with Argon, pulsed into the cell through a magnetic valve. The mass spectra of the ESI solutions are characterised by the almost exclusive presence of the intense signals corresponding to the proton-bound complex $[M{\cdot}H{\cdot}G]^+$. These non-covalent charged aggregates were isolated by broad-band ejection of the not abundant accompanying ions and allowed to react with a neutral gas B, (B = ethylamine, 2-propylamine, (*R*)-2-butylamine, (*S*)-2-butylamine), present in the cell at constant and controlled pressure (from 2.0×10^{-9} to 4.5×10^{-8} mbar, depending upon its reactivity). Comparing the kinetic results obtained with the *quasi*-diasteromeric $[M_S^H{\cdot}H{\cdot}G]^+/[M_R^D{\cdot}H{\cdot}G]^+$ mixture with those obtained with the $[M_S^D{\cdot}H{\cdot}G]^+/[M_R^H{\cdot}H{\cdot}G]^+$ one may provide a way for estimating any hypothetical isotope effect on the kinetics.

8.3 Synthesis of Amidoresorcinarenes and -Cavitands from Achiral Resorcinarenes

8.3.1 Tetracarboxylic acid resorcinarene 39

Resorcinarene tetracarboxylic acid methyl ester **38** (1.50 g, 1.42 mmol) was dissolved in *i*-PrOH (150 mL) and 50 mL of aqueous KOH solution (20% per weight) were added. Solution was heated under reflux for 10 h. The mixture was carefully acidified with diluted HCl under cooling with an ice bath to pH 1 and extracted with ethyl acetate (3 × 150 mL). The combined organic phases were washed with brine and dried with $MgSO_4$. The solvent was reduced to to a volume of few mL under reduced pressure and the solution was stored in the refrigerator overnight. The colourless precipitate was filtered off to yield the tetracarboxylic acid **39** (960 mg, 68%). ^{1}H-NMR (500 MHz, DMSO, 25°C): $\delta = 13.17$ (sb, 4H), 6.95 (s, 4H), 4.60 (t, $^3J = 7.5$ Hz, 4H), 3.33 (s, 24H), 1.75 (sb, 8H), 1.36-1.32 (m, 4H), 0.88 (d, $^3J = 6.3$ Hz,) ppm. MS (MALDI-ToF, 2,5-DHB, positive): calcd. for $C_{56}H_{72}NaO_{16}^+$ ($[M+Na]^+$) 1024.15; found 1024.45.

8.3.2 Tetracarboxylic acid cavitand 42

Cavitand **41** (581 mg, 595 μmol) was dissolved in *i*-PrOH (50 mL) and 20 mL of aqueous KOH solution (20% per weight). The solution was heated under reflux for 10 h. The mixture was carefully acidified to pH 2 with diluted HCl under cooling with an ice bath and extracted with ethyl acetate (3 × 200 mL). The combined organic phases were washed with brine and dried with $MgSO_4$. The solvent was removed under reduced pressure. The colourless residue was suspended in ethyl acetate and the precipitate was filtered off to yield the tetracarboxylic acid **42** (399 mg, 72%). ^{1}H-NMR (500 MHz, DMSO, 25°C): $\delta = 13.23$ (sb, 4H), 7.67 (s, 4H), 5.76 (d, $^2J = 7.5$ Hz, 4H), 4.73 (t, $^3J = 8.2$ Hz, 4H), 4.37 (d, $^2J = 7.53$ Hz, 4H), 3.32 (s, 12H), 2.27 (t, $^2J = 7.22$ Hz, 8H), 1.50-1.45 (m, 4H) 0.98 (d, $^3J = 6.3$ Hz, 24H) ppm. ^{13}C-NMR (125 MHz, DMSO, 25°C): $\delta = 165.3$, 149.5, 138.4, 125.3, 122.9, 99.0, 37.6, 34.1, 25.9, 25.5, 22.5 ppm.

HRMS-ESI: calcd. for $C_{52}H_{57}O_{16}^+$ ($[M+H]^+$) 937.3641; found 937.3651, declination 1.0 mmu/ 1.1 ppm.

8.3.3 General protocol of the amide formation

The corresponding tetracarboxylic acid (1.0 eq.), TBTU (4.1 eq.) and HOBt (4.0 eq.) were suspended in DCM (ca. 1 mL/1 μmol) at 0 °C and NEt_3 (16 eq.) was added. After stirring the solution for 1 h the ice bath cooled phenylalanine methyl ester hydrochloride (4.1 eq.) solution in DCM and NEt_3 (6 eq.) was added slowly. The reaction mixture was stirred at room temperature overnight. Then saturated ammonium chloride solution was added. The phases were separated and the organic phase was washed with brine and dried with $MgSO_4$. The solvent was removed under reduced pressure and the slight yellow residue was filtered through a short column of silica gel (cyclohexane/ethyl acetate 55:45 (v:v)). The amidoresorcinarene was purified by HPLC (cyclohexane/ethyl acetate 55:45 (v:v)).

8.3.4 (*S*)-Tetrakisphenylalanine resorcinarene 44

Resorcinarene **39** (50.0 mg, 50.0 μmol) was reacted to amidoresorcinarene **44** following the general procedure for amide formation. Compound **44** was yielded as glassy solid (19.8 mg, 24%).

^{1}H-NMR (500 MHz, CDCl$_3$): $\delta = 7.22$-7.16 (m, 10-H, 11-H, 12-H, 20H), 6.80 (sb, 3-H, 4H), 5.06 (dd, $^2J = 13.0$ Hz, $^3J = 6.7$ Hz, NH, 4H), 4.49 (t, $^3J = 7.5$ Hz, H$_\alpha$, 4H), 3.28 (s, 13-H, 12H), 3.49 (sb, OMe, 12H), 3.28 (dd, $^2J = 13.9$ Hz, $^3J = 5.3$ Hz, 9-H, 4H), 3.19 (dd, $^2J = 14.0$ Hz, $^3J = 7.0$ Hz, 9-H, 4H), 1.57 (sb, H$_\beta$, 8H), 1.55-1.47 (m, H$_\gamma$, 4H), 0.92 (d, $^3J = 6.3$ Hz, H$_\delta$, 24H) ppm. ^{13}C-NMR (125 MHz, CDCl$_3$): $\delta = 171.6$, 166.3, 153.9, 136.4, 129.4, 128.5, 127.8, 126.9, 125.2, 61.9, 53.9, 52.2, 44.0, 38.6, 37.8, 34.8, 25.8, 23.0, 22.7 ppm. HRMS-ESI: calcd. for $C_{96}H_{120}N_5O_{20}^+$ $[M+NH_4]^+$ 1662.8521; found 1662.8524, declination 0.3 mmu/ 0.2 ppm.

8.3.5 (*R*)-Tetrakisphenylalanine resorcinarene 45

Resorcinarene **39** (49.8 mg, 49.7 μmol) was reacted to amidoresorcinarene **45** following the general procedure for amide formation. Compound **45** was yielded as glassy solid (14.7 mg, 18%).

^{1}H-NMR (500 MHz, CDCl$_3$): $\delta = 7.23$-7.17 (m, 10-H, 11-H, 12-H, 20H), 6.80 (sb, 3-H, 4H), 5.06 (dd, $^2J = 13.0$ Hz, $^3J = 6.5$ Hz, NH, 4H), 4.49 (t, $^3J = 7.5$ Hz, H$_\alpha$, 4H), 3.28 (s, 13-H, 12H), 3.50 (sb, OMe, 24H), 3.28 (dd, $^2J = 13.9$ Hz, $^3J = 5.3$ Hz, 9-H, 4H), 3.19 (dd, $^2J = 14.0$ Hz, $^3J = 7.0$ Hz, 9-H, 4H), 1.57 (sb, H$_\beta$, 8H), 1.56-1.47 (m, H$_\gamma$, 4H), 0.92 (d, $^3J = 6.3$ Hz, H$_\delta$, 24H) ppm. ^{13}C-NMR (125 MHz, CDCl$_3$): $\delta = 171.6$, 166.2, 153.9, 136.4, 129.4, 128.5, 127.8, 126.9, 125.2, 61.9, 53.9, 52.1, 44.0, 38.6, 37.8, 34.8, 25.8, 23.0, 22.7 ppm. HRMS-ESI: calcd. for $C_{96}H_{116}N_4O_{20}Na^+$ ($[M+Na]^+$) 1666.8075; found 1667.8087, declination 1.2 mmu/ 0.7 ppm.

8.3.6 (*S*)-Tetrakisphenylalanine cavitand 46

Cavitand **41** (100 mg, 107 μmol) was reacted to amidoresorcinarene **46** following the general procedure for amide formation. Compound **46** was yielded as colourless solid (57.6 mg, 34%).

^{1}H-NMR (500 MHz, CDCl$_3$): $\delta = 7.26$ (t, $^3J = 7.5$ Hz, 11-H, 11´-H, 8H), 7.20 (d, $^3J = 7.5$ Hz, 12-H, 4H), 7.16 (t, $^3J = 7.5$ Hz, 10-H, 10´-H, 8H), 7.07 (s, 3-H, 4H), 6.36 (d, $^3J = 8.2$ Hz, NH, 4H), 5.41 (d, $^2J = 7.5$ Hz, 14-H$_{\text{outer}}$, 4H), 4.96 (dd, $^2J = 13.5$ Hz, $^3J = 6.0$ Hz, 8-H, 4H), 4.87 (t, $^3J = 8.2$ Hz, H$_\alpha$, 4H), 4.51 (d, $^2J = 7.5$ Hz, 14-H$_{\text{inner}}$, 4H), 3.69 (s, 13-H, 12H), 3.18 (dd, $^2J = 14.1$ Hz, $^3J = 5.3$ Hz, 9-H, 4H), 3.10 (dd, $^2J = 13.8$ Hz, $^3J = 6.3$ Hz, 9-H, 4H), 2.10-2.00 (m, H$_\beta$, 8H), 1.56-1.48 (m, H$_\gamma$, 4H), 1.00 (dd, $^3J = 6.3$ Hz, $^4J = 5.0$ Hz, H$_\delta$, 24H) ppm.

^{13}C-NMR (125 MHz, CDCl$_3$): $\delta = 171.6$, 163.8, 151.9, 151.5, 138.2, 135.8, 129.3, 128.6, 127.0, 125.2, 121.5, 100.1, 53.4, 52.3, 38.7, 37.9, 34.0, 25.9, 22.9, 22.8 ppm. HRMS-ESI: calcd. for $C_{92}H_{101}N_4O_{20}^+$ ([M+H]$^+$) 1581.7004; found 1581.7028, declination 2.4 mmu/ 1.5 ppm.

8.3.7 (*R*)-Tetrakisphenylalanine cavitand 47

Cavitand **41** (54.3 mg, 58.0 μmol) was reacted to amidoresorcinarene **47** following the general procedure for amide formation. Compound **47** was yielded as colourless solid (20.2 mg, 22%).

^{1}H-NMR (500 MHz, CDCl$_3$): $\delta = 7.26$ (t, $^3J = 7.5$ Hz, 11-H, 11´-H, 8H), 7.20 (d, $^3J = 7.5$ Hz, 12-H, 4H), 7.16 (t, $^3J = 7.5$ Hz, 10-H, 10´-H, 8H), 7.07 (s, 3-H, 4H), 6.36 (d, $^3J = 8.2$ Hz, NH, 4H), 5.40 (d, $^2J = 7.5$ Hz, 14-H$_{\text{outer}}$, 4H), 4.94 (dd, $^2J = 13.3$ Hz, $^3J = 6.0$ Hz, 8-H, 4H), 4.87 (t, $^3J = 8.1$ Hz, H$_\alpha$, 4H), 4.51 (d, $^2J = 7.5$ Hz, 14-H$_{\text{inner}}$, 4H), 3.68 (s, 13-H, 12H), 3.18 (dd, $^2J = 14.1$ Hz, $^3J = 5.3$ Hz, 9-H, 4H), 3.10 (dd, $^2J = 13.8$ Hz, $^3J = 6.3$ Hz, 9-H, 4H), 2.10-2.01 (m, H$_\beta$, 8H), 1.56-1.48 (m, H$_\gamma$, 4H), 1.00 (dd, $^3J = 6.3$ Hz, $^4J = 5.0$ Hz, H$_\delta$, 24H) ppm. ^{13}C-NMR (125 MHz, CDCl$_3$): $\delta = 171.6$, 163.8, 151.9, 151.4, 138.2, 135.7, 129.3, 128.6, 127.0, 125.2, 121.5, 100.1, 53.3, 52.3, 38.7, 37.9, 34.0, 25.9, 22.9, 22.8 ppm. HRMS-ESI: calcd. for $C_{92}H_{101}N_4O_{20}^+$ ([M+H]$^+$) 1581.7004; found 1581.7035, declination 3.0 mmu/ 2.0 ppm.

8.4 Synthesis of Tetrabiaryl ether 55

8.4.1 Tetrakis-(2´-bromobenzyl)ether tetramethoxyresorcinarene *rac*-54

NaH (60% in paraffin oil, 2.20 g, 55.0 mmol) was washed with cyclohexane and suspended in dry DMF (50 mL). A solution of *rccc*- 2,8,14,20-tetraisobutyl-4,10,16,22-tetra-*O*-methyl-resorcin[4]arene (*rac*-**19**; 2.00 g, 2.60 mmol) in dry DMF (30 mL) was added dropwise, and the suspension was stirred for 0.5 h at ambient temperature. 2-Bromobenzyl ether (2.78 g, 11.1 mmol, 4.3 equiv.) was dissolved in DMF (10 mL) and added dropwise. After the mixture was stirred for 12 h, methanol (5 mL) was added to remove the excess amount of NaH. The solvent was removed in vacuo, and the residue was dissolved in water and $CHCl_3$. The layers were separated, and the aqueous phase was extracted with $CHCl_3$ (2×40 mL). The combined organic phase was washed with brine, dried with anhydrous $MgSO_4$ and evaporated under reduced pressure. The colourless solid was recrystallised from $CHCl_3$/MeOH (4:1, v:v) to give *rac*-**54** as colourless crystals (3.15 g, 84 %). M.p. 210-212 °C. ^{1}H-NMR (500 MHz, $CDCl_3$): $\delta = 7.530$ (dd, $^3J = 8.2$ Hz, $^4J = 1.3$ Hz, 4H, 3-H), 7.305 (d, $^3J = 7.6$ Hz, 4H, 6-H), 7.159 (td, $^3J = 6.6$ Hz, $^4J = 1.3$ Hz, 4H, 5-H), 7.118 (td, $^3J = 7.5$ Hz, $^4J = 1.3$ Hz, 4H, 4-H), 6.697 (s, 4H, ArH *meta* $ArOCH_3$), 6.384 (s, 4H, ArH *ortho* $ArOCH_3$), 5.030 (d, $^2J = 12.6$ Hz, 4H, OCH_2), 4.819 (d, $^2J = 13.2$ Hz, 4H, OCH_2), 4.715 (t, $^3J = 7.6$ Hz, 4H, H_α), 3.424 (s, 12H, OCH_3), 1.758 (m, 8H, H_β), 1.598 (m, 4H, H_γ), 0.897 (d, $^3J = 6.3$ Hz, 12H, H_δ), 0.863 (d, $^3J = 6.3$ Hz, 12H, H_δ) ppm. ^{13}C-NMR (125 MHz, $CDCl_3$): $\delta = 155.64$ ($ArOCH_3$), 154.55 ($ArOCH_2$), 136.97 (C-1´), 132.10 (C-3´), 129.25 (C-6´), 128.81 (C-4´), 127.36 (C-5´), 126.45 (Ar_q), 126.39 (Ar_q), 125.97 (Ar_q), 121.94 (ArBr), 97.51 (ArH *ortho* CO), 69.98 (OCH_2), 55.59 (OCH_3), 43.81 (C_β), 33.46 (C_α), 25.94 (C_γ), 22.89 (C_δ), 22.79 (C_δ) ppm. IR (KBr): $\widetilde{\nu} = 2951$, 2864, 2831, 1610, 1582, 1498, 1464, 1444, 1405, 1381, 1364, 1297, 1192, 1130, 1098, 1042, 1026, 944, 912, 813, 781, 750, 664, 613 cm^{-1}. UV/Vis (cyclohexane): λ_{max} (ϵ, mol^{-1}dm^{3}cm^{-1}) = 224 (64000), 286 (17000) nm. HRMS-ESI: calcd. for $C_{76}H_{88}Br_4NO_8^+$ $[M+NH_4]^+$ 1458.3238; found 1458.3246, declination 0.8 mmu/ 0.6 ppm. Elemental Analysis: $C_{76}H_{84}O_8Br_4$ (1445.1): calcd. C 63.17, H 5.86; found C 63.07, H 5.98.

rac-**54**: Crystal size 0.30×0.30×0.26 mm, monoclinic, $P2_1/c$, a = 19.1950(2) Å, b = 23.9900(3) Å, c = 15.98900(10) Å, $\beta = 111.2580(5)°$, $Z = 4$, $V = 6861.76(10)$ ^{3}, $\rho_{calcd.} =$ 1.399 mg m^{-3}, $2\Theta_{max} = 54.96°$, $\mu = 2.401$ mm^{-1}, $F(000) = 2976$, 817 parameters, $R_1 =$

0.0500, $wR_2 = 0.1299$ {for 12184 reflections $[I > 2\sigma(I)]$}, $R = 0.0682$, $wR(F_2) = 0.1425$ (for 15680 unique reflections), $R_{\text{int}} = 0.057$, $S = 1.035$, $\Delta\rho$ (min/max) = -1.59/2.81 eÅ^{-3}.

8.4.2 Tetrakis-(2´-bromobenzyl)ether tetramethoxyresorcinarene (*M*,*R*)-(–)-54

NaH (60% in paraffin oil, 130 mg, 3.25 μmol) was washed twice with cyclohexane and suspended in dry DMF (6 mL). A solution of (*P*,*S*)-(+)-**19** (143 mg, 186 μmol) in dry DMF (12 mL) was added dropwise, and the suspension was stirred for 0.5 h at room temperature. 2-Bromobenzyl ether (398 mg, 1.59 mmol) was dissolved in DMF (3 mL) and added dropwise. After the mixture was stirred for 12 h, methanol (5 mL) was added to remove the excess amount of NaH. The solvent was removed in vacuo, and the residue was dissolved in water and $CHCl_3$. The phases were separated, and the aqueous phase was extracted with $CHCl_3$ (3×15 mL). The combined organic phase was washed with brine, dried with anhydrous $MgSO_4$ and evaporated under reduced pressure. The colourless residue was purified by column chromatography (SiO_2; cyclohexane/ethyl acetate, 9:1) to yield 247 mg of (*M*,*R*)-(–)-**54** (92 %). $[\alpha]_D^{25}$ = -4.2 (c = 0.69, $CHCl_3$). HRMS-ESI: calcd. for $C_{76}H_{88}Br_4NO_8^+$ $[M+NH_4]^+$ 1458.3238; found 1458.3217, declination 2.1 mmu/ 1.4 ppm.

8.4.3 Tetrakis-(2´-bromobenzyl)ether tetramethoxyresorcinarene (*P*,*S*)-(+)-54

NaH (60% in paraffin oil, 30.0 mg, 750 μmol) was washed twice with cyclohexane and suspended in dry DMF (6 mL). A solution of (*M*,*R*)-(–)-**19**(72.0 mg, 93.6 μmol) in dry DMF (5 mL) was added dropwise, and the suspension was stirred for 0.5 h at room temperature. 2-Bromobenzyl ether (103 mg, 412 μmol) was dissolved in DMF (8 mL) and added. After the mixture was stirred for 12 h, methanol (5 mL) was added to remove the excess amount of NaH. The solvent was removed in vacuo, and the residue was taken up with water (40 mL) and $CHCl_3$ (30 mL). The phases were separated, and the aqueous phase was extracted with $CHCl_3$ (3×15 mL). The combined organic phase was washed with brine, dried with anhydrous $MgSO_4$ and evaporated under reduced pressure and purified by column chromatography (cyclohexane/ethyl acetate, 4:1) to yield the colourless solid of (*P*,*S*)-(+)-**54** (98.0 mg, 72%). $[\alpha]_D^{25}$

= +5.6 (c = 1.00, $CHCl_3$). HRMS-ESI: calcd. for $C_{76}H_{88}Br_4NO_8^+$ $[M+NH_4]^+$ 1458.3238; found 1458.3244, declination 0.6 mmu/ 0.4 ppm.

Tetrabiaryl Ether *rac*-**55**: *rac*-**54** (500 mg, 346 μmol), dried K_2CO_3 (383 mg, 2.77 mmol) and DMA (10 mL) were placed and in a two-necked round-bottom flask. The suspension was degassed by three freeze-pump-thaw cycles. $Pd(OAc)_2$ (67.0 mg, 298 μmol) and $PCy_3{\cdot}HBF_4$ (206 mg, 559 μmol) were added under an argon atmosphere. The yellow mixture was heated to 130 °C for 20 h. The suspension turned black and was filtered through silica gel. The solvent was removed under reduced pressure, and the residue was purified by column chromatography (SiO_2; cyclohexane/ethyl acetate, 95:5). The colourless solid was recrystallised from $CHCl_3$/MeOH (4:1, v:v) to yield *rac*-**55** (60.2 mg, 16%). M.p. 207°C (decomp.). ^{1}H-NMR (500 MHz, $CDCl_3$, 57°C): $\delta = 8.121$ (d, $^3J = 6.9\,Hz$, 4H, 10-H), 7.029-7.160 (m, 12H, 7-H, 8-H, 9-H), 6.728 (s, 4H, 3-H), 4.848 (d, $^2J = 11.9\,Hz$, 4H, 6-H), 4.759 (t, $^3J = 7.5\,Hz$, 4H, H_α), 4.637 (d, $^2J = 12.6\,Hz$, 4H, 6-H), 3.285 (s, 12H, 11-H), 1.811 (m, 8H, H_β), 1.682 (m, 4H, H_β), 1.027 (d, $^3J = 6.9\,Hz$, 12H, H_δ), 1.010 (d, $^3J = 6.9\,Hz$, 12H, H_δ) ppm. ^{13}C-NMR (125 MHz, $CDCl_3$): $\delta = 154.31$ (C-1), 151.91 (C-4a), 131.97 (Ar_q), 129.67 (Ar_q), 128.21 (C-7 or C-8 or C-9), 126.66 (C-7 or C-8 or C-9), 126.27 (C-3), 125.67 (C-10), 124.11 (C-7 or C-8 or C-9), 115.52 (C-10b), 68.38 (C-6), 59.74 (OCH_3), 44.05 (C_β), 34.34 (C_α), 25.97 (C_γ), 22.88 (C_δ) ppm. UV/Vis (cyclohexane): $\lambda_{max}\,(\epsilon, mol^{-1}dm^3cm^{-1}) = 224$ (68000), 278 (50000), 316 (16000) nm. HRMS-ESI: calcd. for $C_{76}H_{84}NO_8^+$ $[M+NH_4]^+$ 1138.6192; found 1138.6200, declination 0.9 mmu/ 0.8 ppm. Elemental Analysis: $C_{76}H_{80}O_8{\cdot}CHCl_3$ (1240.8): calcd. C 74.53, H 6.58; found C 74.52, H 6.33.

rac-**55·1.5CHCl$_3$**: Crystal size 0.30×0.22×0.08 mm, triclinic, $P\bar{1}$, a = 12.4810(2) Å, b = 15.5000(3) Å, c = 18.5860(4) Å, α = 98.1190(9)°, β = 108.1580(10)°, γ = 95.1430(10)°, Z = 2, V = 3347.95(11) ^{3}, $\rho_{calcd.}$ = 1.290 mg m^{-3}, $2\Sigma_{max}$ = 54.96°, μ = 0.254 mm^{-1}, $F(000)$ = 1374, 841 parameters, R_1 = 0.0610, wR_2 = 0.1585 {for 11846 reflections [$I > 2\sigma(I)$]}, R = 0.0799, $wR(F_2)$ = 0.1745 (for 15260 unique reflections), R_{int} = 0.042,S = 1.023, $\Delta\rho$ (min/max) = -0.75/0.61 Å^{-3}.

(*M*,*R*)-(–)-**Tetrabiaryl Ether** (*M*,*R*)-(–)-**55**: (*M*,*R*)-(–)-**54** (200 mg, 138 μmol), dried K_2CO_3 (174 mg, 1.26 mmol) and DMA (10 mL) were placed and in a two-necked round-bottom flask. The suspension was degassed by two freeze-pump-thaw cycles. $Pd(OAc)_2$ (50.1 mg, 223 μmol) and $PCy_2{\cdot}HBF_4$ (162 mg, 440 μmol) were added under an argon atmosphere. The yellow mixture was heated to 130 °C for 20 h. The suspension turned black and was filtered through silica gel. The solvent was removed under reduced pressure, and the residue was purified by column chromatography (SiO_2; cyclohexane/ethyl acetate, 95:5) to yield (*M,R*)-(−)-**55** as a colourless solid (18.1 mg, 12%). $[\alpha]_D^{25}$ = -7.1 (c = 1.00, $CHCl_3$). HRMS-ESI: calcd. for $C_{76}H_{88}NO_8$ $[M+NH_4]^+$ 1138.6192; found 1138.6199, declination 0.8 mmu/ 0.7 ppm.

(*P,S*)-(+)-**Tetrabiaryl Ether** (*P,S*)-(+)-**55**: (*P,S*)-(+)-**54** (80.0 mg, 55.3 μmol), dried K_2CO_3 (86.1 mg, 623 mmol) and DMA (10 mL) were placed and in a two-necked round-bottom flask. The suspension was degassed by three freeze-pump-thaw cycles. $Pd(OAc)_2$ (18.0 mg, 80.0 μmol) and $PCy_3{\cdot}HBF_4$ (24.7 mg, 162 μmol) were added under an argon atmosphere. The yellow mixture was heated to 130 °C for 20 h. The suspension turned black and was filtered through silica gel. The solvent was removed under reduced pressure, and the residue was purified by column chromatography (SiO_2; cyclohexane/ethyl acetate, 95:5) to yield (*P,S*)-(+)-**55** as a colourless solid (10.3 mg, 17%). $[\alpha]_D^{25}$ = +7.2 (c = 1.00, $CHCl_3$). HRMS-ESI: calcd. for $C_{76}H_{88}NO_8$ $[M+NH_4]^+$ 1138.6192; found 1138.6199, declination 0.8 mmu/ 0.7 ppm.

8.4.4 Synthesis of Tetrakis-(2´-bromo-4´-(methoxycarbonyl))tetramethoxyresorcinarene 58

NaH (60% in paraffin oil) was washed twice with cyclohexane and suspended in dry DMF (70 mL) under an argon atmosphere. A solution of *rccc*-2,8,14,20-tetraundecyl-4,10,16,22-tetra-*O*-methylresorcin[4]arene (*rac*-**49**; 2.26 g, 1.95 mmol) in DMF (20 mL) was added dropwise, and the suspension was stirred for 2 h at ambient temperature. Methyl 3-bromo-4-(bromomethyl)benzoate (4.00 g, 11.7 mmol, 6.0 equiv.) was dissolved in DMF (10 mL) and added dropwise. After the mixture was stirred for 1 h, the reaction was quenched with diluted hydrochloric acid (2 M) under cooling with an ice bath. Then ethyl acetate was added (120 mL) and the two phases were separated. The aqueous phase was extracted with ethyl acetate (80 mL) and the combined phases were washed with water (50 mL) and brine (80 mL). The solvent was evaporated under reduced pressure and the light brown residue was purified by column chromatography (SiO_2; cyclohexane/ethyl acetate, 8:1) to yield 2.18 g (54%) of *rac*-**58**. ^{1}H-NMR (500 MHz, $CDCl_3$): $\delta = 8.19$ (d, $^4J = 1.3$ Hz, 4H, 3´-H), 7.81 (dd, $^4J = 0.6$ Hz, $^3J = 8.2$ Hz, 4H, 5´-H), 7.40 (d, $^3J = 7.5$ Hz, 4H, 6´-H), 6.72 (s, 4H), 6.36 (s, 4H), 5.03 (d, $^2J = 13.8$ Hz, 4H), 4.85 (d, $^2J = 13.8$ Hz, 4H), 4.55 (t, $^3J = 7.5$ Hz, 4H), 3.90 (s, 12H), 3.46 (s, 12H), 1.87-1.86 (m, 8H), 1.24-1.19 (m, 72H), 0.84 (t, $^3J = 6.9$ Hz, 12H) ppm. ^{13}C-NMR

(125 MHz, $CDCl_3$): $\delta = 165.5$, 155.7, 154.3, 142.1, 133.2, 130.6, 128.3, 126.6, 126.4, 126.1, 121.1, 97.4, 69.7, 55.7, 52.3, 35.8, 34.6, 31.9, 30.0, 29.82, 29.75, 29.71, 29.35, 28.3, 22.7, 14.1 ppm. MS (MALDI-ToF, 2,5-DHB, positive): calcd. for $C_{112}H_{148}Br_4NaO_{16}^+$ ($[M+Na]^+$) 2092.97; found 2092.85.

8.5 Synthesis of the Labelled Aldehyde 76

8.5.1 1-Dodecene-12,12,12-*d*$_3$ 73

10-Undecen-1-ol *p*-toluenesulfonate (**75**; 12.6 g, 38.8 mmol) was dissolved in 160 mL THF under argon atmosphere. $CuCl_2$ (163 mg, 1.21 mmol) and 1-phenylpropyne (593 mg, 5.11 mmol) were added and the solution turned orange. The mixture was cooled with an ice bath and MeMgI-*d*$_3$ (75.0 mL, 75.0 mmol, 1.0 M in diethyl ether) was added slowly with a syringe. A colourless solid precipitates and the solution was stirred at room temperature for 18 h. Sat. ammonium chloride solution (100 mL) was carefully added and then diethyl ether (100 mL). The phases were separated and the organic phase was washed with sat. ammonium chloride solution (80 mL), brine (80 mL) and dried with $MgSO_4$. The solvents were removed under reduced pressure. The yellow oil was placed on a silica gel column and eluted with cyclohexane to yield **73** as a colourless oil (6.124 g, 92%). ^{1}H-NMR (600 MHz, $CDCl_3$): $\delta = 5.80$ (dddd, $^4J = 6.7$ Hz, $^4J = 6.7$ Hz, $^3J = 10.2$ Hz, $^2J = 17.0$ Hz, 1H), 4.98 (ddd, $^4J = 1.9$ Hz, $^3J = 3.8$ Hz, $^2J = 17.0$ Hz, 1H), 4.91 (ddd, $^4J = 1.5$ Hz, $^3J = 3.4$ Hz, $^2J = 10.2$ Hz, 1H), 2.05-2.00 (m, 2H), 1.39-1.34 (m, 2H), 1.27-1.24 (m, 14H) ppm. ^{13}C-NMR (150 MHz, $CDCl_3$): $\delta = 139.3$, 114.1, 33.8, 31.8, 29.6, 29.5, 29.4, 29.2, 29.0, 26.9, 22.4, 13.3, 13.2, 13.1 ppm. HRMS-EI: calcd. for $C_{12}H_{21}D_3$ 171.2066; found 171.2071,, declination 0.5 mmu/ 2.7 ppm.

8.5.2 1-Undecanal-11,11,11-*d*$_3$ 76

1-Dodecene-12,12,12-*d*$_3$ **73** (4.006 g, 23.4 mmol) and $RuCl_3 \cdot 3\ H_2O$ (222 mg, 849 μmol) were dissolved in 120 mL of acetonitrile and water (92:8) under argon atmosphere. Sodium periodate (12.48 g, 58.3 mmol) was added in three portions and the green suspension was stirred for 16 h. A solution of sodium thiosulfate (30 mL, 5% by weight) was added and after stirring for additional 30 min diethyl ether (100 mL) was added. The phases were separated and the aqueous phase was extracted with diethyl ether (3 × 100 mL). The combined organic phases were washed with water (80 mL), brine (80 mL) and dried with $MgSO_4$. The solvents were removed under reduced pressure and the yellow oil was purified by silica gel column chromatography (cyclohexane/ethyl acetate 95:5) to yield the aldehyde **76** as a colourless oil (2.503 g, 62%). IR: $\widetilde{\nu} = 3280$, 2915, 2848, 2715, 2218, 2121, 2073, 1726, 1469, 1411, 1385, 1120, 1052, 1024, 995, 959, 744, 718 cm^{-1}. ^{1}H-NMR (500 MHz, $CDCl_3$): $\delta = 9.74$ (s, 1H), 2.39 (td, $^4J = 1.7$ Hz, $^3J = 7.2$ Hz, 2H), 1.63-1.57 (m, 2H), 1.27-1.23 (m, 14H) ppm.

^{13}C-NMR (125 MHz, $CDCl_3$): $\delta = 203.0$, 43.9, 31.8, 29.5, 29.4, 29.3, 29.1, 22.4, 22.1, 13.3, 13.2, 13.0 ppm. HRMS-ESI: calcd. for $C_{16}H_{31}N_3OD_3^+$ (derivatized with Girard T reagent) 287.2885; found 287.2884, declination 0.1 mmu/ 0.3 ppm.

8.6 Synthesis of racemic Tetramethoxyresorcinarenes 79 and 80

8.6.1 Tetramethoxyresorcinarene *rac*-79

3-Methoxyphenol (3.650 g, 29.4 mmol) and 1-undecanal (**78**) (5.030 g, 29.5 mmol) were dissolved in DCM (100 mL) and cooled to -10 °C under argon atmosphere. $BF_3{\cdot}OEt_2$ (7.50 mL, 59.7 mmol) was added slowly with a syringe. The red reaction mixture was stirred for 2 h at room temperature. The solution was washed with water (3 × 150 mL), brine (100 mL), dried with $MgSO_4$ and the solvent was removed under reduced pressure. The brown residue was treated with methanol in an ultrasonic bath to yield the resorcinarene *rac*-**79** as a colourless powder (4.064 g, 50%). M. p. 100°C. IR: $\widetilde{\nu} = 3381$, 2918, 2849, 1618, 1587, 1495, 1466, 1453, 1425, 1340, 1293, 1237, 1192, 1159, 1096, 1087, 1004, 900, 882, 856, 832, 720, 700, 561, 532 cm^{-1}. ^{1}H-NMR (500 MHz, $CDCl_3$): $\delta = 7.50$ (s, 4H), 7.19 (s, 4H), 6.32 (s, 4H), 4.25 (t, $^3J = 7.5$ Hz, 4H), 3.81 (s, 12H), 2.18-2.14 (m, 8H), 1.35-1.24 (m, 64H), 0.87 (t, $^3J = 6.9$ Hz, 12H) ppm. ^{13}C-NMR (125 MHz, $CDCl_3$): $\delta = 153.6$, 152.9, 124.7, 124.6, 123.7, 100.0, 55.8, 33.9, 33.0, 31.9, 29.7, 29.7, 29.4, 28.1, 22.7, 14.1 ppm. HRMS-ESI: calcd. for $C_{72}H_{113}O_8^+$ ($[M+H]^+$) 1105.8430; found 1105.84295, declination 0.1 mmu/ 0.1 ppm. Elemental Analysis: $C_{72}H_{112}O_8$ (1105.7): calcd. C 78.21, H 10.21; found C 77.90, H 9.83.

8.6.2 Tetramethoxyresorcinarene-d_{12} *rac*-80

3-Methoxyphenol (1.789 g, 14.4 mmol) and 1-undecanal-11,11,11-d_3 **76** (2.503 g, 14.4 mmol) were dissolved in DCM (50 mL) and cooled to 10 °C under argon atmosphere. $BF_3{\cdot}OEt_2$ (3.7 mL, 29.5 mmol) was added slowly with a syringe. The red reaction mixture was stirred for 3 h at room temperature. The solution was washed with water (3 × 80 mL), brine (80 mL), dried with $MgSO_4$ and the solvent was removed under reduced pressure. The red to brown residue was recrystallized from methanol to yield the resorcinarene *rac*-**80** as light

yellow crystals (2.274 g, 56%). M. p. 102°C. IR: $\widetilde{\nu} = 3379$, 2918, 2849, 2211, 2121, 2070, 1618, 1587, 1495, 1466, 1425, 1340, 1293, 1236, 1191, 1159, 1098, 1085, 1052, 1030, 1007, 898, 856, 832, 722, 601, 561, 532, 515, 490 cm^{-1}. ^1H-NMR (500 MHz, $CDCl_3$): $\delta = 7.51$ (s, 4H), 7.21 (s, 4H), 6.34 (s, 4H), 4.27 (t, $^3J = 7.5\,Hz$, 4H), 3.82 (s, 12H), 2.20-2.16 (m, 8H), 1.37-1.26 (m, 64H) ppm. ^{13}C-NMR (125 MHz, $CDCl_3$): $\delta = 153.6$, 152.9, 124.7, 124.6, 123.7, 100.0, 55.8, 33.9, 33.0, 31.9, 29.7, 29.7, 29.4, 28.1, 22.4 ppm. HRMS-ESI: calcd. for $C_{72}H_{101}O_8D_{12}^+$ ($[M+H]^+$) 1117.9183; found 1117.9178, declination 0.5 mmu/ 0.4 ppm. Elemental Analysis: $C_{72}H_{100}O_8D_{12}$ (1117.7): calcd. C 77.37, H 11.18; found C 77.22, H 11.32.

8.7 Resolution of the Tetramethoxyresorcinarene enantiomers

8.7.1 General Procedure of the Diastereomer Formation

The corresponding resorcinarene, K_2CO_3 (5 eq.) and 4-dimethylaminopyridine (2 mol%) were dissolved or suspended in dry THF and dry acetonitrile (2:3, 30 mL/mmol) under an argon atmosphere. A solution of freshly prepared (*S*)-(+)-10-camphorsulfonyl chloride (1.8 eq.) in THF was added and the cloudy mixture was stirred over night. Et_2O was added and the mixture was acidified with diluted hydrochloric acid. The phases were separated and the organic layer was washed with brine and dried with $MgSO_4$. The solvents were removed under reduced pressure. The starting material was removed from the crude product by flash column chromatography on silica gel (cyclohexane/ethyl acetate 65:35). The diastereomers were purified by silica gel HPLC (cyclohexane/ethyl acetate 81:19) and yielded as colourless to yellow foams.

8.7.2 Diastereomers 81a and 81b of Tetramethoxyresorcinarene 79

General procedure diastereomers with tetramethoxyresorcinarene *rac*-**79** (3.936 g, 3.56 mmol), K_2CO_3 (2.680 g, 19.4 mmol), 4-dimethylaminopyridine (8.0 mg, 65.5 μmol) and (*S*)-(+)-10-camphorsulfonyl chloride (1.643 g, 6.55 mmol). The starting material (*rac*-**79**) was removed from the diastereomeric mixture by flash column chromatography on silica gel (cyclohexane/ethyl acetate 65:35). The diastereomers were purified by silica gel HPLC (cyclohexane/ethyl acetate 81:19) and yielded as yellow foams of **81a** (277 mg, 6%) and **81b** (284 mg, 6%).

Diastereomer (*S*,*R*,*S*,*S*,*S*)-(+)-81a

$[\alpha]_D^{25}$ = +215.6 (c = 5.5, $CHCl_3$). IR: $\widetilde{\nu}$ = 3398, 2921, 2852, 1745, 1618, 1587, 1495, 1465, 1372, 1351, 1291, 1237, 1195, 1168, 1093, 1054, 1008, 905, 835, 811, 731, 648, 609, 527 cm^{-1}. ^{1}H-NMR (500 MHz, $CDCl_3$): δ = 7.31 (s, 1H), 7.25 (s, 1H), 7.23 (s, 1H), 7.18 (s, 1H), 7.17 (s, 1H), 7.11 (s, 1H), 7.10 (s, 1H), 6.91 (s, 1H), 6.34 (s, 1H), 6.33 (s, 1H), 6.28 (s, 1H), 4.70 (dd, ^3J = 6.9 Hz, ^2J = 9.0 Hz, 1H), 4.29-4.20 (m, 3H), 3.90 (s, 3H), 3.82 (d, ^2J = 14.8 Hz, 1H), 3.80 (s, 6H), 3.71 (s, 3H), 3.29 (d, ^2J = 14.9 Hz, 1H), 2.52 (ddd, ^4J = 3.7 Hz, ^3J = 11.1 Hz, ^2J = 14.5 Hz, 1H), 2.40 (ddd, ^4J = 3.5 Hz, ^3J = 4.3 Hz, ^2J = 18.4 Hz, 1H), 2.19-1.92 (m, 11H), 1.68 (ddd, ^4J = 4.8 Hz, ^3J = 9.3 Hz, ^2J = 14.1 Hz, 1H), 1.41 (ddd, ^4J = 3.8 Hz, ^3J = 9.1 Hz, ^2J = 12.8 Hz, 1H), 1.36-1.18 (m, 64H), 1.13 (s, 3H), 0.90 (s, 3H), 0.87 (t, ^3J = 6.9 Hz, 12H) ppm. ^{13}C-NMR (125 MHz, $CDCl_3$): δ = 214.1, 156.0, 154.0, 153.6, 153.2, 153.0, 152.5, 145.3, 131.8, 131.2, 126.1, 124.8, 124.7, 124.5, 124.1, 124.0, 123.7, 123.6, 122.7, 104.6, 99.8, 99.7, 58.2, 56.3, 55.8, 55.6, 47.8, 47.6, 43.0, 42.5, 35.8, 34.3, 34.1, 33.4, 33.2, 32.9, 31.9, 29.9, 29.8, 29.7, 29.6, 29.4, 28.0, 27.9, 26.8, 25.4, 22.7, 19.9, 19.7, 14.1 ppm. HRMS-ESI: calcd. for $C_{82}H_{130}NO_{11}S^+$ $[M+NH_4]^+$ 1336.9359; found 1336.9342, declination 1.7 mmu/ 1.3 ppm.

Diastereomer (*S*,*S*,*R*,*R*,*R*)-(–)-81b

$[\alpha]_D^{25}$ = -147.5 (c = 5.7, $CHCl_3$). IR: $\widetilde{\nu}$ = 3405, 2920, 2851, 1747, 1618, 1587, 1495, 1465, 1354, 1293, 1237, 1195, 1169, 1094, 1054, 1014, 903, 836, 811, 722, 610, 528 cm^{-1}. ^{1}H-NMR (500 MHz, $CDCl_3$): δ = 7.33 (s, 1H), 7.29 (s, 1H), 7.25 (s, 1H), 7.18 (s, 1H), 7.16 (s, 1H), 7.14 (s, 1H), 7.13 (s, 1H), 6.93 (s, 1H), 6.34 (s, 1H), 6.32 (s, 1H), 6.28 (s, 1H), 4.66 (dd, ^3J = 7.2 Hz, ^2J = 8.9 Hz, 1H), 4.29-4.20 (m, 3H), 3.90-3.87 (m, 4H), 3.81 (s, 3H), 3.80 (s, 3H), 3.71 (s, 3H), 3.24 (d, ^2J = 14.7 Hz, 1H), 2.54 (ddd, ^4J = 3.8 Hz, ^3J = 11.4 Hz, ^2J = 14.3 Hz, 1H), 2.39 (ddd, ^4J = 3.3 Hz, ^3J = 4.6 Hz, ^2J = 18.6 Hz, 1H), 2.17-1.93 (m, 11H), 1.74 (ddd, ^4J = 4.7 Hz, ^3J = 9.6 Hz, ^2J = 14.0 Hz, 1H), 1.45 (ddd, ^4J = 3.9 Hz, ^3J = 9.3 Hz, ^2J = 12.7 Hz, 1H), 1.35-1.19 (m, 64H), 1.13 (s, 3H), 0.88-0.85 (m, 15H) ppm. ^{13}C-NMR (125 MHz, $CDCl_3$): δ = 214.0, 156.0, 154.0, 153.5, 153.2, 153.1, 153.0, 152.5, 145.1, 131.5, 131.1, 126.2, 124.8, 124.6, 124.1, 124.0, 123.6, 122.7, 122.7, 104.3, 99.9, 99.8, 99.7, 57.9, 56.3, 55.8, 55.6, 47.9, 47.6, 42.9, 42.4, 35.8, 34.4, 34.2, 34.0, 33.3, 33.1, 33.0, 31.9, 29.9, 29.8, 29.7, 29.6, 29.4, 28.0, 27.9, 26.9, 25.1, 22.7, 19.9, 19.7, 14.1 ppm. HRMS-ESI: calcd. for $C_{82}H_{126}O_{11}SNa^+$ ([M+Na]$^+$) 1341.8913; found 1341.8903, declination 1.1 mmu/ 0.8 ppm.

8.7.3 Diastereomers 82a and 82b of Tetramethoxyresorcinarene 80

General procedure diastereomers with tetramethoxyresorcinarene-d_{12} *rac*-**80** (1.888 g, 1.69 m-mol), K_2CO_3 (1.220 g, 8.83 mmol), 4-dimethylaminopyridine (5.0 mg, 40.9 μmol) and (*S*)-(+)-10-camphorsulfonyl chloride (765 mg, 3.05 mmol). The starting material (*rac*-**80**) was removed from the diastereomeric mixture by flash column chromatography on silica gel (cyclohexane/ethyl acetate 65:35). The diastereomers were purified by silica gel HPLC (cyclohexane/ethyl acetate 81:19) and yielded as yellow foams of **82a** (198 mg, 9%) and **82b** (195 mg, 9%).

Diastereomer (*S*,*R*,*S*,*S*,*S*)-(+)-82a

$[\alpha]_D^{25}$ = +51.4 (c = 1.0, $CHCl_3$). IR: $\tilde{\nu}$ = 3397, 2920, 2851, 2210, 2121, 2074, 1740, 1617, 1586, 1495, 1464, 1371, 1355, 1291, 1236, 1195, 1169, 1090, 1048, 1009, 903, 834, 810, 722, 607, 527 cm^{-1}. ^{1}H-NMR (500 MHz, $CDCl_3$): δ = 7.31 (s, 1H), 7.25 (s, 1H), 7.23 (s, 1H), 7.18 (s, 1H), 7.17 (s, 1H), 7.12 (s, 1H), 7.10 (s, 1H), 6.90 (s, 1H), 6.34 (s, 1H), 6.33 (s, 1H), 6.28 (s, 1H), 4.69 (dd, ^3J = 6.9 Hz, ^2J = 9.3 Hz, 1H), 4.29-4.20 (m, 3H), 3.89 (s, 3H), 3.82 (d, ^2J = 14.8 Hz, 1H), 3.80 (s, 6H), 3.71 (s, 3H), 3.29 (d, ^2J = 14.9 Hz, 1H), 2.52 (ddd, ^4J = 3.9 Hz, ^3J = 11.5 Hz, ^2J = 14.2 Hz, 1H), 2.40 (ddd, ^4J = 3.6 Hz, ^3J = 4.4 Hz, ^2J = 18.5 Hz, 1H), 2.23-1.92 (m, 11H), 1.68 (ddd, ^4J = 4.7 Hz, ^3J = 9.3 Hz, ^2J = 14.1 Hz, 1H), 1.41 (ddd, ^4J = 3.7 Hz, ^3J = 9.1 Hz, ^2J = 12.7 Hz, 1H), 1.36-1.22 (m, 64H), 1.13 (s, 3H), 0.90 (s, 3H) ppm. ^{13}C-NMR (125 MHz, $CDCl_3$): δ = 214.1, 156.0, 154.0, 153.6, 153.1, 153.0, 152.5, 145.3, 131.8, 131.2, 126.1, 124.8, 124.6, 124.4, 124.1, 123.9, 123.7, 123.6, 122.7, 104.5, 99.8, 99.7, 58.1, 56.3, 55.8, 55.6, 47.8, 47.6, 42.9, 42.4, 35.8, 34.3, 34.1, 33.4, 33.2, 32.9, 31.8, 29.9, 29.8, 29.7, 29.7, 29.6, 29.4, 28.0, 27.9, 27.9, 26.7, 25.4, 22.4, 19.8, 19.7, 13.3, 13.2, 13.0 ppm. HRMS-ESI: calcd. for $C_{82}H_{118}NO_{11}SD_{12}^+$ [M+NH$_4$]$^+$ 1349.0112; found 1349.0099, declination 1.4 mmu/ 1.0 ppm.

Diastereomer (*S*,*S*,*R*,*R*,*R*)-(−)-82b

$[\alpha]_D^{25}$ = -32.4 (c = 1.0, $CHCl_3$). IR: $\tilde{\nu}$ = 3402, 2920, 2851, 2209, 2123, 2074, 1743, 1617, 1586, 1495, 1464, 1354, 1292, 1236, 1194, 1169, 1090, 1052, 1010, 904, 835, 810, 722, 609, 527 cm^{-1}. ^{1}H-NMR (500 MHz, CDCl$_3$): $\delta = 7.33$ (s, 1H), 7.30 (s, 1H), 7.26 (s, 1H), 7.19 (s, 1H), 7.17 (s, 1H), 7.12 (s, 2H), 6.94 (s, 1H), 6.34 (s, 1H), 6.33 (s, 1H), 6.29 (s, 1H), 4.67 (dd, $^{3}J = 7.2$ Hz, $^{2}J = 8.9$ Hz, 1H), 4.30-4.21 (m, 3H), 3.91-3.88 (m, 4H), 3.81 (s, 3H), 3.80 (s, 3H), 3.72 (s, 3H), 3.25 (d, $^{2}J = 14.8$ Hz, 1H), 2.54 (ddd, $^{4}J = 3.9$ Hz, $^{3}J = 11.6$ Hz, $^{2}J = 14.1$ Hz, 1H), 2.39 (ddd, $^{4}J = 3.3$ Hz, $^{3}J = 4.6$ Hz, $^{2}J = 18.6$ Hz, 1H), 2.20-1.93 (m, 11H), 1.75 (ddd, $^{4}J = 4.7$ Hz, $^{3}J = 9.3$ Hz, $^{2}J = 14.1$ Hz, 1H), 1.44 (ddd, $^{4}J = 3.7$ Hz, $^{3}J = 9.1$ Hz, $^{2}J = 12.7$ Hz, 1H), 1.36-1.17 (m, 64H), 1.14 (s, 3H), 0.86 (s, 3H) ppm. ^{13}C-NMR (125 MHz, CDCl$_3$): $\delta = 214.0$, 156.0, 154.0, 153.5, 153.2, 153.1, 153.0, 152.5, 145.1, 131.5, 131.1, 126.2, 124.8, 124.6, 124.1, 124.0, 123.6, 122.7, 122.7, 104.3, 99.9, 99.8, 99.7, 60.4, 57.9, 56.2, 55.8, 55.6, 47.8, 47.6, 42.9, 42.4, 35.8, 34.4, 34.3, 34.0, 33.3, 33.1, 33.0, 31.8, 29.9, 29.8, 29.7, 29.6, 29.4, 28.0, 27.9, 26.8, 25.1, 22.4, 19.9, 19.7, 13.3, 13.2, 13.0 ppm. HRMS-ESI: calcd. for $C_{82}H_{118}NO_{11}SD_{12}^{+}$ [M+NH$_4$]$^{+}$ 1349.0112; found 1349.0135, declination 1.4 mmu/ 1.0 ppm.

8.7.4 General procedure cleavage of the auxiliaries

The corresponding diastereomer was dissolved in ethanol (20 mL) and an aqueous solution of KOH (10 mL, 20% by weight) was added. After the mixture was heated under refluxed for 2 h the red solution was acidified with conc. hydrochloric acid and extracted with dichloromethane (3 × 80 mL). The combined organic phases were washed with water (80 mL) and brine (100 mL), dried with MgSO$_4$ and the solvent was removed under reduced pressure. The glassy solid was placed on a column of silica gel and eluted with cyclohexane/ethyl acetat 65:35 to yield the enantiomers.

8.7.5 Tetramethoxyresorcinarene (*P*,*S*)-(+)-79

Diastereomer **81a** (275 mg, 208 μmol) was converted into the enantiomer following the general procedure cleavage of the auxiliaries to yield (*P*,*S*)-(+)-**79** as a colourless glassy solid (148 mg, 64%). $[\alpha]_{\mathrm{D}}^{25} = +48.5$ (c = 1.0, CHCl$_3$). CD (cyclohexane): $\lambda_{\mathrm{max}}(\Delta\epsilon) = 212$ (+52), 225 (-11), 237 (+21), 284 (-14), 302 (+22). IR: $\widetilde{\nu} = 3404$, 2922, 2852, 1619, 1589, 1496, 1466, 1427, 1334, 1293, 1237, 1197, 1165, 1093, 1014, 902, 835, 535 cm^{-1}. ^{1}H-NMR (600 MHz, CDCl$_3$): $\delta = 7.48$ (s, 4H), 7.19 (s, 4H), 6.32 (s, 4H), 4.24 (t, $^{3}J = 7.9$ Hz, 4H), 3.81 (s, 12H), 2.20-2.11 (m, 8H), 1.38-1.33 (m, 8H), 1.31-1.21 (m, 56H), 0.87 (t, $^{3}J = 6.8$ Hz, 12H) ppm.

^{13}C-NMR (150 MHz, CDCl$_3$): $\delta = 153.6$, 152.9, 124.7, 124.6, 123.7, 100.0, 55.9, 34.0, 33.0, 31.9, 29.7, 29.6, 29.4, 28.1, 22.7, 14.1 ppm. HRMS-ESI: calcd. for $C_{72}H_{116}NO_8^+$ [M+NH$_4$]$^+$ 1122.8696; found 1122.8680, declination 1.6 mmu/ 1.4 ppm.

8.7.6 Tetramethoxyresorcinarene (*M*,*R*)-(–)-79

Diastereomer **81b** (280 mg, 212 μmol) was converted into the enantiomer following the general procedure cleavage of the auxiliaries to yield (*M*,*R*)-(–)-**79** as a colourless glassy solid (167 mg, 71%). $[\alpha]_D^{25}$ = -47.4 (c = 1.0, CHCl$_3$). CD (cyclohexane): $\lambda_{max}(\Delta\epsilon) = 213$ (-49), 225 (+11), 237 (-20), 284 (+14), 302 (-19). IR: $\tilde{\nu} = 3406$, 2922, 2852, 1619, 1589, 1496, 1466, 1426, 1334, 1293, 1237, 1197, 1165, 1092, 1013, 902, 835, 521 cm^{-1}. ^{1}H-NMR (600 MHz, CDCl$_3$): $\delta = 7.48$ (s, 4H), 7.19 (s, 4H), 6.32 (s, 4H), 4.25 (t, $^3J = 7.6$ Hz, 4H), 3.81 (s, 12H), 2.20-2.11 (m, 8H), 1.38-1.33 (m, 8H), 1.31-1.21 (m, 56H), 0.87 (t, $^3J = 7.2$ Hz, 12H) ppm. ^{13}C-NMR (150 MHz, CDCl$_3$): $\delta = 153.6$, 152.9, 124.7, 124.6, 123.7, 100.0, 55.9, 34.0, 33.0, 31.9, 29.7, 29.6, 29.4, 28.1, 22.7, 14.1 ppm. HRMS-ESI: calcd. for $C_{72}H_{116}NO_8^+$ [M+NH$_4$]$^+$ 1122.8696; found 1122.8672, declination 2.3 mmu/ 2.1 ppm.

8.7.7 Tetramethoxyresorcinarene-d_{12} (*P*,*S*)-(+)-80

Diastereomer **82a** (195 mg, 146 μmol) was converted into the enantiomer following the general procedure cleavage of the auxiliaries to yield (*P*,*S*)-(+)-**80** as a colourless glassy solid (133 mg, 82%). $[\alpha]_D^{25}$ = +49.2 (c = 1.0, CHCl$_3$). CD (cyclohexane): $\lambda_{max}(\Delta\epsilon) = 213$ (+50), 224 (-11), 237 (+21), 285 (-14), 302 (+21). IR: $\tilde{\nu} = 3405$, 2921, 2852, 2209, 2121, 2074, 1619, 1589, 1496, 1466, 1427, 1334, 1293, 1235, 1197, 1165, 1090, 1054, 1011, 903, 835, 528 cm^{-1}. ^{1}H-NMR (600 MHz, CDCl$_3$): $\delta = 7.48$ (s, 4H), 7.19 (s, 4H), 6.32 (s, 4H), 4.25 (t, $^3J = 7.6$ Hz, 4H), 3.81 (s, 12H), 2.18-2.14 (m, 8H), 1.38-1.32 (m, 8H), 1.30-1.22 (m, 56H) ppm. ^{13}C-NMR (150 MHz, CDCl$_3$): $\delta = 153.6$, 153.0, 124.7, 124.6, 123.7, 100.0, 55.9, 34.0, 33.0, 31.9, 29.8, 29.7, 29.7, 29.4, 28.1, 22.4 ppm. HRMS-ESI: calcd. for $C_{72}H_{104}NO_8D_{12}^+$ [M+NH$_4$]$^+$ 1134.9449; found 1134.9439, declination 1.1 mmu/ 1.0 ppm.

8.7.8 Tetramethoxyresorcinarene-d_{12} (*M*,*R*)-(–)-80

Diastereomer **82b** (192 mg, 144 μmol) was converted into the enantiomer following the general procedure cleavage of the auxiliaries to yield (*M*,*R*)-(–)-**80** as a colourless glassy solid (137 mg, 85%). $[\alpha]_{\mathrm{D}}^{25}$ = -48.0 (c = 1.0, $CHCl_3$). CD (cyclohexane): $\lambda_{\mathrm{max}}(\Delta\epsilon) = 213$ (-50), 225 (+11), 237 (-21), 285 (+14), 302 (-21). IR: $\widetilde{\nu} = 3409$, 2921, 2852, 2208, 2121, 2074, 1619, 1589, 1496, 1466, 1427, 1334, 1293, 1235, 1196, 1165, 1090, 1054, 1012, 903, 835, 529 cm^{-1}. ^1H-NMR (600 MHz, $CDCl_3$): $\delta = 7.48$ (s, 4H), 7.19 (s, 4H), 6.32 (s, 4H), 4.25 (t, $^3J = 7.6$ Hz, 4H), 3.81 (s, 12H), 2.18-2.14 (m, 8H), 1.38-1.32 (m, 8H), 1.30-1.22 (m, 56H) ppm. ^{13}C-NMR (150 MHz, $CDCl_3$): $\delta = 153.6$, 153.0, 124.7, 124.6, 123.7, 100.0, 55.9, 34.0, 33.0, 31.9, 29.8, 29.7, 29.7, 29.4, 28.1, 22.4 ppm. HRMS-ESI: calcd. for $C_{72}H_{104}NO_8D_{12}^+$ $[M+NH_4]^+$ 1134.9449; found 1134.9436, declination 1.3 mmu/ 1.1 ppm.

8.8 Synthesis of Octahydroxyresorcinarenes

8.8.1 General procedure Octahydroxyresorcinarenes

Resorcinol and the corresponding aldehyde were dissolved in equimolar amounts in EtOH and hydrochloric acid (conc.). The red solution was heated under reflux for 3 h. The resorcinarene precipitated as yellow solid that was filtered off and washed with water. The light yellow solid was treated with MeOH in an ultrasonic bath and the colourless to light yellow solid was recrystallised from MeOH.

8.8.2 Octahydroxyresorcinarene 83

Resorcinol (3.00 g, 27.2 mmol) and 1-undecanal (**78**, 4.69 g, 27.2 mmol) were reacted to the octahydroxy resorcinarene **83** giving a colourless to light yellow solid (414 mg, 6%). ^1H-NMR (500 MHz, $CDCl_3$): $\delta = 9.61$ (s, 4H), 9.33 (s, 4H), 7.20 (s, 4H), 6.11 (s, 4H), 4.29 (t, $^3J = 7.3$ Hz, 4H), 2.22-2.09 (m, 8H), 1.39-1.26 (m, 64H, 0.88 (t, $^3J = 6.8$ Hz, 12H) ppm. ^{13}C-NMR (125 MHz, Acetone-d_6): $\delta = 152.6$, 125.3, 125.1, 103.5, 34.3, 33.0, 32.7, 29.3, 29.0, 28.8, 28.7, 28.6, 23.3, 14.4 ppm. HRMS-ESI: calcd. for $C_{68}H_{108}NO_8^+$ $[M+NH_4]^+$ 1066.8070; found 1066.8099, declination 3.0 mmu/ 2.8 ppm.

8.8.3 Octahydroxyresorcinarene-*d*$_{12}$ 84

Resorcinol (381 mg, 3.46 mmol) and 1-undecanal-11,11,11-*d*$_3$ (**76**; 600 mg, 3.46 mmol) were reacted to the octahydroxy resorcinarene **84** giving a colourless to light yellow solid (29.0 mg, 4%). ^{1}H-NMR (500 MHz, CDCl$_3$): $\delta = 9.60$ (s, 4H), 9.33 (s, 4H), 7.20 (s, 4H), 6.11 (s, 4H), 4.29 (t, $^3J = 7.3$ Hz, 4H), 2.22-2.09 (m, 8H), 1.39-1.26 (m, 64H) ppm. ^{13}C-NMR (125 MHz, Acetone-*d*$_6$): $\delta = 152.6$, 125.3, 125.1, 103.5, 34.3, 33.0, 32.7, 29.3, 29.0, 28.8, 28.7, 28.5, 22.8 ppm. HRMS-ESI: calcd. for $C_{68}H_{96}NO_8D_{12}{}^+$ [M+NH$_4$]$^+$ 1078.8823; found 1078.8843, declination 2.0 mmu/ 1.9 ppm.

8.9 Synthesis of Octamethoxyresorcinarenes

8.9.1 General procedure of the methylation reaction

NaH (60% in paraffin oil) was washed with cyclohexane and suspended in dry DMF (10 mL) under an argon atmosphere. The racemic, inherently chiral resorcinarene was dissolved in 5 mL DMF and added dropwise to the suspension. After stirring for 2 h MeI (2 eq. per functionality) was slowly added under ice bath cooling and the solution was stirred overnight. The yellow solution was acidified with hydrochloric acid to pH 1 and DCM was added (80 mL). The layers were separated and the aqueous phase was extracted twice with DCM (50 mL). The combined organic phases were washed twice with acidified (40 mL) water and with brine (40 mL). The solution was dried with MgSO$_4$ and the solvent was evaporated under reduced pressure. The resorcinarenes were recrystallised from DCM and MeOH.

8.9.2 Octamethoxyresorcinarene 85

Resorcinarene **79** (200 mg, 181 μmol) was reacted to the octamethylated resorcinarene **85** giving colourless crystals (164 mg, 78%). ^{1}H-NMR (500 MHz, CDCl$_3$): $\delta = 6.58$ (s, 4H), 6.29 (s, 4H), 4.41 (t, $^3J = 7.6$ Hz, 4H), 3.57 (s, 24H), 1.80-1.76 (m, 8H), 1.30-1.22 (m, 56H), 0.84 (t, $^3J = 7.2$ Hz, 12H) ppm. ^{13}C-NMR (125 MHz, CDCl$_3$): $\delta = 155.8$, 126.2, 126.1, 97.1, 56.2, 35.4, 34.6, 31.9, 30.0, 29.9, 29.7, 29.4, 28.2, 22.7, 14.1 ppm. HRMS-ESI: calcd. for $C_{76}H_{124}NO_8^+$ [M+NH$_4$]$^+$ 1178.9322; found 1178.9324, declination 0.2 mmu/ 0.2 ppm.

8.9.3 Octamethoxyresorcinarene-d_{12} 86

Resorcinarene **80** (200 mg, 179 μmol) was reacted to the octamethylated resorcinarene **86** giving colourless crystals (181 mg, 86%). ^{1}H-NMR (500 MHz, CDCl$_3$): $\delta = 6.58$ (s, 4H), 6.29 (s, 4H), 4.41 (t, $^3J = 7.6$ Hz, 4H), 3.57 (s, 24H), 1.81-1.76 (m, 8H), 1.30-1.22 (m, 56H) ppm. ^{13}C-NMR (125 MHz, CDCl$_3$): $\delta = 155.8$, 126.2, 126.1, 97.1, 56.2, 35.4, 34.6, 31.9, 30.0, 29.9, 29.7, 29.7, 29.4, 28.2, 22.4, 13.4, 13.2, 13.1 ppm. HRMS-ESI: calcd. for $C_{76}H_{112}NO_8D_{12}^+$ $[M+NH_4]^+$ 1191.0075; found 1191.0080, declination 0.5 mmu/ 0.4 ppm.

Abbreviations

amu	atomic mass unit
B	base
Boc	*tert*-butyloxycarbonyl
CD	circular dichroism
CSA	camphor sulfonic acid
CSA-Cl	camphor sulfonic acid chloride
Cy	cyclohexyl
DCM	dichloromethane
de	diastereomeric excess
DIBAL-H	diisobutylaluminiumhydride
DMA	*N,N*-dimethylacetamide
DMAP	4-*N,N*-dimethylaminopyridine
DMF	*N,N*-dimethylformamide
EI	electron ionisation
ESI	electrospray ionisation
eq.	equivalent
FAB	fast atom bombardement
FT-ICR	Fourier transform ion cyclotron resonance
G	guest
HOBt	1-hydroxy-1*H*-benzotriazol
HPLC	high performance liquid chromatography
ICR	ion cyclotron resonance
k	reaction rate
K	equilibrium constant
K_{IE}	kinetic isotope effect
M	host
m/z	mass to charge ratio

MALDI-ToF	matrix assisted laser desorption ionisation-time of flight
MeCN	acetonitrile
MeI	methyl iodide
MeI-d_3	methyl iodide-d_3
MeMgI	methylmagnesium iodide
MeMgI-d_3	methylmagnesium iodide-d_3
MS	mass spectrometry
NBS	*N*-bromosuccinimide
NMR	nuclear magnetic resonance
PA	proton affinity
ρ	enantioselectivity of achiral reacting gases
RT	room temperature
TBTU	1-[bis(dimethylamino)methyliumyl]-1H-benzotriazol-3-oxid tetrafluoroborate
THF	tetrahydrofuran
ξ	enantioselectivity of chiral reacting gases

Glossary

In the following there are terms explained that are used in stereochemical descriptions and in mass spectrometry. The terms and definitions are taken from the IUPAC Recommendations in 1996 on "Basic Terminology of Stereochemistry",[106] IUPAC Recommendations on "Glossary of Terms Used in Physical Organic Chemistry",[107] "Stereochemistry of Organic Compounds",[108] "Mass Spectrometric Desk Reference",[109] and from a glossary published by Eames *et al.*[80]

- Chiral recognition: A term used for discrimination between enantiomers, or between enantiotopic ligands, achieved by appropriatly structured reagents or catalysts, either natural, such as enzymes, or synthetic. A broader term is stereoisomer discrimination.
- Isotopomer: Isotopically enriched analogue of a compound differing from each other only in the quantity of an isotope of one of the constituent atoms.

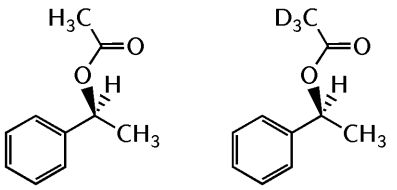

- Isotopologue: A molecular entity that differs only in isotopic composition (number of isotopic substitutions).
- Racemate: A composite (solid, liquid, gaseous, in solution) of equimolar quantities of two enantiomeric species. In the chemical name or formula it may be distinguished from the individual enantiomers by the prefix ±- or *rac*- or by the descriptors *R* and *S*. Synonym: Racemic mixture.
- Racemic compound: A racemate in which two enantiomers form a crystalline compound (which can be recognized from the melting phase diagram or by X-ray structure analysis: The unit cell contains equal numbers of enantiomeric molecules).

- Stereoisotopomers: Isomers with the same topicity (topos ($\tau o \rho o \sigma$, greek), place) of molecular entities, having the same spatial arrangement of the substituents but are non-superimposable.
- Stereoselectivity: The preferential formation of one stereosiomer over another in a chemical reaction.
- Topicity: The stereochemical relationship of substituents relative to the structure to which they are attached.
- *Quasi*-enantiomers: A pair of molecules that have a non-superimposable non-mirror image but have opposite relative configurations at all stereogenic centers. Thus (*S*)-2-bromobutane is the quasienantiomer of (*R*)-2-chlorobutane.

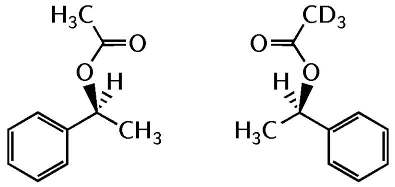

- *Quasi*-racemate: A 1:1 mixture of *quasi*-enantiomers that form a compound, an eutectic, or a solid solution.

Bibliography

[1] a) J.-M. Lehn, *Supramolecular Chemistry*, VCH, Weinheim **1995**; b) J.-M. Lehn, *Chem. Soc. Rev.* **2007**, *36*, 151–160.

[2] J. W. Steed, J. L. Atwood, *Supramolecular Chemistry*, Wiley, Chichester, 2nd Ed. **2009**.

[3] J. Vicens, V. Böhmer (Editor), *Calixarenes - A Versatile Class of Macrocyclic Compounds*, Kluwer Academic Publishers **1991**.

[4] V. Böhmer, *Angew. Chem. Int. Ed.* **1995**, *34*, 713–745.

[5] M. O. Vysotsky, C. Schmidt, V. Böhmer, *Advances in Supramolecular Chemistry*, 139233, JAI Press, Stamford, **2000**.

[6] B. Botta, M. Cassani, I. D´Acquarica, D. Misiti, D. Subissati, G. Delle Monache, *Curr. Org. Chem.* **2005**, *9*, 337–355.

[7] B. Botta, M. Cassani, I. D´Acquarica, D. Subissati, G. Zappia, G. Delle Monache, *Curr. Org. Chem.* **2005**, *9*, 1167–1202.

[8] N. K. Beyeh, M. Kogej, A. Ahman, K. Rissanen, C. A. Schalley, *Angew. Chem. Int. Ed.* **2006**, *45*, 5214–5218.

[9] R. L. McGillivray, J. L. Atwood, *Nature* **1997**, *389*, 469–472.

[10] T. Gerkensmeier, W. Iwanek, C. Agena, R. Fröhlich, S. Kotila, C. Näther, J. Mattay, *Eur. J. Org. Chem.* **1999**, 2257–2262.

[11] H. Dodziuk (Editor), *Cyclodextrines and Their Complexes - Chemistry, Analytical Methods, Applications*, Wiley-VCH, Weinheim **2006**.

[12] K. Tsubaki, M. Nuruzzaman, T. Kusumoto, N. Hayashi, W. Bin-Gui, K. Fuji, *Org. Lett.* **2001**, *3*, 4071–4073.

[13] Y. Kubo, S. Maeda, S. Tokita, M. Kubo, *Nature* **1996**, *382*, 522–524.

[14] C. D. Gutsche, *Calixarenes Revisited*, The Royal Society of Chemistry, Cambridge, **1998**.

[15] J. W. Steed, J. L. Atwood, *Supramolecular Chemistry*, John Wiley & Sons, Chichester, **2009**.

[16] P. Timmerman, W. Verboom, D. N. Reinhoudt, *Tetrahedron* **1996**, *6352*, 2663–2704.

[17] J. Pfeiffer, V. Schurig, *J. Chromatogr. A* **1999**, *840*, 145–150.

[18] V. Schurig, *Chirality* **2005**, *17*, S205–S226.

[19] J. R. Fraser, B. Borecka, J. Trotter, J. C. Sherman, *J. Org. Chem.* **1995**, *60*, 1207–1213.

[20] R. G. Chapman, J. C. Sherman, *J. Am. Chem. Soc.* **1998**, *120*, 9818–9826.

[21] H. E. K. Huttunen-Hennelly, J. C. Sherman, *Peptide Science* **2007**, *90*, 37–50.

[22] H. E. K. Huttunen-Hennelly, J. C. Sherman, *Org. Biomol. Chem.* **2007**, *5*, 3637–3650.

[23] C. Berghaus, M. Feigel, *Eur. J. Org. Chem.* **2003**, 3200–3208.

[24] C. M. Hülsbusch, M. Feigel, *J. Incl. Phenom. Macrocycl. Chem.* **2007**, *59*, 53–63.

[25] A. Shivanyuk, K. Rissanen, S. K. Körner, D. M. Rudkevich, J. Rebek, Jr., *Helv. Chim. Acta* **2000**, *83*, 1778–1790.

[26] P. Amrhein, A. Shivanyuk, D. W. Johnson, J. Rebek, *J. Am. Chem. Soc.* **2002**, *124*, 10349–10358.

[27] P. Soncini, S. Bonsignore, E. Dalcanale, *J. Org. Chem.* **1992**, *57*, 4608–4612.

[28] B. Botta, G. Delle Monache, P. Salvatore, F. Gasparrini, C. Villani, M. Botta, F. Corelli, A. Tafi, E. Gacs-Baitz, S. Santini, C. Carvalho, D. Misiti, *J. Org. Chem.* **1997**, *62*, 932–938.

[29] B. Botta, I. D´Acquarica, L. Nevola, F. Sacco, Z. Valbuena Lopez, G. Zappia, C. Fraschetti, M. Speranza, A. Tafi, F. Caporuscio, M. C. Letzel, J. Mattay, *Eur. J. Org. Chem.* **2007**, 5995–6002.

[30] B. Botta, G. Delle Monache, C. Fraschetti, L. Nevola, D. Subissati, M. Speranza, *Int. J. Mass Spectrom.* **2007**, *267*, 24–29.

[31] B. Botta, A. Tafi, F. Caporuscio, M. Botta, L. Nevola, I. D´Acquarica, C. Fraschetti, M. Speranza, *Chem. Eur. J.* **2008**, *14*, 3585–3595.

[32] B. Botta, C. Fraschetti, F. R. Novara, A. Tafi, F. Sacco, L. Mannina, A. P. Sobolev, J. Mattay, M. C. Letzel, M. Speranza, *Org. Biomol. Chem.* **2009**, *7*, 1798–1806.

[33] B. Botta, C. Fraschetti, I. D´Acquarica, M. Speranza, F. R. Novara, J. Mattay, M. C. Letzel, *J. Phys. Chem. A* **2009**, *113*, 14625–14629.

[34] B. Botta, D. Subissati, A. Tafi, G. Delle Monache, A. Filippi, M. Speranza, *Angew. Chem. Int. Ed.* **2004**, *43*, 4767–4770.

[35] M. Pietraszkiewicz, P. Prus, R. Bilewicz, *Pol. J. Chem.* **1999**, *73*, 2035–2042.

[36] W. Iwanek, J. Mattay, *Liebigs Ann.* **1995**, *8*, 1463–1466.

[37] W. Iwanek, M. Urbaniak, *Polish J. Chem.* **1999**, *73*, 2067–2072.

[38] N. K. Beyeh, D. Fehér, M. Luostarinen, C. A. Schalley, K. Rissanen, *J. Incl. Phenom. Macrocycl. Chem.* **2006**, *56*, 381–394.

[39] A. Szumna, *Org. Biomol. Chem.* **2007**, *5*, 1358–1368.

[40] B. Kuberski, M. Pecul, A. Szumna, *Eur. J. Org. Chem.* **2008**, 3069–3078.

[41] M. J. McIldowie, M. Mocerino, B. W. Skelton, H. A. White, *Org. Lett.* **2000**, *2*, 3869–3871.

[42] J. Y. Boxhall, P. C. B. Page, M. R. J. Elsegood, Y. Chan, H. Heaney, K. E. Holmes, M. J. McGrath, *Synlett* **2003**, 1002–1006.

[43] B. R. Buckley, P. C. Bulman Page, Y. Chan, H. Heaney, M. Klaes, M. J. McIldowie, V. McKee, J. Mattay, M. Mocerino, E. Moreno, B. W. Skelton, A. H. White, *Eur. J. Org. Chem.* **2006**, 5135–5151.

[44] M. Klaes, C. Agena, M. Köhler, M. Inoue, T. Wada, Y. Inoue, J. Mattay, *Eur. J. Org. Chem.* **2003**, 1404–1409.

[45] M. Klaes, B. Neumann, H.-G. Stammler, J. Mattay, *Eur. J. Org. Chem.* **2005**, 864–868.

[46] M. J. McIldowie, M. Mocerino, M. I. Ogdena, B. W. Skelton, *Tetrahedron* **2007**, *63*, 10817–10825.

[47] D. Moore, S. E. Matthews, *J. Incl. Phenom. Macrocycl. Chem.* **2009**, *65*, 137–155.

[48] M. Luostarinen, K. Salorinne, H. Lähteenmäki, H. Mansikkamäki, C. A. Schalley, M. Nissinen, K. Rissanen, *J. Incl. Phenom. Macrocycl. Chem.* **2007**, *58*, 71–80.

[49] T. J. Wenzel, *Discrimination of Chiral Compounds Using NMR Spectroscopy*, John Wiley & Sons, Hoboken, **2007**.

[50] C. A. Schalley (Editor), *Analytical Methods in Supramolecular Chemistry*, Wiley-VCH, Weinheim **2007**.

[51] C. A. Schalley, A. Springer, *Mass Spectrometry and Gas-Phase Chemistry of Non-Covalent Complexes*, John Wiley & Sons, Hoboken, **2009**.

[52] M. Sawada, Y. Takai, H. Yamada, S. Hirayama, T. Kaneda, T. Tankaka, K. Kamada, T. Mizooku, S. Takeuchi, K. Ueno, K. Hirose, Y. Tobe, K. Naemura, *J. Am. Chem. Soc.* **1995**, *117*, 7726–7736.

[53] M. Sawada, Y. Takai, H. Yamada, J. Nishida, T. Kaneda, R. Arakawa, M. Okamoto, K. Hirose, T. Tanaka, K. Naemura, *J. Chem. Soc., Perkin Trans. 2* **1998**, 701–710.

[54] N. Kuhnert, A. Le-Gresley, D. C. Nicolau, A. Lopez-Periago, *J. Label. Compd. Radiopharm.* **2007**, *50*, 1215–1223.

[55] C. Fraschetti, M. Pierini, C. Villani, F. Gasparrini, S. L. Mortera, M. Speranza, *Chem. Commun.* **2009**, 5430–5432.

[56] A. Mehdizadeh, M. C. Letzel, M. Klaes, C. Agena, J. Mattay, *Eur. J. Mass. Spectrum.* **2004**, *10*, 649–655.

[57] T. Schröder, R. Brodbeck, M. C. Letzel, A. Mix, B. Schnatwinkel, M. Tonigold, D. Volkmer, J. Mattay, *Tetrahedron Lett.* **2008**, *49*, 5939–5942.

[58] C. Agena, Dissertation, Bielefeld University **2002**.

[59] a) L. M. Tunstad, J. A. Tucker, E. Dalcanale, J. Weiser, J. A. Byrant, J. C. Sherman, R. C. Helgeson, C. B. Knobler, D. J. Cram, *J. Org. Chem.* **1989**, *54*, 1305–1312; b) J. A. Bryant, M. T. Blanda, M. Vincenti, D. J. Cram, *J. Am. Chem. Soc.* **1991**, *113*, 2176–2172; c) J. L. Irwin, M. S. Sherburn, *Org. Lett.* **2001**, *3*, 225–227.

[60] I. Stoll, J. Eberhard, R. Brodbeck, W. Eisfeld, J. Mattay, *Chem. Eur. J.* **2008**, *14*, 1155–1163.

[61] I. Stoll, A. Mix, A. B. Rozhenko, B. Neumann, H.-G. Stammler, J. Mattay, *Tetrahedron* **2008**, *64*, 3813–3825.

[62] L. A. Carpino, H. Imazumi, A. El-Faham, F. J. Ferrer, C. Zhang, Y. Lee, B. M. Foxman, P. Henklein, C. Hanay, C. Mügge, H. Wenschuh, J. Klose, M. Beyermann, M. Bienert, *Angew. Chem. Int. Ed.* **2002**, *41*, 441–445.

[63] N. Sewald, H.-D. Jakubke, *Peptides: Chemistry and Biology*, Wiley-VCH, Weinheim **2003**.

[64] G. D. Fasman (Editor), *Circular dichroism and the conformational analysis of biomolecules*, Plenum Press, New York **1996**.

[65] F. Gruppi, F. Boccini, L. Elviri, E. Dalcanale, *Tetrahedron* **2009**, *66*, 7289–7295.

[66] a) N. Nishimura, K. Kobayashi, *Angew. Chem. Int. Ed.* **2008**, *47*, 6255–6258; b) N. Nishimura, K. Yoza, K. Kobayashi, *J. Am. Chem. Soc.* **2010**, *132*, 777–790.

[67] T. M. Altamore, E. S. Barrett, P. J. Duggan, M. S. Sherburn, M. L. Szydzik, *Org. Lett.* **2002**, *4*, 3489–3491.

[68] M. Pietraszkiewicz, P. Prus, O. Pietraszkiewicz, *Tetrahedron* **2004**, *60*, 10747–10752.

[69] L.-C. Campeau, M. Parisien, M. Leblanc, K. Fagnou, *J. Am. Chem. Soc.* **2004**, *126*, 9186–9187.

[70] L.-C. Campeau, M. Parisien, A. Jean, K. Fagnou, *J. Am. Chem. Soc.* **2006**, *128*, 581–590.

[71] M. Paletta, *Untersuchungen zur Erweiterung der Kavität inhärent chiraler Resorc[4]arene*, Diploma Thesis, Bielefeld University **2006**.

[72] a) K.-C. Kong, C.-H. Cheng, *J. Am. Chem. Soc.* **1991**, *113*, 6313–6315; b) D. K. Morita, J. K. Stille, J. R. Norton, *J. Am. Chem. Soc.* **1995**, *117*, 8576–8581; c) F. E. Goodson, T. I. Wallow, B. M. Novak, *J. Am. Chem. Soc.* **1997**, *119*, 12441–12453; d) V. V. Grushin, *Organometallics* **2000**, *19*, 1888–1900.

[73] T. E. Barder, S. D. Walker, J. R. Martinelli, S. L. Buchwald, *J. Am. Chem. Soc.* **2005**, *127*, 4685–4696.

[74] D. P. Curran, F. Yang, J. Cheong, *J. Am. Chem. Soc.* **2002**, *124*, 14993–15000.

[75] D. D. Hennings, S. Iwasa, V. H. Rawal, *J. Org. Chem.* **1997**, *62*, 2–3.

[76] a) G. Bringmann, T. Hartung, L. Göbel, O. Schupp, C. L. J. Ewers, B. Schöner, R. Zagst, K. Peters, H. G. von Schnering, C. Burschka, *Liebigs Ann. Chem.* **1992**, 225–232; b) G. Bringmann, J. R. Jansen, *Heterocycles* **1989**, *28*, 137–142.

[77] R. J. Abraham, J. Fisher, *NMR Spectroscopy*, Wiley, New York **1988**.

[78] F. Vögtle, A. Hünten, E. Vogel, S. Bischbeck, O. Safarowsky, J. Recker, A. Parham, M. Knott, W. Müller, U. Müller, Y. Okamoto, T. Kubota, W. Lindner, E. Francotte, S. Grimme, *Angew. Chem. Int. Ed.* **2001**, *40*, 2468–2471.

[79] N. Berova, K. Nakanishi, R. W. Woody (Editor), *Cicular Dichroism - Principles and Applications*, Wiley-VCH, 2. Ed. **2000**.

[80] J. Eames, M. J. Suggate, *J. Label. Compd. Radiopharm.* **2004**, *47*, 705–717.

[81] G. E. Keck, M. B. Andrus, D. R. Romer, *J. Org. Chem.* **1990**, *56*, 417–420.

[82] M. Gangoda, R. K. Gilpin, J. Figueirinhas, *J. Phys. Chem.* **1989**, *93*, 4815–4818.

[83] X. Qin, T. Tzvetkov, X. Liu, D.-C. Lee, L. Yu, D. C. Jacobs, *J. Am. Chem. Soc.* **2004**, *126*, 13232–13233.

[84] B. Chantegrel, C. Deshayes, A. Doutheau, J. P. Steghens, *Lipids* **2002**, *37*, 1013–1018.

[85] J. Terao, H. Todo, S. A. Begum, H. Kuniyasu, N. Kambe, *Angew. Chem. Int. Ed.* **2007**, *46*, 2086–2089.

[86] D. Yang, C. Zhang, *J. Org. Chem.* **2001**, *66*, 4814–4818.

[87] a) A. Girard, G. Sandulesco, *Helv. Chim. Acta* **1936**, *19*, 1095–1107; b) A. M. Gaddis, R. Ellis, G. T. Currie, *Nature* **1961**, *191*, 1391–1392.

[88] B. R. Buckley, J. Y. Boxhall, P. C. Bulman Page, Y. Chan, M. R.J. Elsegood, H. Heaney, K. E. Holmes, M. J. McIldowie, V. McKie, M. J. McGrath, M. Mocerino, A. M. Poulton, E. P. Sampler, B. W. Skelton, A. H. White, *Eur. J. Org. Chem.* **2006**, 5117–5134.

[89] a) J. B. Niederl, H. J. Vogel, *J. Am. Chem. Soc.* **1940**, *62*, 2512–2514; b) H. Erdtman, S. Högberg, S. Abrahamsson, B. Nilsson, *Tetrahedron Lett.* **1968**, *14*, 1679–1682; c) P. Timmerman, W. Verboom, D. N. Reinhoudt, *Tetrahedron* **1996**, *52*, 2663–2704.

[90] G. S. Coumbarides, M. Dingjan, J. Eames, M. J. Suggate, *J. Label. Compd. Radiopharm.* **2006**, *49*, 153–161.

[91] W. L. Meyer, A. P. Lobo, *J. Am. Chem. Soc.* **1966**, *88*, 3181–3182.

[92] C. Schiel, G. A. Hembury, V. V. Borovkov, M. Klaes, C. Agena, T. Wada, S. Grimme, Y. Inoue, J. Mattay, *J. Org. Chem.* **2006**, *71*, 976–982.

[93] A. Filippi, A. Giardini, S. Piccirillo, M. Speranza, *Int. J. Mass Spectrom.* **2000**, *198*, 137–163.

[94] C. A. Schalley, *Int. J. Mass Spectrom.* **2000**, *194*, 11–39.

[95] J. S. Brodbelt, *Int. J. Mass Spectrom.* **2000**, *200*, 57–69.

[96] M. Vincenti, A. Irico, *Int. J. Mass Spectrom.* **2002**, *214*, 23–26.

[97] M. Speranza, F. Gasparrini, B. Botta, C. Villani, D. Subissati, C. Fraschetti, F. Subrizi, *Chirality* **2009**, *21*, 69–86.

[98] M. Speranza, *Int. J. Mass. Spectrom.* **2004**, *232*, 277–317.

[99] M. Sawada, Y. Takai, T. Kaneda, R. Arakawa, M. Okamoto, H. Doe, T. Matsuo, K. Naemura, K. Hirose, Y. Tobe, *Chem. Commun.* **1996**, 1735–1736.

[100] M. Sawada, H. Yamaoka, Y. Takai, Y. Kawai, H. Yamada, T. Azuma, T. Fujioka, T. Tanaka, *Int. J. Mass. Spectrom.* **1999**, *193*, 123–130.

[101] J. Guo, J. Wu, G. Siuzdak, M.G. Finn, *Angew. Chem. Int. Ed.* **1999**, *38*, 1755–1758.

[102] M. M. Stone, A. H. Franz, C. B. Lebrilla, *J. Am. Soc. Mass Spectrom.* **2002**, *13*, 964–974.

[103] J. A. Loo, *Int. J. Mass Spectrom.* **2000**, *200*, 175–186.

[104] M. Mäkinen, P. Vainiotalo, K. Rissanen, *J. Am. Soc. Mass Spectrom.* **2002**, *13*, 851–861.

[105] A. B. Rozhenko, W. W. Schoeller, M. C. Letzel, Björn Decker, C. Agena, J. Mattay, *Chem. Eur. J.* **2006**, *12*, 8995–9000.

[106] G. P. Moss, *Pure & Appl. Chem.* **1996**, *68*, 2193–2222.

[107] P. Muller, *Pure & Appl. Chem.* **1994**, *66*, 1077–1184.

[108] E. L. Eliel, S. H. Wilen, *Stereochemistry of Organic Compounds*, John Wiley & Sons, New York **1994**.

[109] D. Sparkman, *Mass Spectrometry Desk Reference*, Global View Publishing, Pittsburgh **2006**

Appendix

- Table 8.1: Rate constants (cm^3 $molecule^{-1}$ s^{-1}) measured for the reaction between $[M{\cdot}H{\cdot}G]^+$ and 2-propylamine. Enantioselectivity $\rho = k_{homo}/k_{hetero}$.
- Table 8.2: Rate constants (cm^3 $molecule^{-1}$ s^{-1}) measured for the reaction between $[M{\cdot}H{\cdot}G]^+$ and ethylamine. Enantioselectivity $\rho = k_{homo}/k_{hetero}$.
- Table 8.3: Rate constants (cm^3 $molecule^{-1}$ s^{-1}) measured for the reaction between $[M{\cdot}H{\cdot}G]^+$ and 2-butylamine. Enantioselectivity $\rho = k_{homo}/k_{hetero}$; $\xi = (k_R)/(k_S)$.
- Table 8.4: Kinetic isotope effect $K_{IE} = k_H/k_D$ measured for the reactions of $[M{\cdot}H{\cdot}G]^+$ with ethylamine, 2-propylamine and 2-butylamine.

Table 8.1: Rate constants (cm^3 molecule^{-1} s^{-1}) measured for the reaction between $[M{\cdot}H{\cdot}G]^+$ and 2-propylamine. Enantioselectivity $\rho = k_{homo}/k_{hetero}$.

Host M	Guest G	k × 10^{10}	ρ	% *eff*
M_S^H	A_2	4.456±0.2372	0.700±0.053	37.4
M_R^D		6.369±0.3420		53.4
M_S^D		4.007±0.1893	0.595±0.040	33.6
M_R^H		6.738±0.3195		56.5
M_S^H	A_5	2.619±0.1014	2.029±0.111	22.0
M_R^D		1.291±0.0502		10.8
M_S^D		2.942±0.1236	2.202±0.131	24.7
M_R^H		1.336±0.0562		11.2
M_S^H	A_7	7.153±0.2437	0.946±0.046	60.0
M_R^D		7.562±0.2624		63.4
M_S^D		7.175±0.2209	0.989±0.043	60.2
M_R^H		7.255±0.2230		60.9
M_S^H	E_1	1.391±0.0383	0.737±0.029	11.7
M_R^D		1.887±0.0536		15.8
M_S^D		1.236±0.0342	0.610±0.024	10.4
M_R^H		2.024±0.0570		17.0
M_S^H	E_6	1.993±0.0794	0.798±0.045	16.7
M_R^D		2.498±0.0989		21.0
M_S^D		1.987±0.0794	0.752±0.042	16.7
M_R^H		2.643±0.1044		22.2
M_S^H	E_9	1.708±0.0743	1.091±0.067	14.3
M_R^D		1.566±0.0676		13.1
M_S^D		1.779±0.0775	1.100±0.068	14.9
M_R^H		1.618±0.0711		13.6
M_S^H	E_{10}	1.500±0.0469	0.705±0.031	12.6
M_R^D		2.129±0.0664		17.9
M_S^D		1.614±0.0611	0.706±0.036	13.5
M_R^H		2.286±0.0775		19.2

Host M	Guest G	k × 10^{10}	ρ	% *eff*
M_S^H	N_6	0.0639±0.0018	0.472±0.018	0.54
M_R^D		0.1354±0.0035		1.14
M_S^D		0.0844±0.0022	0.843±0.032	0.71
M_R^H		0.1000±0.0028		0.84
M_S^H	N_{12}	0.0263±0.0013	3.886±0.287	0.22
M_R^D		0.1022±0.0053		0.86
M_S^D		0.0285±0.0014	3.095±0.269	0.24
M_R^H		0.0882±0.0041		0.74
M_S^H	N_{13}	0.0057±0.0001	0.894±0.038	0.05
M_R^D		0.0051±0.0002		0.04
M_S^D		0.0055±0.0001	0.981±0.036	0.05
M_R^H		0.0054±0.0001		0.04
M_S^H	N_{14}	0.0625±0.0026	1.515±0.089	0.52
M_R^D		0.0947±0.0039		0.79
M_S^D		0.0666±0.0027	1.189±0.068	0.56
M_R^H		0.0792±0.0031		0.66

Table 8.2: Rate constants (cm^3 molecule^{-1} s^{-1}) measured for the reaction between [M·H·G]$^+$ and ethylamine. Enantioselectivity $\rho = \mathrm{k}_{\mathrm{homo}}/\mathrm{k}_{\mathrm{hetero}}$.

Host M	Guest G	k × 10^{11}	ρ	% *eff*
M^{H}_{S}	A_1	51.41±2.4477	0.994±0.067	40.7
M^{D}_{R}		51.74±2.4571		41.0
M^{D}_{S}		47.79±2.2706	0.934±0.063	37.9
M^{H}_{R}		51.88±2.4334		41.1
M^{H}_{S}	A_2	3.710±0.0904	0.391±0.014	2.94
M^{D}_{R}		9.488±0.2385		7.51
M^{D}_{S}		3.499±0.0788	0.398±0.015	2.77
M^{H}_{R}		8.803±0.2626		6.97
M^{H}_{S}	A_4	5.258±0.1348	0.565±0.020	4.16
M^{D}_{R}		9.307±0.2353		7.37
M^{D}_{S}		5.011±0.1260	0.532±0.019	3.97
M^{H}_{R}		9.422±0.2505		7.46
M^{H}_{S}	A_7	32.00±1.148	0.863±0.044	25.3
M^{D}_{R}		37.06±1.314		29.3
M^{D}_{S}		36.59±1.403	0.994±0.054	29.0
M^{H}_{R}		36.82±1.425		29.2
M^{H}_{S}	E_1	0.655±0.0250	0.533±0.029	0.53
M^{D}_{R}		1.230±0.0048		0.97
M^{D}_{S}		0.610±0.0232	0.525±0.028	0.48
M^{H}_{R}		1.162±0.0435		0.92
M^{H}_{S}	E_9	2.902±0.1800	0.859±0.075	2.30
M^{D}_{R}		3.377±0.2064		2.67
M^{D}_{S}		2.729±0.1694	0.949±0.083	2.16
M^{H}_{R}		2.875±0.1791		2.28
M^{H}_{S}	N_6	0.0333±0.0011	0.594±0.026	0.026
M^{D}_{R}		0.0559±0.0017		0.044
M^{D}_{S}		0.0324±0.0010	0.641±0.027	0.026
M^{H}_{R}		0.0505±0.0015		0.041

Table 8.3: Rate constants (cm^3 molecule^{-1} s^{-1}) measured for the reaction between $[M{\cdot}H{\cdot}G]^+$ and 2-butylamine. Enantioselectivity $\rho = k_{homo}/k_{hetero}$; $\xi = (k_R)/(k_S)$.

		(*R*)-2-butylamine		(*S*)-2-butylamine				
Host M	Guest G	$k \times 10^{10}$	ρ	$k \times 10^{10}$	ρ	% *eff* $_R$	% *eff* $_S$	ξ
M_S^H	A_1	9.355±0.2536	1.064±0.041	9.518±0.4665	1.097±0.076	82.6	84.0	0.98±0.055
M_R^D		8.793±0.2383		8.676±0.4257		77.6	76.6	1.01±0.057
M_S^D		8.172±0.2311	0.958±0.038	8.821±0.4539	0.924±0.067	72.1	77.8	0.93±0.054
M_R^H		8.527±0.2337		9.545±0.4893		75.3	84.2	0.89±0.052
M_S^H	A_2	7.472±0.3237	0.932±0.057	7.423±0.213	0.941±0.038	65.9	65.5	1.01±0.052
M_R^D		8.015±0.3446		7.885±0.227		70.7	69.6	1.02±0.053
M_S^D		6.093±0.2668	0.760±0.048	6.963±0.200	0.827±0.034	53.8	61.5	0.87±0.045
M_R^H		8.014±0.3592		8.419±0.242		70.7	74.3	0.95±0.050
M_S^H	A_3	10.18±0.4248	0.964±0.057	7.218±0.3397	0.983±0.065	89.8	63.7	1.41±0.089
M_R^D		10.56±0.4424		7.343±0.3466		93.2	64.8	1.44±0.091
M_S^D		9.791±0.4110	0.940±0.056	6.999±0.3289	0.932±0.062	86.4	61.8	1.40±0.088
M_R^H		10.41±0.4362		7.511±0.3532		91.9	66.3	1.38±0.076
M_S^H	A_4	7.624±0.3306	0.950±0.059	8.302±0.4073	1.080±0.075	67.3	73.3	0.92±0.058
M_R^D		8.025±0.3601		7.689±0.3830		70.8	67.9	1.04±0.070
M_S^D		7.181±0.3203	0.852±0.054	7.114±0.3375	0.837±0.056	63.4	62.3	1.01±0.066
M_R^H		8.425±0.3743		8.499±0.4023		74.4	75.0	0.99±0.064

		(*R*)-2-butylamine		(*S*)-2-butylamine				
Host M	Guest G	k × 10^{10}	ρ	k × 10^{10}	ρ	% *eff*$_\mathrm{R}$	% *eff*$_\mathrm{S}$	ξ
M_S^H	A_5	6.607±0.2816	1.306±0.083	6.551±0.3005	1.438±0.093	58.3	57.8	1.01±0.063
M_R^D		5.057±0.2361		4.555±0.2063		44.6	40.2	1.11±0.072
M_S^D		7.546±0.3266	1.624±0.103	6.603±0.2916	1.565±0.972	66.6	58.3	1.14±0.070
M_R^H		4.648±0.2152		4.220±0.1845		41.0	37.2	1.10±0.070
M_S^H	A_6	9.907±0.3817	0.951±0.051	7.237±0.3334	0.987±0.064	87.4	63.9	1.37±0.082
M_R^D		10.16±0.3884		7.329±0.3332		89.7	64.7	1.39±0.082
M_S^D		9.879±0.3787	0.977±0.064	6.880±0.3108	0.977±0.062	87.2	60.7	1.43±0.085
M_R^H		10.39±0.3975		7.041±0.3185		91.7	62.1	1.48±0.088
M_S^H	A_8	0.0124±0.0005	0.546±0.028	0.0141±0.0004	0.691±0.031	0.11	0.12	0.88±0.043
M_R^D		0.0228±0.0008		0.0204±0.0007		0.20	0.18	1.11±0.054
M_S^D		0.0119±0.0005	0.482±0.024	0.0129±0.0004	0.637±0.028	0.10	0.11	0.92±0.048
M_R^H		0.0247±0.0008		0.0203±0.0006		0.22	0.18	1.21±0.053
M_S^H	E_1	2.885±0.0695	0.771±0.026	4.190±0.2984	0.817±0.082	25.5	37.0	0.69±0.052
M_R^D		3.709±0.0895		5.131±0.3641		32.7	45.3	0.72±0.054
M_S^D		2.896±0.0708	0.734±0.026	3.595±0.2248	0.778±0.069	25.6	30.9	0.80±0.083
M_R^H		3.947±0.1003		4.619±0.2885		34.8	40.8	0.85±0.057
M_S^H	E_6	5.151±0.1965	0.817±0.044	3.375±0.1591	0.837±0.055	45.5	29.8	1.01±0.063
M_R^D		6.304±0.2413		4.034±0.1837		55.6	35.6	1.11±0.072
M_S^D		4.541±0.1694	0.752±0.040	3.163±0.1438	0.770±0.050	40.1	27.9	1.14±0.070
M_R^H		6.035±0.2293		4.111±0.1883		53.3	36.3	1.10±0.070

		(R)-2-butylamine		(S)-2-butylamine				
Host M	Guest G	k × 10^{10}	ρ	k × 10^{10}	ρ	% eff_R	% eff_S	ξ
M_S^H	N_1	1.275±0.0390	0.772±0.033	0.8706±0.0245	0.980±0.039	11.2	7.68	1.46±0.060
M_R^D		1.650±0.0505		0.8887±0.0249		14.6	7.84	1.86±0.077
M_S^D		1.268±0.0362	0.823±0.033	0.8879±0.0235	0.981±0.037	11.2	7.84	1.43±0.055
M_R^H		1.541±0.0428		0.9046±0.0241		13.6	7.98	1.70±0.065
M_S^H	N_4	0.0173±0.0005	0.580±0.022			0.15		
M_R^D		0.0298±0.0008				0.26		
M_S^D		0.0170±0.0004	0.574±0.022			0.15		
M_R^H		0.0297±0.0008				0.26		
M_S^H	N_6	0.4290±0.0182	0.541±0.032	0.5110±0.0157	0.757±0.033	3.79	4.51	0.84±0.044
M_R^D		0.7933±0.0328		0.6752±0.0214		7.00	5.96	1.17±0.061
M_S^D		0.4651±0.0190	0.651±0.037	0.4709±0.0138	0.685±0.029	4.10	4.15	0.99±0.050
M_R^H		0.7143±0.0279		0.6878±0.0204		6.30	6.07	1.04±0.051
M_S^H	N_{11}	3.140±0.0852	0.931±0.035	2.204±0.0571	1.085±0.040	27.7	19.4	1.42±0.053
M_R^D		3.374±0.0907		2.031±0.0531		29.8	17.9	1.66±0.062
M_S^D		2.761±0.0824	0.887±0.037	2.115±0.0541	0.987±0.036	24.4	18.7	1.30±0.051
M_R^H		3.112±0.0895		2.142±0.0545		27.5	18.9	1.45±0.056
M_S^H	N_{12}	0.1364±0.0057	3.940±0.233	0.1758±0.0180	2.653±0.387	1.20	1.55	0.78±0.086
M_R^D		0.5374±0.0226		0.4665±0.0490		4.74	4.12	1.15±0.130
M_S^D		0.1495±0.0064	3.065±0.188	0.1762±0.0180	2.825±0.407	1.32	1.55	0.85±0.094
M_R^H		0.4583±0.0205		0.4977±0.0508		4.04	4.39	0.92±0.103

		(*R*)-2-butylamine		(*S*)-2-butylamine				
Host M	Guest G	k × 10^{10}	ρ	k × 10^{10}	ρ	% *eff* $_{\mathrm{R}}$	% *eff* $_{\mathrm{S}}$	ξ
M_S^H	N_{13}	0.0303±0.0010	1.020±0.046	0.0388±0.0013	0.783±0.036	0.27	0.34	0.78±0.060
M_R^D		0.0309±0.0009		0.0304±0.0010		0.27	0.27	1.02±0.045
M_S^D		0.0332±0.0009	1.144±0.047	0.0358±0.0011	0.877±0.038	0.29	0.32	0.93±0.038
M_R^H		0.0380±0.0011		0.0314±0.0010		0.33	0.28	1.21±0.052
M_S^H	N_{14}	0.3501±0.0146	1.569±0.094	0.2550±0.0121	1.318±0.088	3.09	2.25	1.37±0.086
M_R^D		0.5492±0.0233		0.3360±0.0160		4.85	2.97	1.63±0.104
M_S^D		0.3777±0.0159	1.360±0.081	0.3120±0.0137	0.939±0.058	3.33	2.75	1.21±0.074
M_R^H		0.5137±0.0215		0.2930±0.0130		4.53	2.59	1.75±0.107

Table 8.4: Kinetic isotope effect $K_{IE} = k_H/k_D$ measured for the reactions of $[M{\cdot}H{\cdot}G]^+$ with ethylamine, 2-propylamine and 2-butylamine.

	ethylamine		2-propylamine		2-butylamine	
Guest G	M_S^H/M_S^D	M_R^H/M_R^D	M_S^H/M_S^D	M_R^H/M_R^D	M_S^H/M_S^D	M_R^H/M_R^D
A_1	1.07	1.00				
A_2	1.06	0.93				
A_3					1.04	0.98
A_4	1.05	1.01			1.06	1.05
A_5			0.89	1.03	0.87	0.92
A_6					1.02	0.96
A_7	0.87	0.99	1.00	0.96		
A_8					1.04	1.08
E_1	1.07	0.94	1.12	1.07	1.00	1.06
E_9	1.06	0.85	0.96	1.03		
E_{10}			0.93	1.07		
N_1					1.00	0.93
N_4					1.02	1.00
N_6	1.03	0.90	0.76	0.74	0.92	0.90
N_{11}					1.14	0.92
N_{12}			0.92	0.86	0.91	0.85
N_{13}			1.07	1.02	1.08	1.03
N_{14}			0.94	0.84	0.93	0.93